1997

Modeling electrokinetically enhanced transport of multispecies in porous media under transient electrical field

Xuefeng Cao
Lehigh University

Cao, Xuefeng

Modeling Electrokinetically Enhanced Transport of Multispecies in Porous Media...

June 1, 1997

MODELING ELECTROKINETICALLY ENHANCED TRANSPORT OF MULTISPECIES IN POROUS MEDIA UNDER TRANSIENT ELECTRICAL FIELD

by

Xuefeng Cao

A Thesis

Presented to the Graduate and Research Committee

of Lehigh University

in Candidacy for the Degree of

Master of Science

in

Civil and Environmental Engineering

Lehigh University

May 1997

CERTIFICATE OF APPROVAL

This thesis is accepted and approved in partial fulfillment of the requirements for the Master of Science.

5/3/97
Date

Sibel Pamukcu
Thesis Advisor

Le-Wu Lu
Chairperson of Department

ACKNOWLEDGEMENTS

I would like to express my sincere appreciation to my advisor, Dr. Sibel Pamukcu, for her support, encouragement and valuable guidance throughout this research. Her constant concerns toward both my academic progress and my personal life have made my study at Lehigh a precious experience.

I am deeply indebted to Dr. Cetin Seren for his detailed instruction in computer programming and providing many hours of consultation and cooperation. Many Thanks are extended to Dr. Gerard Lennon for his valuable suggestions to the numerical model. Thanks are also due to Mesut Pervizpour, Salome Romero, Antoinette Weeks and other graduate students in Fritz lab who are not named here for their friendship and valuable assistance to my study and research.

I would also like to express my gratitude to my parents and my sisters for their love, encouragement and full support during my study.

This study was funded by the National Science Foundation through Grant No. MSS-9216291.

TABLE OF CONTENTS

LIST OF TABLES

LIST OF FIGURES

ABSTRACT

A modified mathematical model is developed for multispecies transport under transient electric field. Coupled potential differences (chemical and electrical potentials) are incorporated in the model. A set of differential equations addressing mass and charge balances are formulated. Chemical reactions, including electrolysis, water auto-ionization, sorption/desorption and precipitation reactions, are described using algebraic equations. The varying electric conductivity, electric field, current and voltage are also simulated in the model.

Transport of a multispecies system including hydrogen, hydroxyl, lead and nitrate ions are modeled. The distribution of species concentration, pH, electric field and conductivity are predicted. Associated chemical reactions are evaluated. The model predictions are reasonable and agree well with available experimental observations reported in literature.

Finite Difference Method is used to solve the PDE equations numerically. An iterative scheme is applied in computing. Program is developed using C++ and object-oriented technology. The program is developed to model multi-component transport process under a constant voltage difference, but can be easily converted to simulate the process under constant current. Because of the highly modular feature of object-oriented programming, the program can be used in many ways, such as being adapted into the core simulator of a knowledge-based program.

CHAPTER 1
INTRODUCTION

1.1 Statement of Problem

Migration of contaminant in soil, especially heavy metals released from DOE weapons complexes, industrial operations, and all other human activities, is a widespread problem for the nation's health and groundwater supply. The removal of such contaminants from soil using current technologies, i.e., excavation, landfill, vapor extraction, vitrification, etc., is either cost-expensive or technique-ineffective in some cases. For example, there are currently no mature technologies that are widely employed in engineering practices to fine-grained soil decontamination. With increasing demand for cost-effective and environmentally safe insitu remediation technologies, many studies have been conducted in search of such an innovative approach.

Electroremediation is probably one of the most promising insitu soil decontamination technologies capable of removing organic and inorganic contaminants and radionuclides. By using a low level direct current (DC) electrical potential difference across electrode pairs placed in ground, contaminants in the soil are moved under the action of the electrical field. Extraction of contaminants by electrokinetic method is based on the assumption that the contaminant is in liquid phase in the soil pores. This involves contaminant adsorption, transport, capture, and removal from soils. Principle mechanisms of electrokinetic decontamination are electroosmosis, electrophoresis, and electro-migration of ionic and polar species.

Although electrokinetic technology has been used for decades in construction for

soil stability, injection of grouts, and barriers of waste reservoir, its application to insitu removal of contaminants is still in stages of development. Most efforts are restricted to the laboratory. Limited field tests have been carried out. Some confusions still exist to the process of the coupling flow driven by electrical, chemical and hydraulic gradients. To convert the proposed electrokinetic processing method into an engineered technology, a thorough understanding of the electrokinetic phenomena is essential.

Mathematical models are effective approach to describe, explain, and predict the electrokinetic processing. These models, backed up by experiment data, will help determine the efficiency of the experiment scheme, offer theoretical support, prompt engineering application, and even help save money, time, and energy on developing this technology.

Several models have been developed since late 1980's. Although they have been shown to fit both theory and laboratory experiment data well, most of these models could only deal with single ion migration and neglect some important factors, such as changing electric field, electrode reactions, effective ion mobilities and chemical reactions between species, etc.

Multicomponent species transport model under transient electric field is challenging yet important to better understand the fundamental mechanisms, and is gaining increasing attention. Such a model is needed to develop the analysis tools in engineering the implemented techniques, too.

1.2 Objectives of Study

The main objective of this study is to investigate the existing electrokinetic mass transport models, analyze possible influence factors to the soil decontamination processing and present a modified mathematical model of electrokinetic mass transport which is able

to deal with multicomponent transport and incorporate those considerations previously ignored in other models. These considerations are:

1. Electrode reactions that control the chemistry in electrode solutions and thus lead to a transient boundary flux.
2. The influence of precipitation reactions which often happens during heavy metal transport especially in a high pH environment.
3. The changing electrical field due to re-distribution of charged concentration.
4. Effective ionic mobilities in pore fluid.
5. Effects of a multi-species mass transport system.
6. Sorption and desorption reactions.
7. Different voltage control scheme (i.e., the application of constant voltage through soil column).

Solution procedure developed in this study will serve as a basis for future development. This is a first step toward the goal of setting up a knowledge based system which should be able to model the transport process under different conditions. Model development and programming are the very important parts of this study.

1.3 Summary of Work

In this research, the mechanism and complex phenomena of electrokinetic decontamination process are studied. Existing models are evaluated, paying special attention to those of Acar and Alshawabkeh (1996) and Denisov and Probstein (1996). Boundary conditions, chemical equilibrium, transport coefficient, and electric field distribution, are given detailed consideration. Previously obtained laboratory data by Lehigh researchers (Pamukcu and Wittle, 1992) are used in model runs and verification. Based on these efforts, the existing models are optimized and modified to account for

coupled multicomponent species transport under the combined effects of diffusion, electromigration, electroosmosis, changing electric field, adsorption, and chemical reactions. Various chemical reactions in the pore fluid, such as sorption, precipitation/dissolution, water autoionization and electrolysis reactions are considered in the resulting one-dimensional model.

An object-oriented program (OOP) is developed to perform the numerical modeling. Finite difference method is employed to solve the partial difference governing equations (PDE). The program is constructed in a way that it is adaptable for future development and this development is not limited by its current structure.

CHAPTER 2
THEORY AND BACKGROUND

2.1 Theoretical Aspects of Electrokinetics

The electrokinetic phenomena is based on the relative motion between a charged surface and the bulk solution at its interface. The macroscopic motion observed experimentally is the result of the interactions of two charged phases at microscopic level. The formation of electric double layer at the charged surface of clay particles explains these electrokinetic phenomena of interest: electroosmosis, electrophoresis, and electromigration.

2.1.1 The Electric Double Layer

Consider a negatively charged clay colloid surface in contact with a water solution containing ions. The attraction to counterions and repulsion to co-ions, when combined with the mixing tendency resulting from the random thermal motion of the ions, leads to the formation of electric double layer, which is known as Gouy-Chapman theory (Gouy,1910; Chapman,1913) . A schematic of ion distributions adjacent to a clay particle in suspension is shown in Figure 2.1 .

According to Stern (1924), electric double layer is composed of a fixed layer

(Stern layer) and a diffuse layer (Gouy layer). In the Stern layer, the ions are assumed to oscillate about fixed adsorption sites, whereas, in the diffuse layer, ions are assumed to undergo Brownian motion. In a porous plug of clay, the surface becomes negatively charged when wetted with water. This charge is balanced by the adjoining Stern layer of liquid, which carries positively charged ions. The thickness of Stern layer is approximately the radius of a hydrated cation adsorbed on the clay particle surface. Stern layer and diffuse layer are divided by three planes: one is the plane of the clay-water interface; a second is the outer Helmholtz plane (O.H.P); and the third is the plane of shear as shown in Figure 2.2 . The O.H.P is the plane that defines the outer limit of the Stern layer, the layer of positively charged ions that are condensed on the clay particle surface. The drop in potential in Stern layer is linear from surface potential of ψ_0 to ψ_d at the O.H.P. The plane of shear is the plane at which the mobile portion of the diffuse layer can "slip" or flow past the charged surface. Potential at this shear plane is referred to as the electrokinetic potential or zeta(ζ) potential. Potential distribution in diffuse layer is given by Poisson-Boltzmann equation, which describes an exponential fall of the potential.

Integrating Poisson-Boltzmann equation with appropriate boundary conditions will give us the thickness of the diffuse layer, which is indirectly related to the ionic concentration in the bulk solution and the valence of the counterion. In applying double layer theory to clays, it is often assumed that the Stern layer is absent, hence, the diffuse layer begins at the clay-water interface[1]. The exact location of shear plane is still a matter of debate.

[1]Low (1987) indicated that the diffuse layer does not begin at the clay-water interface. The conclusion is reinforced by additional data presented by Low(1981), Chan et al(1984), and Miller (1984).

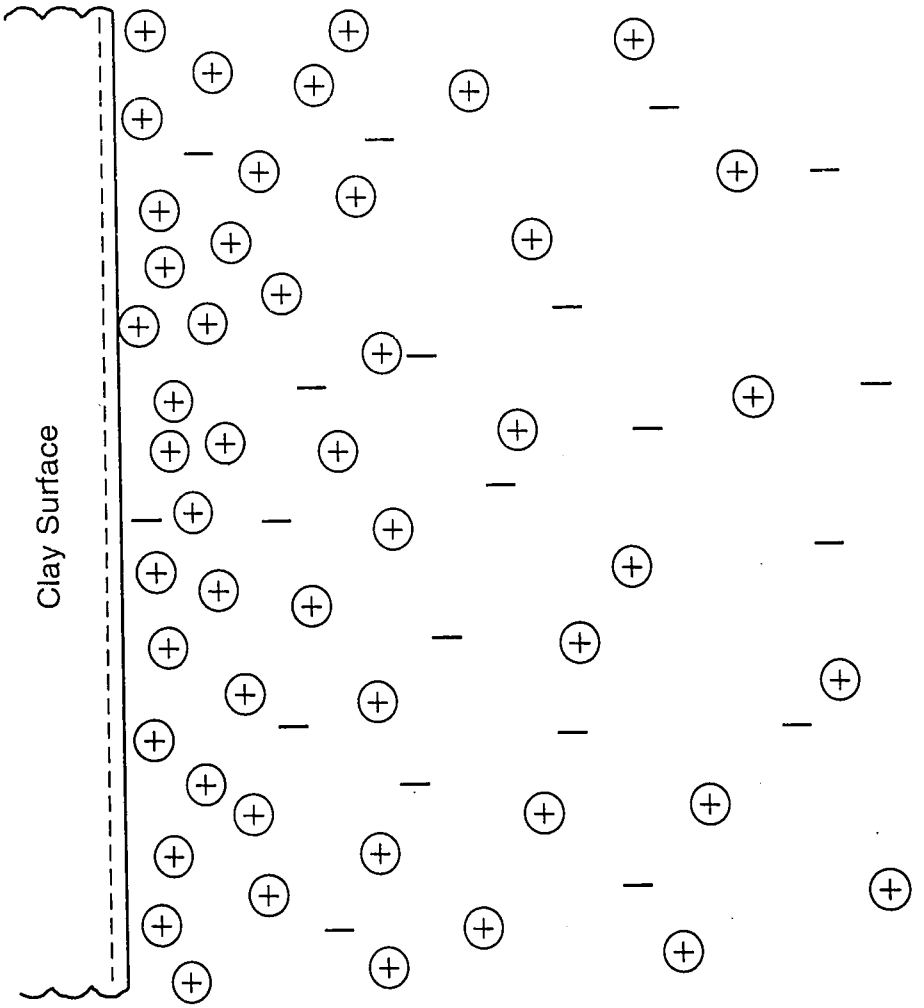

Figure 2.1. The Charged Ion Distributions Adjacent to A Clay Surface (Mitchell, 1993)

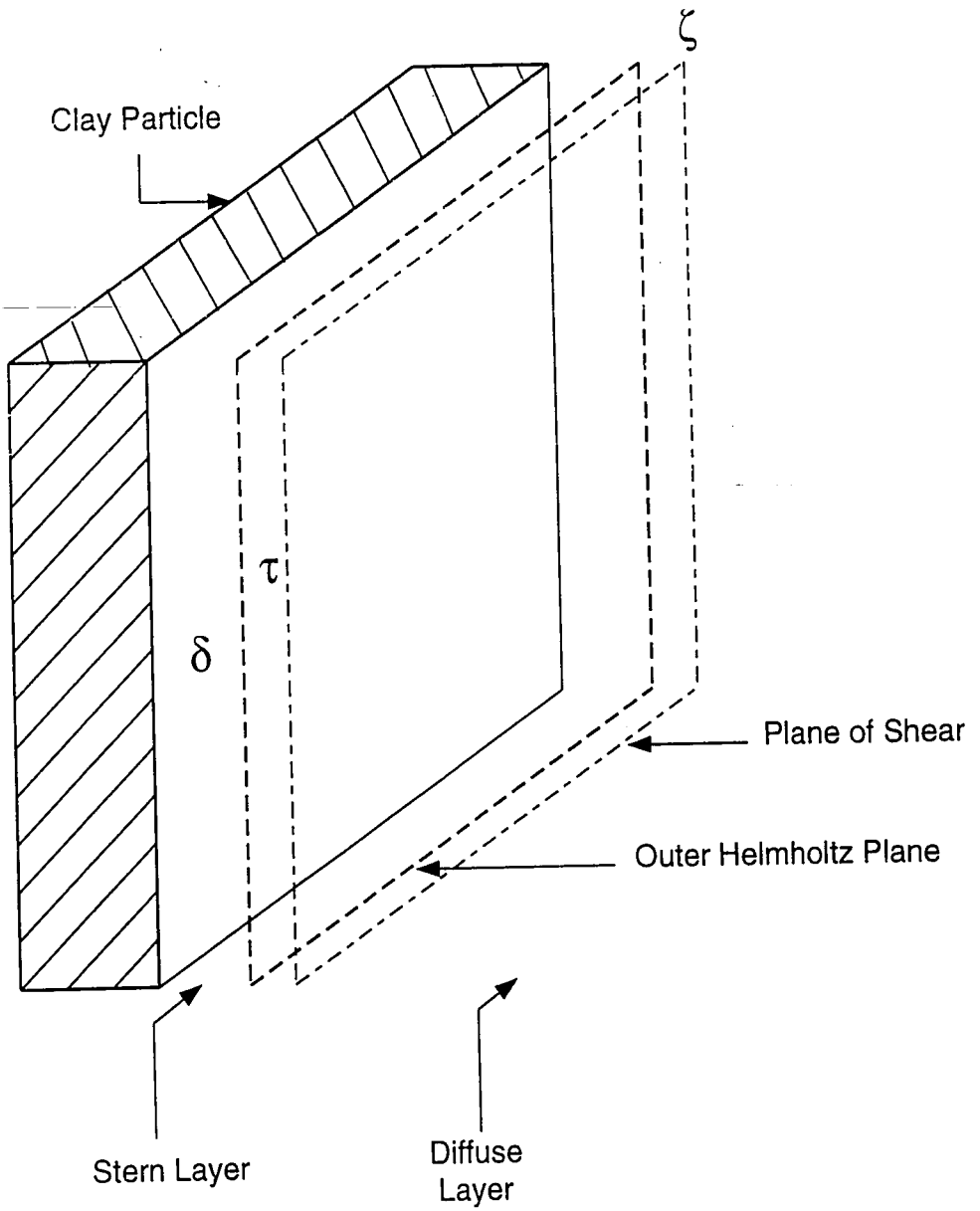

Figure 2.2. Model of The Electric Double Layer of Clay Particles

2.1.2 Electrophoresis

Electrophoresis is defined as the migration of charged colloids in solid-liquid mixture under electric potential gradient. Here we mean the movement of colloidal particles, not small ions. The motion of small ions is called ionic migration.

For clay-water system, if we place a direct current (DC) field across its suspension, negatively charged clay particles migrate toward the anode, as shown in Figure 2.3. The un-restrained particle transport through water in a poorly consolidated system will likely compact the soil to the anode, and disintegrate it on the cathode side.

In a compact system of porous plug, electrophoresis is of less importance due to restrained solid phase. But in the process of soil decontamination, electrophoresis of clay colloids could still play an important role.

2.1.3 Electroosmosis

Electroosmosis is complement of electro-phoresis. The latter involves discrete particle transport through water, while the electroosmosis involves water transport through a continuous soil particle network. When an electric field is applied, the surface or particle is fixed, the mobile diffuse layer moves, carrying solution with it, this is called electroosmosis. The movement of diffuse layer is, actually, described as that charged ions migrate under the field, carrying their water of hydration and exert a viscous drag on the water around them. Fig 2.4 shows the development of electro-osmotic flow.

In negatively charged clay particles, more cations than anions will generate a net water flow toward cathode. See Figure 2.5 . The ability of electroosmosis to produce a rapid flow of water in a compact, low permeability soil makes it significant to soil

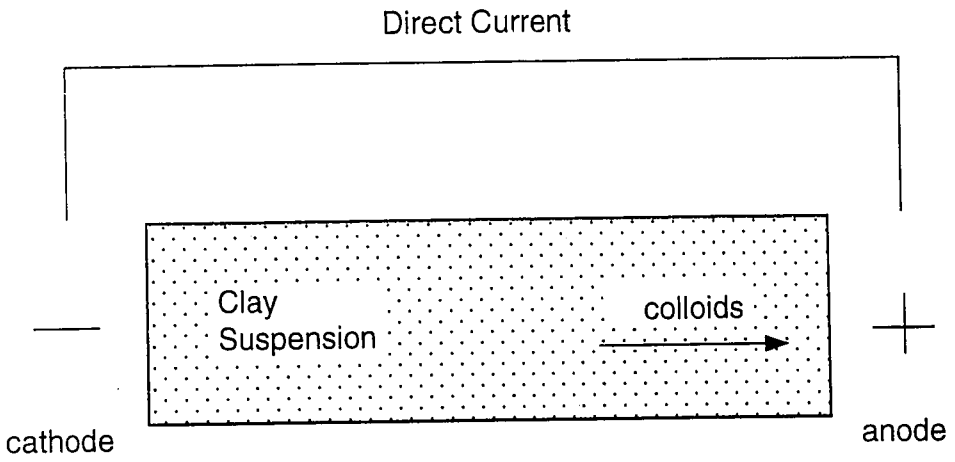

Figure 2.3 Electrophoresis in Clay-Water Suspension

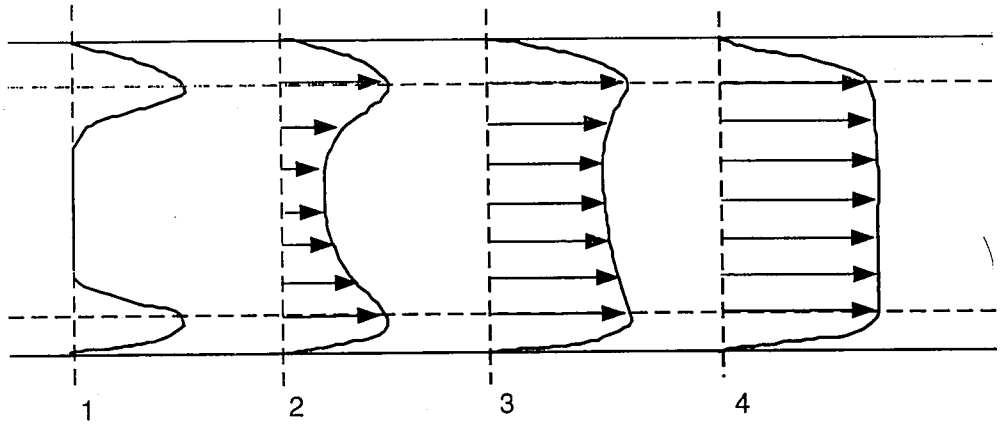

Figure 2.4 Development of Electroosmotic Flow; arrows represent flow velocities: From 1-4, switching on of field - steady state flow. Dashed lines are outer boundary of diffuse layer.

decontamination process by advection.

2.1.4 Electro-migration

Charged ions moving toward the oppositely charged electrode relative to solution is called electromigration. In a dilute system or a porous medium with moderately concentrated aqueous solution of electrolytes, electro-migration of ions is the major cause of current conduction.

For convenience the relationships between the various electrokinetic effects, they are summarized in table 2-1 (Adamson, 1990).

Table 2-1

Electrokinetic Effects

Potential	Nature of Solid Surface	
	Stationary [a]	Moving [b]
Applied	Electroosmosis	Electrophoresis
Induced	Streaming Potential	Migration Potential

[a] For example, a wall or apparatus surface.

[b] For example, a colloidal particle.

The streaming potential is the electrical potential difference due to water flow through soil under a hydraulic gradient. Double-layer charges are displaced in the direction of flow, and thus produces a potential difference between the ends of soil mass. Sometimes this streaming potential may decrease the effect of electroosmosis by reversing the situation in electroosmosis.

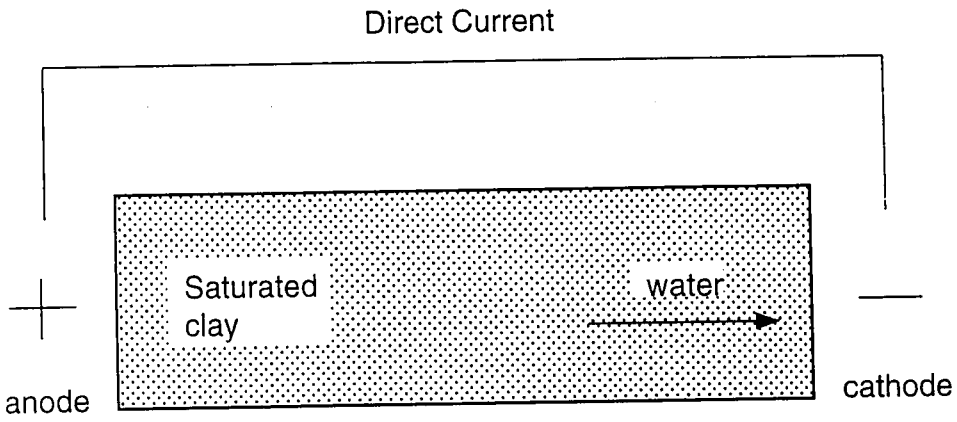

Figure 2.5 Electroosmosis in Saturated Clay

Electroosmotic flow under electric potential differences depends mainly on the porosity and the zeta potential and is independent to the pore size distribution or the presence of macro-pores (Acar, 1993). So electroosmosis is an efficient method to generate a uniform fluid and mass transport in clayey soils. Relative contribution of electroosmosis and ion migration to the total mass transport varies according to soil types, water content, types of ion species, pore fluid concentration and processing conditions. In silts and low-activity clays, electroosmotic flow reaches maximum. But the mass transport by ionic migration is always much higher than the mass transport by electroosmotic advection (at least 10 times higher). The effect of electroosmosis will decrease significantly when pH and zeta potential drops in the later stages of electrokinetic process (Hamed, 1991 and Pamukcu and Wittle, 1992). We will further discuss this in next chapters.

When micelles (charged particles) are formed with other species in the processing fluid, or when we deal with slurries, electrophoresis becomes significant (Pamukcu, 1994).

2.2 Historical Development of Electrokinetics

Although electrokinetic remediation technology is getting attention only in recent years, the first observation of electrokinetic phenomena was almost 200 years dated back. In the following centuries after its discovery, the electrokinetics has experienced great development, and has been applied to many science and engineering fields besides soil decontamination.

2.2.1 Observations and Development

In 1808, Reuss observed the electrokinetic phenomena when a DC current was applied to a clay-water mixture. Water moved through the capillary towards the cathode under the electric field. When the electric potential was removed, the flow of water immediately stopped. Napier (1846) distinguished electroosmosis from electrolysis. And in 1861, Quincke found the electric potential difference through a membrane resulted from streaming potential.

Helmholtz first treated electroosmotic phenomena analytically in 1879. A mathematical basis was provided. Pellat (1904) and Smoluchowski (1921) later modified it to also apply to electrophoretic velocity. Helmholtz-Smoluchowski (H-S) theory deals with electroosmotic/electrophoretic velocity of a fluid of certain viscosity and dielectric constant through a surface-charged porous medium of zeta potential (ζ), under an electric gradient. The H-S equation is as follows:

$$U_{EO} = \frac{\epsilon \zeta}{\mu} \frac{\partial \phi}{\partial x} \qquad [2\text{-}1]$$

U_{EO} = electroosmotic (electrophoretic) velocity
ϵ = permittivity of fluid in free space
μ = viscosity of fluid
$\partial\phi/\partial x$ = electric gradient

ζ varies with pH and ionic concentration of the pore fluid, which, as well as the electric gradient term therefore is not constant during the electrokinetic process in soils. This makes it difficult to assess a velocity term for the duration of electroosmotic transport.

Spiegler in 1958 gave another approach to electrokinetic process in porous medium. According to Spiegler, the electroosmotic flow is the difference between the measured flow and the ion hydration water in moles per Faraday. He suggested the opposite water transport induced by electromigration of anions. So the net water flow toward the cathode may be retarded by this opposite transport if anion concentration in

free water exceeds that of the cations.

Khan (1991) also proposed a modified theory of electroosmotic flow through soil. He separated the total current into a clay surface current and a pore water current. The voltage V, is expressed as parallel currents through soil:

$$V = I_s R_s = I_o R_o \qquad [2\text{-}2a]$$

I_s = surface current
R_s = surface resistance of soil
I_o = current carried by pore water
R_o = resistance of pore water

and the electroosmotic velocity of water thus directly depends on the surface current of soil:

$$U_{EO} = K I_s \qquad [2\text{-}2b]$$

where K is a constant coefficient including permittivity of fluid, dielectric constant of soil, viscosity, surface potential and surface resistance of soil.

The zeta potential in Khan's proposal is defined at the outer limit of the Stern layer and will be a constant surface potential that is invariant with respect to electrolyte concentration. Therefore, the true electroosmotic flow becomes independent to electrolyte concentration in the pore fluid.

2.2.2 Investigation and Application

In 1939, Leo Casagrande demonstrated that by using electroosmosis to soils with

high water content, the quick increase in the effective stresses in the soil will increase shear-strength of the soil to such a degree that even steep cuts will remain stable. Leo Casagrande first applied electrokinetics for soil stabilization in a construction project in Germany. Two years later, in 1941, Casagrande again utilized electro-osmosis to foundation engineering successfully. It was indicated from Casagrande's practice, that small reductions in water content by electroosmosis could produce significant increases in soil strength. From then on, electrochemical processing of soils has been investigated and used in many field protects. Besides its applications in chemistry, petroleum, and bio-science, in geotechnical engineering, electrokinetic treatment has been utilized in:

(1) improvement of excavation stability
(2) pore water tension development
(3) electrochemical induration/hardening
(4) fine-grained soils' stabilization
(5) consolidation and densification
(6) groundwater flow reversal and barrier system

To reduce the expenditures of electrical energy, several strategies can be employed including the use of polarity or current reversals (Gray&Somogyi, 1977); stepped voltages (Lockhart, 1983) and applying electro-osmotic dewatering technology only to soils with relatively low electrolyte concentration.

Active researches in geo-environmental field also indicated the great potential of electrokinetics in waste disposal, for example, the dewatering of waste sludge slimes; flow barriers; insitu generation of reactants for cleanup and/or electrolysis of contaminants; and decontamination of soils and groundwater.

2.3 Application of Electrokinetics to Soil Decontamination

Since the first use of electrokinetics to dewatering soils and sludges by Casagrande in 1949, research in electrokinetic decontamination of soils has accelerated in the past decade. Much of the work has focused on utilizing the technique for soil densification as an aid in containment facilities (Mitchell, Renaud & Probstein, 1986). Others have studied the effects of electrolysis on soil chemistry and the use of electrokinetics to contaminant removal from soil (Segall, et al. 1980; Putnam 1988; Acar, et al. 1989). The feasibility and cost effectiveness of the technique in the latter purpose have been demonstrated through laboratory studies and pilot scale studies.

Following the detection of high concentration of metals and organics in electroosmotically drained water of a dredged sludge by Segall and co-workers (1980), Banarjee and co-workers (1988) published a feasibility study for the potential application of electrokinetics for chromium decontamination; Acar and coworkers (1989) realized the importance of pH gradient generated from anode through cathode by the process; and in the same year, Lageman (Lageman, 1989) attempted to utilize pH gradient by controlling the chemical environment around the electrodes. Studies were also performed on the electrically induced movement of ions in sand at the University of Manchester in 1980 (Hamnet, 1980). It was observed that the process was more efficient in those fine-grained soils.

Pamukcu et al. (1991) presented the effects of speciation and precipitation on the efficiency of electrokinetic transport of zinc through soil. They found that zinc may be removed from both anode and cathode ends. Other lab studies further substantiated the applicability of the technique to a wide range of contaminants in soils (Khan et al. 1989; Hamed et al. 1991; Bruell and co-workers 1992; Pamukcu and Wittle 1992; Wittle and Pamukcu 1993; Acar et al. 1993, 1994, 1995; Hicks and Tondorf 1994; Acar and Alshawabkeh 1996). These studies showed that heavy metals and other cationic species can be removed from the soil either with the effluent or deposited at or close to the cathode. Acar et al. (1993), Pamukcu and Wittle (1994) and Yeung et al. (1996) also studied different enhancement technologies for electrokinetic transport.

Kaolinite specimens prepared with organic molding fluids demonstrated successful application of the electrokinetics in transport of the benzene, toluene, ethylene and m-xylene compounds (Bruell et al. 1992; Segal et al. 1992). High degrees of removal of phenol and acetic acid were also observed by Shapiro and Probstein (1993). Acar et al. (1992) reported removal of phenol from saturated kaolinite. Wittle and Pamukcu (1993) and Pamukcu (1994) investigated removal of organics such as chlorinated hydrocarbons and PAHs from different soil types.

CHAPTER 3
THE ELECTROKINETIC DECONTAMINATION PROCESSES

3.1 Lab Experiments

Electrokinetic decontamination involves complex physical and chemical processes. Previous and current research has made better understanding of the processing through large amount of lab experiments and careful analysis of the data. Although there exist differences in both equipment set-up and concentration of contaminants used among these bench-scale laboratory tests, all investigations show results consistent with the basic theory; describe different, if not similar, aspects of the processes; and contribute to the development of this technology.

3.1.1 The Electrokinetic Apparatus

Due to different research approach, there is no standard apparatus for measuring electrokinetic flow in soil. Schematic diagram of one equipment developed and used in Lehigh University by Pamukcu and co-workers are given in previous publications (Wittle and Pamukcu 1992; Pamukcu and Wittle 1994).

A one-dimensional consolidometer, a dedicated compression unit is used for

electrokinetic test specimen preparation as shown in Figure 3.1. It applies small increments of sustained stress and allows the excess fluid to drain out of the soil slowly. Homogeneous, near-saturated soil matrices compacted to a constant density and pressure are obtained using this equipment. The densified soil sample is packed into a cylindrical soil chamber in the unit, which may be easily pulled out after consolidation and then mounted in the electrokinetic cell without disturbance. Detailed operation of the unit is presented by Wittle and Pamukcu (1992).

The electrokinetic apparatus consists of a tube to hold the soil sample, a pair of electrodes constructed of graphite rods and placed inside liquid holding reservoirs at ends of the tube, pieces of porous stones to separate soil from liquid reservoirs, and other items for the convenience of measuring flow and potential (Figure 3.2). Wilkowe (1992) presents detailed description of the electrokinetic apparatus (E-K apparatus).

3.1.2 Sample Preparation and Sampling

Pamukcu and Wittle (1992) have explained the sample preparation process in detail. Here is a brief summary:

Contaminated clay slurries (laboratory-prepared soil specimens) are poured into the consolidation unit. The slurries are consolidated under a pre-selected final pressure (i.e. 200kPa). An incremental pressure is applied to approach this during the consolidation process. Clay samples is compressed into compact water saturated soil cylinders.

The soil cylinder is then removed from consolidometer, weighted, and sampled, and mounted into E-K apparatus. When all set-up is completed with electrical and water connections and the air bubbles are removed from the electrode chambers, the electrokinetic unit is ready for experiment.

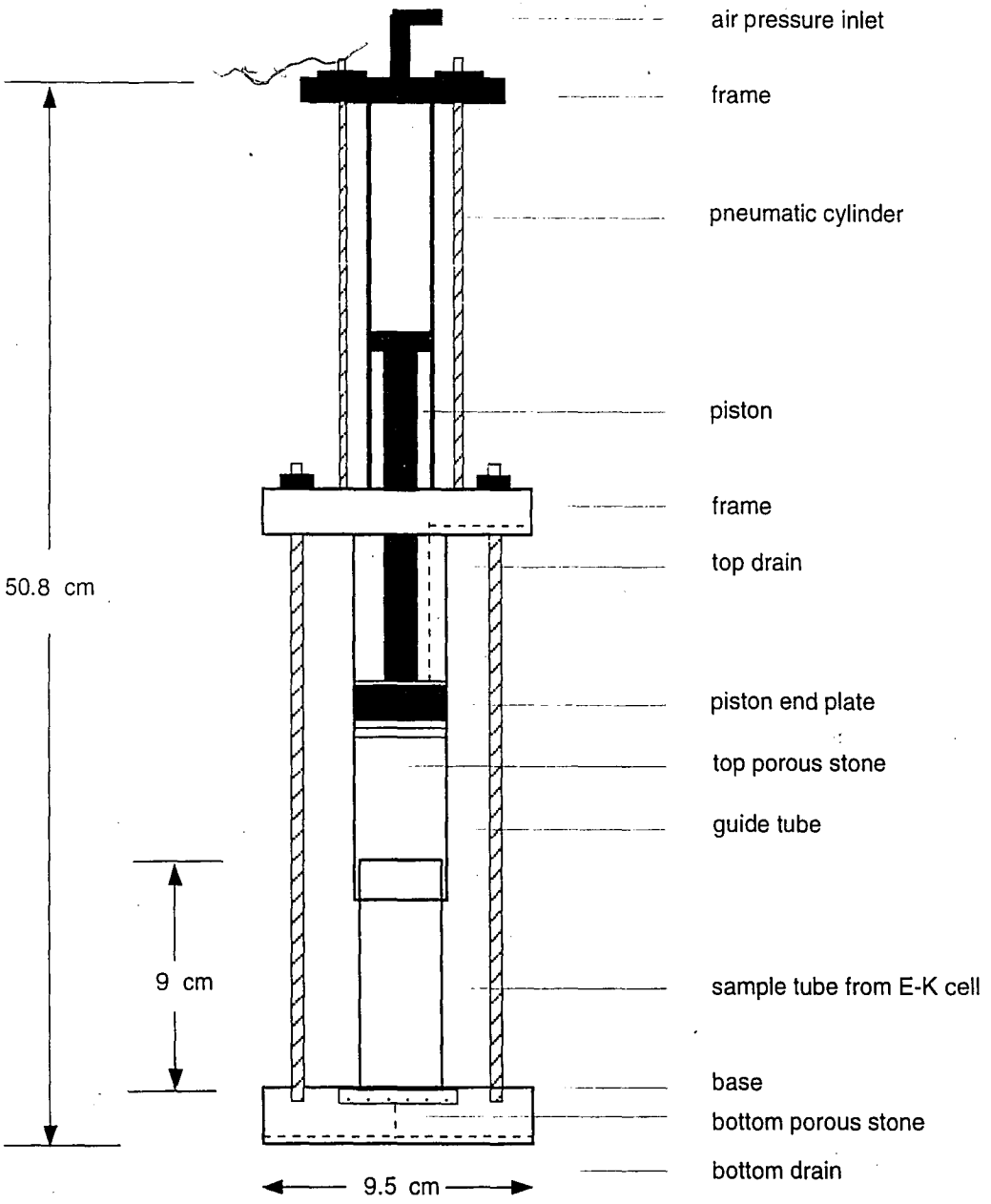

Figure 3.1 Consolidation Apparatus

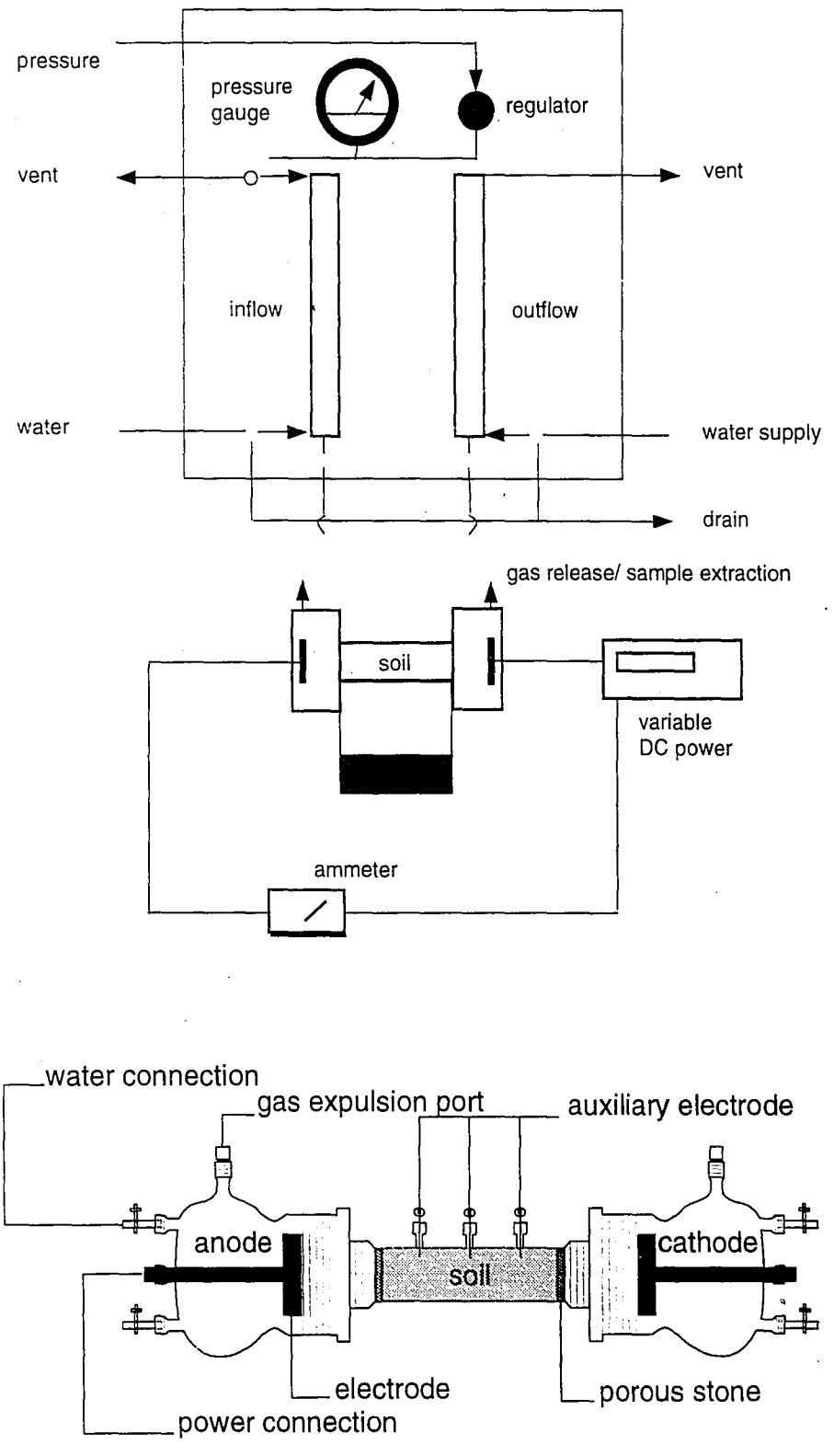

Figure 3.2 Schematic Diagram of the Electrokinetic Apparatus and Control Panel

3.1.3 Electrokinetic Testing

Laboratory investigations can be categorized into two groups. One often performed electrokinetic test tends to obtain a large database by observing the migration trend of each contaminant in the soil sample. This kind of tests is helpful in evaluating the efficiency of electrokinetic removal of various metal species and organic compounds. The other tests are more specified which tend to concentrate on the critical parameters of the process and try to prevent the development of unfavorable factors and enhance the efficiency of this technology. Some chemical or physical enhancement methods are often applied in these tests. pH control and use of surfactants are examples of these measures.

In all E-K tests by the Lehigh researchers, the E-K cell is operated under constant potential. Time-dependent water movement through the soil can be measured on the inflow and outflow tubes on the control panel of the test. The voltage in soil and the current generated are measured simultaneously with the flow measurements. Small amount of electrode chamber waters are sampled at different time periods during a test, and their pH readings are taken. These samples, as well as those collected at the end of experiment, are analyzed for the particular contaminant extracted. Soil specimens are also collected at different measuring points for quantitative analysis.

Detailed testing process is discussed by Pamukcu et al. (1992).

3.2 Observations and Considerations

Electrokinetic processing involves various physical-chemical phenomena. Coupled flow generated in the process effects the contaminating ion/particle removal, and the efficiency of this technology. The physical and chemical properties of soils, contaminants,

and pore fluids play important roles in this technology's removal efficiency. Some major considerations are discussed below.

3.2.1 General Description of Transport Mechanism

Advection of pore fluid due to electroosmotic flow and internally or externally applied hydraulic potential differences, diffusion from concentration gradients, and ion migration due to electrical gradients, together, form the transport mechanism for the movement of contaminants through electrokinetic decontamination. The coupled processes drive an acid front generated by electrolysis that advances across the soil sample and results in desorption of contaminant cations from the soil particle surfaces. These cations along with other ions in the pore fluid flow to the oppositely charged electrode.

A schematic diagram of electroosmotic flow is given in Figure 3.3 .

3.2.2 Electrolysis and Acid Front

Electrolysis reactions dominate the chemistry at the electrodes and soil/electrode interfaces, and directly influence the electrokinetic processing if no external factors control the chemistry of the process water. When electrolysis of water takes place, water molecules are disassociated into their ionic components and following equations describe the process, at anode and cathode site, respectively:

$$2H_2O - 4e^- \Rightarrow O_2\Uparrow + 4H^+ \quad \text{(anode)}$$

$$4H_2O + 4e^- \Rightarrow 2H_2O\Uparrow + 4OH^- \quad \text{(cathode)}$$

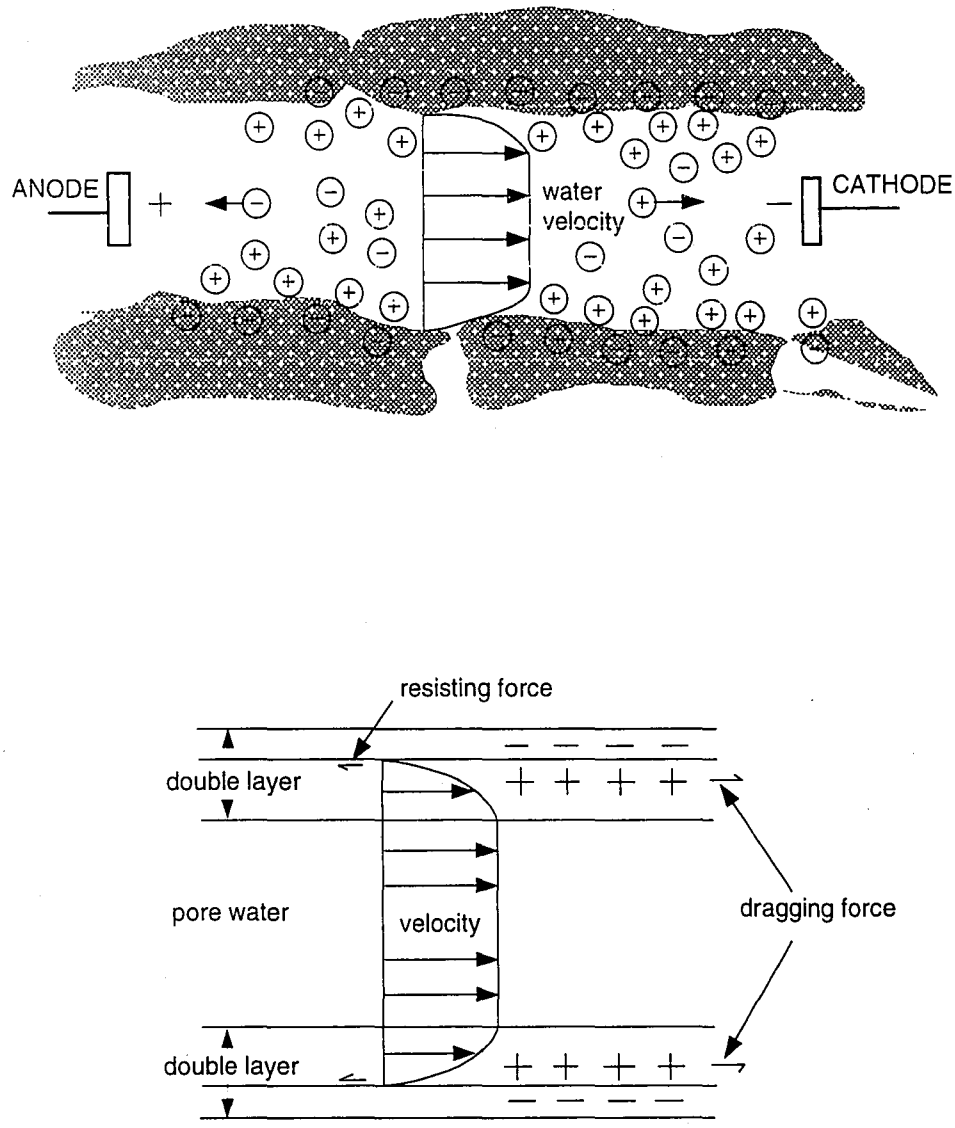

Figure 3.3 Schematic Diagram of Electroosmotic Flow in Microscopic View (After Probstein 1989)

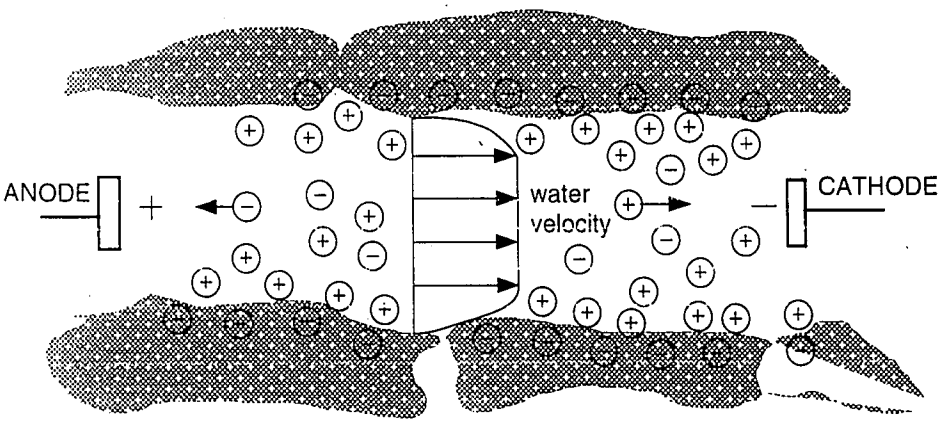

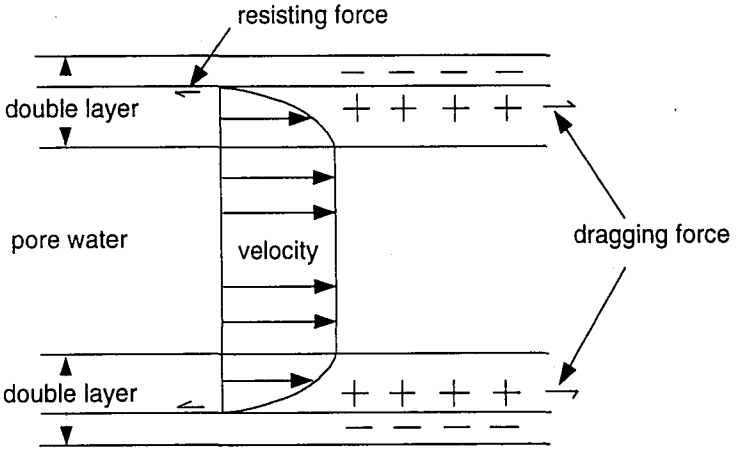

Figure 3.3 Schematic Diagram of Electroosmotic Flow in Microscopic View (After Probstein 1989)

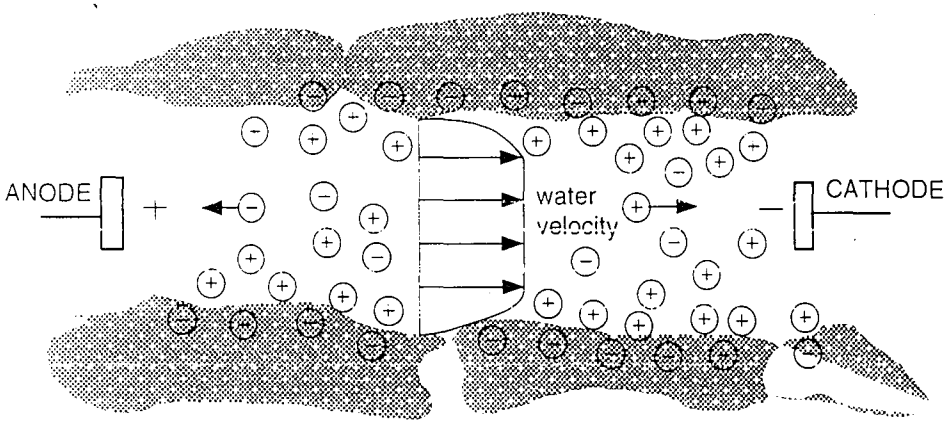

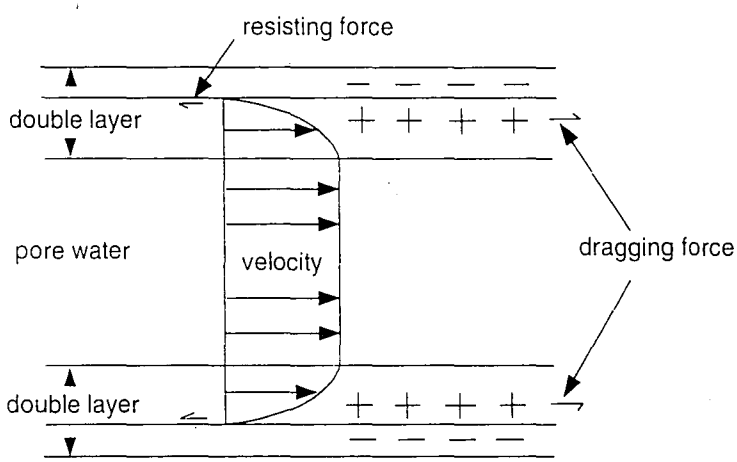

Figure 3.3 Schematic Diagram of Electroosmotic Flow in Microscopic View (After Probstein 1989)

This results in reduction of pH at the anode site and increase of pH at cathode site. We should consider these electrolysis reactions at electrodes together with the mass flux of species in the electric field. Since the mobility of the hydrogen under electrical field is about two times the hydroxyl ion mobility, hydrogen can dominate over hydroxyl ion in the system (Acar and Alshawabkeh, 1993). So in unenhanced electrokinetic remediation, an acid front will be formed and flush through the soil sample. The hydrogens meet the hydroxyl ions close to the cathode compartment, generating water within that zone (Figure 3.4).

The sweep of the acid front across the soil mass has brought many influences to the decontamination process. This pH gradient developed from anode to cathode may assist in desorption of the cationic species concentrated on the soil surface. It also causes the ionic conductivity to decrease significantly. A high pH at cathode end causes soluble contaminants to precipitate out of solution as hydroxide salts in the soil pores approach the interface of soil and electrode water. This can be prevented by using solubility enhancement and conditioning schemes.

Hydrogen transports to the cathode, carrying water and contaminants with, changing physical and chemical properties of the soil particles, pore fluids, and metal ions. This composes the basis of electrokinetic processing. If a suitable pH condition can be maintained throughout the soil sample, so that metals remain in solubilized condition and the soil affinity for these metals is low, then a higher degree of contaminant removal could be reached.

3.2.3 pH and Redox Potential

Redox potential refers to the reduction and oxidation reaction capacity. Redox potential of an ion is directly or indirectly influenced by local electrical field strength, ion

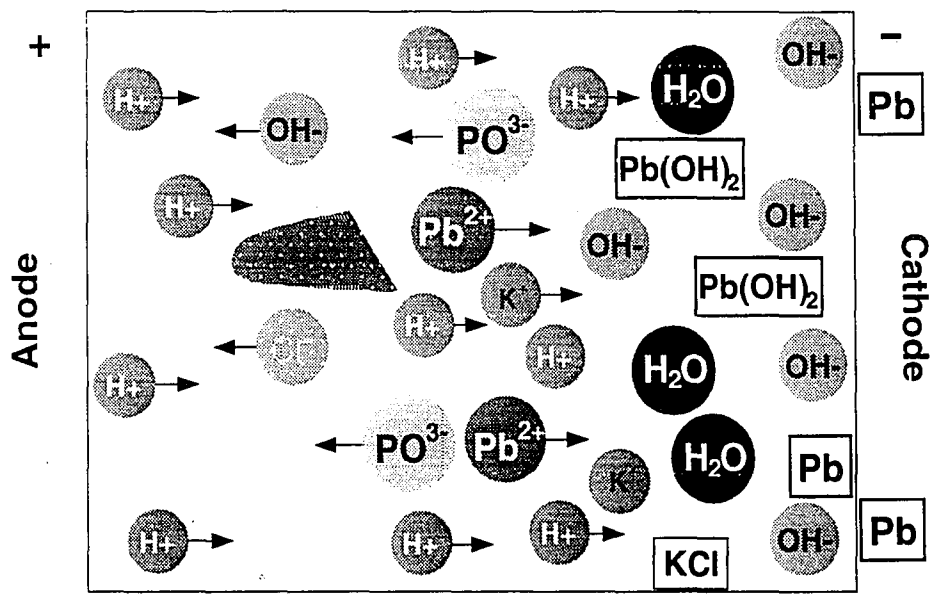

Figure 3.4 Migration of H+/OH- Through Soil Under An Electrical Field, with Existence of Other Ions. (Following Acar et al. 1995)

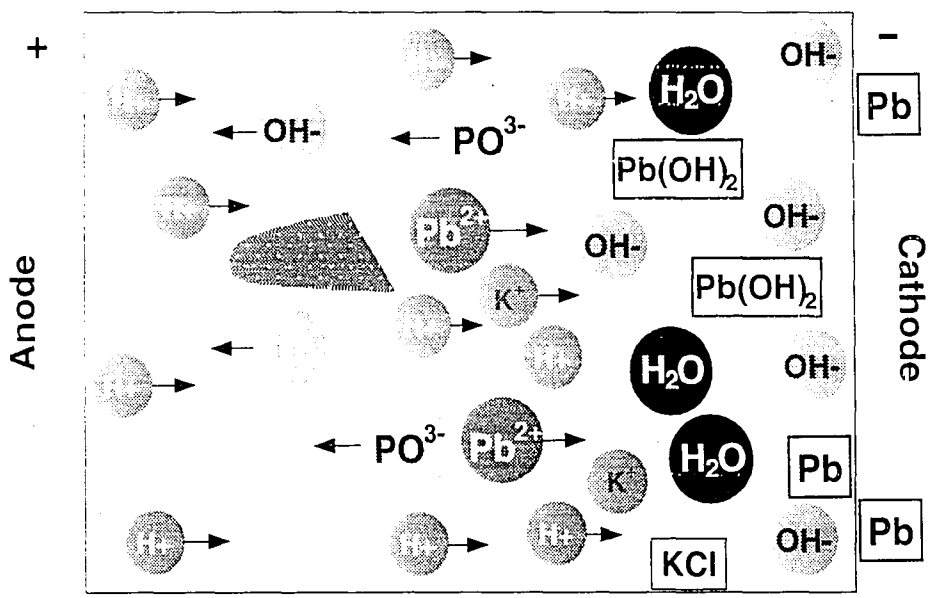

Figure 3.4 Migration of H+/OH- Through Soil Under An Electrical Field, with Existence of Other Ions. (Following Acar et al. 1995)

concentration, and pH environment in the pore fluid. The pH-redox conditions at any point during the treatment would determine the solubility and speciation of most heavy metal constituents. These conditions may limit or enhance the movement of the metals to an electrode site. Building a relationship between redox potential and metal speciation is very helpful to determine the fate of metal ions during an electrokinetic treatment.

3.2.4 Effect of Zeta Potential

We have defined zeta (ζ) potential as the electrical potential at the junction between the fixed and mobile parts of electrical double layer. ζ potential is influenced by the type and concentration of the electrolytes added to the particle suspension. ζ for clay soils is usually negative because of the net negative charge on clay particle surfaces. But it highly depends on pore fluid chemistry, i.e., hydrogen and hydroxyl ions are the potential determining ions, therefore lower pH will reduce ζ in magnitude for clays. At low enough pH, ζ may become positive. Hunter and James (1992) observed that adsorption of partially hydrolyzed metal cations such as Co^{2+}, Cd^{2+}, and Cu^{2+} cause ζ reversals for kaolinite. Figure 3.5 illustrates the relationship of ζ vs pH for kaolinite. As the concentration of hydrolyzable metal ions increases, ζ becomes more positive at low pH levels due to the increased cations. The double layer is compressed and the negatively charged surface is diminished. The effect is largest at an intermediate pH, slightly above which precipitation of metal hydroxide would be expected in the bulk solution.

Change of ζ potential will have a direct effect on the rate of electroosmotic flow. Electroosmotic permeability is influenced by the volume average of the zeta potential (Probstein and Hicks, 1993) (also see equation 4-18). Due to the influence of sorption of hydrolyzable metal ions, the sign reversal of zeta will make the electroosmotic flow not significant in soils with high concentration of heavy metals. In this case, and also for saline soils, electromigration becomes the dominant mechanism of decontamination.

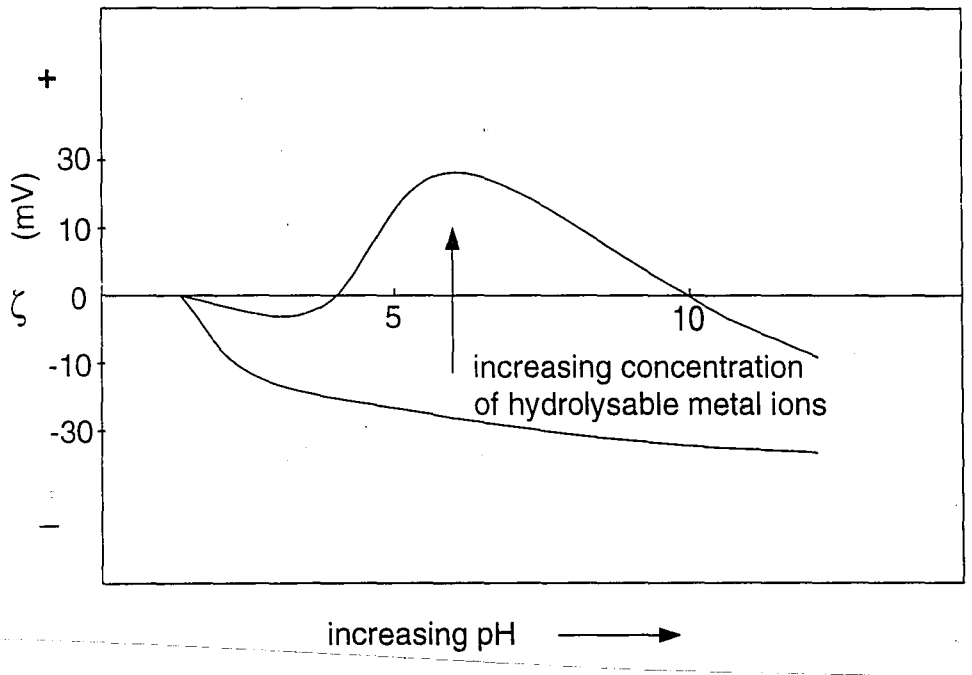

Figure 3.5 Schematic Illustration of The Zeta Potential Behavior of Kaolinite in The Presence and Absence of Hydrolysable Metal Ions (After West and Stewart 1995)

3.2.5 Enhancement and Conditioning

As we have discussed, there are various physical and chemical enhancement methods applicable to the electrokinetic process. A common approach is to inject chemical conditioners at the anode or the cathode. Low concentration acetic acid may be introduced at the anode and cathode to depolarize the cathode reaction. Acetic acid is environmentally safe and most acetate salts are soluble. Acar and Alshawabkeh (1993) gave a detailed explanation on why depolarizing both the cathode and anode reactions could benefit the E-K processing.

Generally, the objectives of chemical conditioners are to remove or avoid the precipitates in the cathode compartment, to slow down the increase of hydrogen ion concentration in the anode compartment, to increase solubility and desorption of metal ions, or to avoid the dissolution and release of silica, alumina, and heavy metals associated with the clay mineral sheets. In the latter case, the use of calcium hydroxide is proposed.

One other option is using chelating agents to complex the metal into a stable form. The complexing agent is expected to bond with the contaminant and prevent the ions from being adsorbed onto the surface of the soil particles. Probstein (1994) explored the use of EDTA in extracting zinc by E-K processing. Wittle and Pamukcu (1993) chose EDA (Ethylenediamine) as a chelating agent in their studies. They showed that the addition of EDA dramatically increased the current efficiency (volume of flow / quantity of electricity) of the E-K process for metal decontamination. Surfactant treatment is often necessary for organic contaminants. Micelles may be an effective enhancement measure for the removal of polar organic compounds.

Physical enhancement is to increase the migration potential of contaminants by either increasing the temperature of the pore fluid (thermal enhancement) or applying low amplitude-high frequency shear or acoustic waves through the soil sample (wave

enhancement). The first one aims to introduce a significant pore pressure quickly thus increase flow rate due to increased water pressure, and promote ion and organic dissolution. The second measure also causes a progressive increase in the pore water pressure, and, may possibly loosen contaminants that may be in the form of colloids or micelles away from the clay surfaces by the particle vibration imparted.

3.3 Other Pertinent Considerations

Physico-chemistry of particles and the chemical environment is important in the electrokinetic decontamination process. These properties, such as cation exchange capacity, surface charge density, zeta potential, and dielectric constant, are dependent on particle surface characteristics. Their combined influence to the efficiency of E-K processing is great yet a very complex one. Better understanding of these basic concepts is required to develop effective soil decontamination technology. We have discussed the pH and zeta potential before. Several other concerns are as the following.

3.3.1 Cation Exchange Capacity

Cation exchange capacity (CEC) is a measure of the degree of the isomorphous substitution. It is the basic phenomena in development of electric charges which affects the flocculation and dispersion process in the clay systems. Cations are attracted and held onto the surfaces and edges to preserve electrical neutrality. These cations can be replaced by cations of other type.

CEC is defined as the quantity of counter ions in the zone adjacent to the charged

surface that can be exchanged for other ions, always expressed as equivalent moles of exchangeable monovalent cations in milliequivalent (meq) per 100g of clay. CEC can be considered a material constant for a given clay. The existence of organic substances, soil particle size, and lattice distortion all affect the magnitude of the CEC. CEC for clay reduces with increasing acidity, increases with increasing ionic strength, and is higher in non-aqueous than in aqueous solvents (Ferris and Jepson, 1975). For strongly sorbed contaminants, decontamination is fast where concentration levels exceed the cation exchange capacity.

Holdridge (1966) studied the sorption of heavy metal cations by clay. Normal cation exchange reactions accounted for a limited proportion of the sorption, but preferential adsorption on the surfaces was responsible for the removal of cations from solution in excess of CEC of the clay.

3.3.2 Electrical Conductivity

The electrical conductance of a colloidal solution comes from the movement of charged colloidal particles and the ions present in the solution. According to Khan's (1991) modified theory of electroosmotic flow (Equation 2-2), the electrical conductivity of a soil can be split into two parts: conductivity of clay surfaces and conductivity of the pore water.

Migration of ions to the electrodes with opposite charge is the basic phenomena when a DC current is added to a soil. The bulk conductivity of soil is dependent on concentration and mobility of the ions present. Increasing electrolyte concentration will increase the electrical conductivity, thus for a constant current, the electrical potential differences will decrease, so will the electrokinetic flow.

Due to electrolysis reactions, the electrolyte concentration inside a porous medium

will rise during the E-K process, resulting in increased conductivity in the vicinity of the anode. Hydrogen ions transfer towards the cathode saturate both the pore fluid and the double layer within the zone close the anode. When the cathode compartment is approached, H+ and other cationic species meet the OH- and form water and precipitation, decreasing the bulk and pore fluid conductivity near the cathode. As a consequence of lower conductivity, the electric gradients within this zone will increase. This will decrease the efficiency of the E-K processing. This effect may be minimized by controlling the electrode chemistry.

3.3.3 Dielectric Constant

Based on the electrical double-layer theory, a shift of ions within the diffuse layer by an external electrical field would result in a dielectric dispersion. Counterions on the surface of the highly charged colloidal particle are strongly bounded by the electrostatic attraction, but ions in the diffuse layer can be moved by an external field, polarizing the ion atmosphere and producing an electric dipole moment of the particle.

In aqueous colloidal solutions, the presence of electrolyte may cause conductivity difference. Dielectric properties could be affected by electrolyte in two ways: the ions may associate and produce ion pairs; ions or their aggregates could influence the solvent's molecular interactions. Debye (1936) indicated that, in electrolytes, very intense fields would be set up around small size ions.

Suspensions of colloidal particles in aqueous electrolyte solutions usually have high dielectric constants at low electro-magnetic frequencies. Low frequency dielectric dispersion is due to the relaxation of double layer polarization. And, low frequency dielectric constant of suspensions is strongly dependent on the zeta potential of the particles (Dukhin and Shilov, 1974). Dielectric constant of Na-mont-morillonite

suspensions responded well to the frequency, while the dilute suspension of kaolinite which is a non-swelling clay showed no dielectric enhancement according to the research of Raythatha and Sen (1986).

Dielectric constant of the soil pore solutions is a key factor in determining both ionic mobilities and electroosmotic permeabilities. Electroosmotic velocity is positively proportional to the value of the dielectric constant as shown in equation 4-17. When an ion is present in a solution at limited concentration (not a dilution), it would be influenced by its dielectric diffusion. Its mobility is thus connected with the dielectric constant. The influence of the dielectric constant toward the equivalent ionic mobility is described in equation 4-12.

CHAPTER 4
THEORETICAL DEVELOPMENT OF THE ELECTROKINETIC TRANSPORT MODEL

4.1 A Brief Overview

4.1.1 Introduction

Electrokinetic decontamination experiments may be a time-consuming process, especially when it is applied to a fine grained soil. While bench-scale experiments help us get first-hand data, it is not effective enough to prove that the electrokinetic (E-K) technology is suitable for field application. Often due to the complexity of the contaminating compounds and the lack of funds, we may not be able to conduct pilot scale tests as many as necessary. Actually, very few large-scale field tests have been done or currently are undertaken. This leaves the technology not convincing enough to the industry.

Laboratory observations help to understand better the process. We can thus draw principles out of so much information, transfer the physical process into a mathematical model, using mathematical language to describe the coupled flow, ion migration and other processes affecting the transport. A mathematical model upgrades our understanding of the E-K processing from direct observation to the general principles. This transport model may help us predict the efficiency of the electrokinetic remediation to a specific ion, in a specific soil. Ultimately, we can change parameters to see its effects on the process. The simulation may be comparable to controlled laboratory test data but obtained far more quickly and less expensively. Ultimately the transport model and the laboratory experiment should support each other.

Modeling coupled transport of fluid, charge, and chemically reactive species is a complex task. Most of the current work is based on a generally accepted transient coupled flux equation, which maintains conservation of mass and energy. Similar partial differential equations have been successfully applied to solve solute transport equations in groundwater simulation due to chemical and hydraulic gradients (Lafolie and Hayot 1993; Moldrup et al. 1992; Leij et al. 1991). Transport models which incorporate electric gradient together with those chemical and hydrochemical factors are very limited (Alshawabkeh and Acar, 1996).

4.1.2 Previous Studies

In recent years, several researchers studied and proposed their theoretical modeling of conduction phenomena under electric field. In most cases, dilute solutions, rapid dissociation-association chemical reactions, and small double layer thickness are assumed. They are all constructed on the second-order differential advection-dispersion equations, while addressing their understanding and concerns toward the process.

Shapiro et al. (1989) and Shapiro and Probstein (1993) presented a general model of electroosmosis. They set up a group of convective diffusion equations with chemical reactions to characterize the transient behavior of concentration fields for a set of chemical species in solution that are transported by convection, migration, and diffusion in an electric field. A steady state electroosmotic flux is assumed by averaging the electrical gradient and zeta potential across the soil sample. In their report in 1993, the results were compared with experiment data for the case of constant voltage at the boundaries, and the comparisons showed a good agreement only in one case of acetic acid removal from a kaolinite specimen. The second experiment data did not show good agreement with model results. Their model did not consider or solve the preservation equation of the electric charge, nor did it account for any sorption reactions.

Acar et al. (1989) proposed their model to describe the single specie migration, i.e., hydrogen transport and pH gradient development, under constant boundary pH values and in a constant electric field. This model provided good qualitative correlation when compared to experiment data. However, the electrical field change was neglected, and the chemical reactions associated with the process were not incorporated either.

Yeung (1990) and Mitchell and Yeung (1991) also built a one-dimensional model for transport of contaminants through a liner in their study of using electrical gradients to retard migration of contamination across earthen barriers. Applying the integral finite difference method, the model reasonably predicted the transport of sodium and chloride ions across the liner. Still, a constant electrical gradient was assumed, and chemical reactions and electrode chemistry were neglected.

Denisov et al. (1996) gave an analytical solution to a more comprehensive one dimensional model, which considered electro-neutrality, changed electrical field, and actually was the first published multi-species modeling for the prevailing mechanism of E-K processing. But it was only aiming to draw a conceptual picture for the whole process. In order to obtain an analytical solution, the model was simplified to keep the electromigration term only, which they stated to be the most important driving force for charged species quantitatively and qualitatively. A ternary system consisting of two cations and one anion was studied, where the porous specimen had a planar geometry and was practically uncharged and chemically inert so as to avoid the influence of electro-osmosis and adsorption of the species. Advection and chemical reactions were neglected. Constant boundary conditions were assumed for each species.

The derived analytical expressions which describe the variation in the medium conductivity were beneficial. The solution offered a way of understanding the E-K processing conceptually. Though their solution was said to be consistent with their experimental results, doubts remain if that is also the case for a medium other than saturated sand which was used in their comparative tests.

Most recently, Alshawabkeh and Acar (1996) modified their previous model by

adding in the factor of metal precipitation, pore pressure development, and introducing a changing electric field. An equation for consolidation process is also included to reflect the influence of changing pore water pressure and the suction that resulted during the process.

This is a fairly good model which has incorporated a few more of the considerations of the process. The changing electric field is said to be considered, but since the model prediction for changing electrical field does not quite agree with the experimental results, the solution scheme remains questionable. A constant electric current is applied through the sample, which is easier to be implemented numerically but usually not the case for practical operation which often uses constant electrical voltage at both ends. Electro-migration mobility in dilute solution is used directly without considering the effect of limited concentrations in pore fluids. A mixed coefficient is selected from the test data to justify the model predictions due to its failure to investigate the relationship between migration mobilities and solute concentration.

4.2 Basic Assumptions

Electrokinetic soil processing is influenced by many factors such as soil mineralogy, surface chemistry, electrochemistry, pH of the pore solution, electrolysis reactions, and physical characteristics of the porous medium. This complexity of the process greatly increases the difficulty to illustrate it using mathematical language. A relatively simplified situation would allow us to reach a satisfactory result with less effort, after all a theoretical solution may not exist under the real conditions.

Following assumptions are employed in this study:

1. Soil medium is isotropic and saturated.
2. Electrical capacitance of the soil is equal to zero everywhere.

3. Typical clayey soil with negatively charged surface and very low hydraulic conductivity is used.
4. Electricity is conducted by the pore fluids and migrating ions only.
5. Isothermal conditions, under constant room temperature.
6. Instant chemical reactions are assumed.

Some of these assumptions were made due to the limited understanding of the effect of the considered factor. For example, a thermal gradient generated during the process may cause some influences to ion transport, and needs to be studied.

4.3 General Governing Equations

As we have discussed above, the basic governing equation for electrokinetic enhanced transport is the advection-diffusion equation. This means, advection (or convection) and diffusion constitute major driving forces for the movement of charged ions. According to their definition, dispersion refers to the movement of species under influence of gradient of chemical potential, i.e., a concentration gradient, which is the most basic thermo-dynamic phenomena in all mass transport processes. While advection is the stirring or hydro-dynamic transport caused by density gradient or forced convection. In our case, the influence of electric field which is the migration of charged species is included in the advection part.

In this chapter, we first introduce the basic equations for mass transfer in aqueous systems. Then, considering the case of electrokinetic processing in porous medium, the basic transient partial differential equation is modified and developed into the governing equation for the proposed modeling. Finally, chemical reactions and boundary conditions are discussed and the complete set of equations are built up for numerical implementation.

4.3.1 Fick's Law of Diffusion

Adolf Eugen Fick first developed the laws of diffusion by means of analogies with Fourier's work (Fourier, 1822), based upon his basic hypothesis (Fick, 1855). He found that the flux is proportional to the concentration gradient. Fick defined a total one-dimensional flux J(x,t) to represent the number of moles of the specie that pass a given cross area normal to the axis of diffusion. This well-known Fick's first law reads as:

$$J(x,t) = -D\frac{\partial c(x,t)}{\partial x} \qquad [4\text{-}1]$$

Where

c = concentration, $[ML^{-3}]$;

x = distance, [L] ;

t = time, [T] ;

The quantity D was defined by Fick as the diffusion constant with units of $[L^2T^{-1}]$.

Fick's second law of diffusion, a basic equation for one-dimensional unsteady-state diffusion, describes the change of concentration with time.

$$\frac{\partial c(x,t)}{\partial t} = -\nabla \cdot J(x,t) = D\frac{\partial^2 c(x,t)}{\partial x^2} \qquad [4\text{-}2]$$

The flux equation implies no convection, yet it is a special case of mass transfer.

4.3.2 The Nernst-Planck Equation

A general one-dimensional transfer to an electrode is governed by Nernst-Planck equation:

$$J_i(x) = -D_i^* \frac{\partial c_i(x)}{\partial x} - \frac{z_i F}{RT} D_i^* c_i \frac{\partial \phi(x)}{\partial x} + c_i v(x) \qquad [4\text{-}3]$$

where

J_i = total flux of species *i*, $[MT^{-1}L^{-2}]$;

D_i^* = effective diffusion coefficient of species *i*, $[L^2T^{-1}]$;

c_i = concentration of species, $[ML^{-3}]$;

z_i = charge of species ;

$\phi(x)$ = electric potential at point x, [V] ;

$v(x)$ = advection velocity, $[LT^{-1}]$;

R = universal gas constant, 8.3144 J/K mol ;

T = absolute temperature, [K] ;

F = Faraday constant, 96,485 C/mol electrons ;

In this equation, $\partial c_i(x)/\partial x$ defines concentration gradient, and $\partial \phi(x)/\partial x$ takes care of the potential gradient. The minus sign arises because the direction of flux opposes the direction of increasing c_i and ϕ.

The flux J_i, according to its definition, is equivalent to a current density which is defined as the flow rate of electrons through a unit cross area ($CT^{-1}L^{-2}$). Relative contributions of diffusion and migration to the flux of a specie, and of the flux to the total current, differ at a given time for different locations in solution. Current i

$$i = i_d + i_m$$

where i_d is the current density due to diffusion and i_m is the current density due to migration. i_m and i_d may be in same or opposite direction, depending on the charge on the electro-active species.

According to Fick's second law,

$$\frac{\partial c_i(x)}{\partial t} = -\nabla J_i(x) \qquad [4\text{-}4]$$

we obtain

$$\frac{\partial c_i(x)}{\partial t} = D_i^* \frac{\partial^2 c_i(x)}{\partial x^2} + \frac{z_i F}{RT} D_i^* c_i(x) \frac{\partial^2 \phi(x)}{\partial x^2} + \frac{z_i F}{RT} D_i^* \frac{\partial c_i(x)}{\partial x} \frac{\partial \phi(x)}{\partial x} - v(x) \frac{\partial c_i(x)}{\partial x} \qquad [4\text{-}5]$$

Note, the last two terms in equation 4-5 can be combined into one advection term which includes both natural advection ($-v(x)\partial c_i(x)/\partial x$) and forced advection under electric field (the 3rd term).

$$\frac{\partial c_i(x)}{\partial t} = D_i^* \frac{\partial^2 c_i(x)}{\partial x^2} + \left[\frac{z_i F}{RT} D_i^* \frac{\partial \phi(x)}{\partial x} - v(x) \right] \frac{\partial c_i(x)}{\partial x} + \frac{z_i F}{RT} D_i^* c_i(x) \frac{\partial^2 \phi(x)}{\partial x^2} \qquad [4\text{-}6]$$

This basic mass transfer equation under electric field is a good start of our study. We will expand it in the electrokinetic case and finally lead to a mass transfer equation under electric field and in the porous medium.

4.3.3 Mass Conservation Equation in Porous Medium

For medium in which the transfer takes place other than aqueous medium, porosity is considered to be an important factor which immediately affect the actual amount of the mass at a given concentration and at a fixed point.

We thus modify 4-4 and 4-6 into the following form:

$$\frac{\partial n c_i(x)}{\partial t} = -\nabla \cdot J_i(x) \qquad [4\text{-}7]$$

where n is soil porosity with unit $[L^3 / L^3]$.

4.4 Theoretical Development

Modification of the one-dimensional Nernst-Planck mass transfer equation is discussed term by term and categorized according to different mass transport mechanism. This requires not only detailed investigation of the influences of different parameters, but also consideration of the laboratory test conditions. The prevailing factors, such as diffusion, electro-migration and electroosmotic flow, are given special emphasis.

4.4.1 Diffusion

Bear (1972) indicated that the mechanical dispersion is a significant mechanism in contaminant transport in groundwater because of relatively high hydraulic conductivity. Yet the molecular diffusion is primary that controls hydrodynamic dispersion in clayey soils due to low advective hydraulic flow.

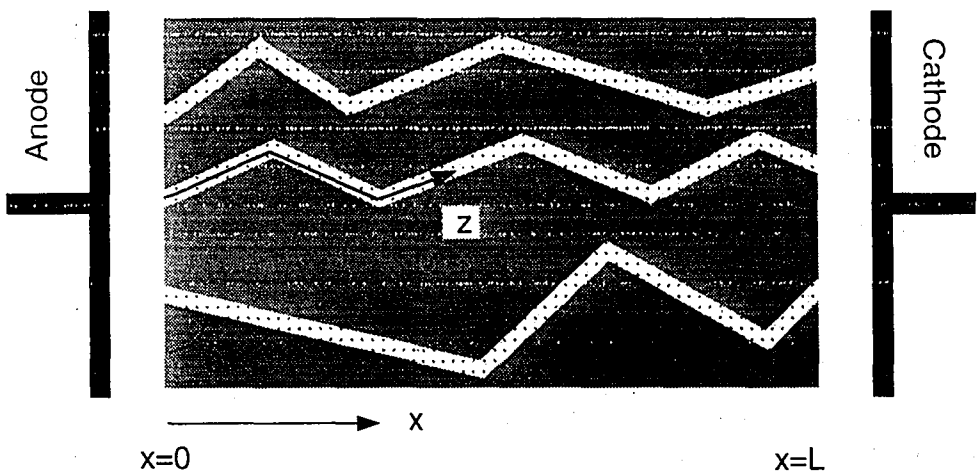

Figure 4.1 Tortuous Path in Porous Medium

In saturated soil, Fick's law of diffusion describes the diffusive mass transport of chemical species under chemical concentration gradient. Equation 4-1 and 4-2 serves as general rules for mass transfer by diffusion. Considering the effect of a longer capillary flow path through porous medium, a tortuosity factor γ is introduced. As described in Figure 4.1, the relation between axial coordinate of the straight circular capillary z and the porous medium coordinate x is given by

$$x = \frac{z}{\gamma}$$

The effective diffusion coefficient D^* is thus given by (Gillham and Cherry, 1982)

$$D^* = \frac{D}{\gamma^2} = D\tau \qquad [4\text{-}8]$$

where τ is called an empirical tortuosity factor of the soil. A summary of various values of τ for different soil types is given in Table 4.1 .

Diffusion coefficients for different ions in infinite dilute solution are given by several researchers. Tables 4.2 and 4.3 lists some of the values for typical anions and cations under ideal conditions. It should be noted that the diffusion coefficient (D) for solute in non-dilute solution is somehow a complex concept and is not a constant in a changing chemical environment (Cussler, 1984). For example, diffusion in concentrated solutions causes convection, the combination of convection and diffusion makes the analysis complicated. This convection should be handled with more complete form of Fick's law in calculating the diffusion coefficient, often including a reference velocity. Coupled concentration gradients in a multicomponent system are also changing the diffusion value. Yet finding how diffusion is related to chemical reaction is a difficult task. Few research data could be found for multicomponent diffusion at a given concentration.

The dilute limit is easier to understand and base upon the qualitative calculations. It is the basis of finding the influence of chemical reaction, dispersion, and mass transfer

Table 4.1 Representative Tortuosity Factors

Soil	Tracer	Saturation	τ
50% Sand:Bentonite Mixture	^{36}Cl	Saturated	0.08-0.12
Bentonite:Sand Mixture	^{36}Cl	Saturated	0.04-0.49
Bentonite:Sand Mixture	^{36}Cl	Saturated	0.59-0.84
Silt Loam	^{36}Cl	Unsaturated	0.05-0.55
Sand	^{36}Cl	Saturated	0.28
Loam	^{36}Cl	Saturated	0.36
Clay	^{36}Cl	Saturated	0.31
Clayey Till	Cl-	Saturated	0.15
Silty Clay	Cl-	Saturated	0.13-0.3
Silty Clay	Cl-	Saturated	0.1
Sandy Loam	Cl-	Unsaturated	0.21-0.35
Silty Clay Loam; Sandy Loam	Cl-	Saturated	0.08-0.22
Kaolinite	Cl-	Saturated	0.12-0.5
Smectite Clay	Cl-	Saturated	0.07-0.24
Clay	Cl-&SO_4^{2-}	Saturated	0.55
Silty Clay Loam; Sandy Loam	Br-	Saturated	0.19-0.3
Kaolinite	Br-	Saturated	0.15-0.42
Smectite Clay	Br-	Saturated	0.08
Sandy Loam	Br-	Saturated	0.25-0.35
Bentonite:Sand Mixture	^{3}H	Saturated	0.01-0.22
Bentonite:Sand Mixture	^{3}H	Saturated	0.33-0.7

Source: Shachelford and Daniel (1991)

coefficients, on diffusion coefficient.

4.4.2 The Convection Term

In Nernst-Planck equation, the convection term is composed of

$$v_{advection} = \frac{z_i F}{RT} D_i^* \frac{\partial \phi(x)}{\partial x} - v(x) \qquad [4\text{-}9]$$

It does not consider the effect of electroosmosis clearly.. In electrokinetic processing, the convection is composed by electromigration, electroosmosis, and advection due to Darcy's law, as described below.

4.4.2.1 Electromigration

Electromigration velocity measures ion movement in the pore water caused by electric field, as expressed in equation 4-9, at infinite dilute solutions

$$u_m = -\frac{zF}{RT} D^* \frac{\partial \phi}{\partial x} \qquad [4\text{-}10]$$

where u_m is the migration velocity with unit [L/T]

Define $v_{m,o} = zFD^*/RT$, then equation 4-10 can be simplified as

Table 4.2 Absolute Values of Diffusion Coefficients and Ionic Mobilities for Cations at Infinite Dilution at 25°C

Cation	$D_j x10^6$ cm^2/sec	$u_j x10^5$ $cm^2/V\ sec$		Cation	$D_j x10^6$ cm^2/sec	$u_j x10^5$ $cm^2/V\ sec$
Ag^+	16.48	61.9		La^{3+}	6.19	72.1
Al^{3+}	5.41	61.0		Li^+	10.29	40.1
Ba^{2+}	8.47	63.6		Mg^{2+}	7.06	55.0
Be^{2+}	5.99	46.6		Mn^{2+}	7.12	55.4
Ca^{2+}	7.92	61.7		NH_4^+	19.57	76.2
Cd^{2+}	7.19	56.0		$N_2H_5^+$	15.71	61.1
Ce^{3+}	6.20	72.5		Na^+	13.34	51.9
Co^{2+}	7.32	54.9		Nd^{3+}	6.16	72.1
$Co(NH_3)^{3+}_6$	9.04	103.6		Ni^{2+}	6.61	51.8
$Co(en)_3^{3+}$	6.63	77.4		Pb^{2+}	9.45	73.6
Cr^{3+}	5.95	-		Pr^{3+}	6.17	72.1
Cs^+	20.56	80.1		Ra^{2+}	8.89	69.2
Cu^{2+}	7.14	57.0		Rb^+	20.72	80.6
Dy^{3+}	5.82	68.1		Sc^{3+}	5.74	67.0
Er^{3+}	5.85	68.4		Sm^{3+}	6.08	71.0
Eu^{3+}	6.02	70.4		Sr^{2+}	7.91	61.6
Fe^{2+}	7.19	56.0		Tl^+	19.89	78.8
Fe^{3+}	6.04	70.5		Tm^{3+}	5.81	67.9
Gd^{3+}	5.97	69.8		UO_2^{2+}	4.26	33.2
H^+	93.11	362.5		Y^{3+}	5.5	64.2
Hg^{2+}	8.47	54.9		Yb^{3+}	5.82	67.6
Ho^{3+}	5.89	68.7		Zn^{2+}	7.03	54.7
K^+	19.57	76.2				

Source: Lide (1994)

Table 4.3 Absolute Values of Diffusion Coefficients and Ionic Mobilities for Anions at Infinite Dilution at 25°C

Anion	D_j x 10^6 cm^2/sec	u_j x10^5 cm^2/V sec		Anion	D_j x 10^6 cm^2/sec	u_j x 10^5 cm^2/V sec
$Au(CN)_2^-$	13.31	51.8		HS-	17.31	67.4
$Au(CN)_4^-$	9.59	37.3		HSO_3^-	13.31	51.8
$B(C_6H_5)_4^-$	5.59	21.8		HSO_4^-	13.31	51.8
Br-	20.80	80.9		$H_2SbO_4^-$	8.25	32.1
Br_3^-	11.45	44.6		I-	20.45	49.6
BrO_3^-	14.83	57.8		IO_3^-	10.78	42.0
Cl-	20.32	79.1		IO_4^-	14.51	56.5
ClO_2^-	13.85	53.9		$N(CN)_2^-$	14.51	56.5
ClO_3^-	17.2	66.9		NO_2^-	19.12	74.4
ClO_4^-	17.92	70.4		NO_3^-	19.02	74.0
CN-	20.77	80.8		$NH_2SO_3^-$	12.86	50.4
CO_3^{2-}	9.23	74.6		N_3^-	18.37	71.5
$Co(CN)_6^{3-}$	8.78	102.5		OCN-	17.20	66.9
CrO_4^{2-}	11.32	88.1		OH-	52.73	205.8
F-	14.75	56.4		PF_6^-	15.15	59.0
$Fe(CN)_6^{4-}$	7.35	115.0		PO_3F^{2-}	8.43	65.6
$Fe(CN)_2^{3-}$	8.96	104.7		PO_4^{3-}	6012	71.5
$H_2AsO_4^-$	9.05	35.2		$P_2O_7^{4-}$	6.39	84.3
HCO_3^-	11.85	46.1		$P_3O_9^{3-}$	7.42	86.6
HF_2^-	19.97	77.7		$P_3O_{10}^{3-}$	5.81	113.0
HPO_4^{2-}	4.39	59.1		ReO_4^-	14.62	56.7
$H_2PO_4^-$	8.79	34.2		SCN-	17.58	68.4
$H_2PO_2^-$	12.25	47.7		SeCN-	17.23	67.0

Source: Lide (1993)

$$u_m = -v_{m,o}\frac{\partial \phi}{\partial x} \qquad [4\text{-}11]$$

$v_{m,o}$ is usually called the ionic mobility [$L^2/T/Volt$].

From equation 4-11, clearly the electromigration velocity depends on the local electric field and differs for each species.

Equations 4-10 and 4-11 are valid for infinitely dilute solutions. In the pore fluids with finite concentrations, which is more close to E-K test situation, influence of inter-ionic attraction should be considered. This influence obviously increases with increasing ionic concentration, and thus lead to decrease of ion equivalent conductances with decrease in degree of ionization (Kortüm and Bockris, 1951).

Debye, Hückel and Onsager gave a quantitative formulation for ion mobility (Kortüm and Bockris, 1951), indicating the mobility of an ion in a binary salt is independent of the other ion in the salt. The result provides a theoretical basis for Kohlrausch's law of the independent migration of ions, according to which the equivalent conductance of an electrolyte is additively composed of mobilities of the constituent ions,

$$\Lambda_v = \Lambda_\infty - \left[\frac{8.205\cdot 10^5}{(\varepsilon T)^{3/2}} z^2 \Lambda_\infty + \frac{82.48\cdot z}{\mu\cdot(\varepsilon T)^{1/2}}\right]\sqrt{z\cdot n_e\cdot c} \qquad [4\text{-}12]$$

where Λ_v = equivalent conductance, [L^2 Ohm^{-1}] ;

Λ_∞ = equivalent conductance at infinite dilution, [L^2 Ohm^{-1}] ;

ε = dielectric constant ;

T = absolute temperature, [K] ;

μ = fluid viscosity, [$ML^{-1}T^{-1}$] ;

z = charge valency ;

n_e = electrochemical valency, i.e., for $CaCl_2$, z+ = 2, z- = 1, while $n_e = z+ \cdot 1 = z- \cdot 2 = 2$;

For a 1-1 valent salt, $z = n_e = 1$, define

$$\alpha = \frac{8.205 \cdot 10^5}{(\varepsilon T)^{3/2}} z^2$$

$$\beta = \frac{82.48\, z}{\mu \cdot (\varepsilon T)^{1/2}} \qquad [4\text{-}13]$$

Equation 4-12 is then rewritten as :

$$\Lambda_v = \Lambda_\infty - \left(\alpha \Lambda_\infty + \beta \right) \sqrt{c} \qquad [4\text{-}14]$$

Applying this equation to ionic mobility at finite concentration gives:

$$v_m = v_{m,o} - (\alpha v_{m,o} + \beta) c^{1/2} \qquad [4\text{-}15]$$

where $v_{m,o}$ is ionic mobility in infinite dilution as we defined before.

For aqueous solution at room temperature (T = 298K), using ε=78.56 and μ=0.008948, equation 4-15 becomes

$$v_m = v_{m,o} - (0.2289 v_{m,o} + 60.21) c^{1/2} \qquad [4\text{-}16]$$

Note, this is for 1,1-valent salt only. For $z_+(z_-) = 2$ or above, this equation should be modified from equation 4-12.

4.4.2.2 Electroosmosis and Electroosmotic Mobility

Electroosmosis velocity can be approximated by Helmholtz-Smoluchowski equation

$$u_{eo} = \frac{\varepsilon \zeta E}{\mu} \qquad [4\text{-}17]$$

where

ε = dielectric constant of pore solution

ζ = local zeta potential [V]

E = local electric field strength, $E=\partial\phi/\partial x$ [V/L]

μ = viscosity of pore solution [FTL^{-2}]

ε is the ratio of the permittivity of the pore solution over its permittivity in vacuum (~ 80 for water at 20°C). Viscosity of water at 20°C is about 10^{-3} kg/m·s. According to Shapiro and co-workers (1993), for a typical water-saturated clay, with ζ potential of 10mV, and an electric field strength of 100V/m, the electroosmotic velocity has a value of 10^{-6} m/s or ~10 cm/day. This is about at least 10 times lower than electromigration velocity (Acar and Alshwabkeh, 1993).

Since ζ potential is a local value and depends on local variables, its volume average at the local position is assumed (Shapiro and Probstein, 1993). Then,

$$v_{eo} = \frac{\varepsilon}{\mu} < \zeta \frac{\partial \phi}{\partial x} > \qquad [4\text{-}18]$$

where <> denotes the average of the scalar product.

By analogy to Darcy's formula, define k_e as the coefficient of electroosmotic permeability of the soil, we get

$$u_{eo} = k_e E \qquad k_e = \frac{\varepsilon \zeta}{\mu} \qquad [4\text{-}19]$$

k_e is considered a constant property of a specific soil in this equation. We have discussed that the zeta potential appearing in k_e expression is not a constant, but a variable depending on pH environment, electrolyte chemistry, and other factors. Contradictory conclusions about the variation of electroosmotic permeability for cohesive soils have appeared. Casagrande (1952) pointed out that electroosmotic permeability is a relatively constant value for different type of soils. However, Gray and Mitchell (1967) indicated that the electroosmotic permeability can vary considerably over a wide range of water contents and soil types. Hamed et al (1991) found that it changes during the course of a prolonged test. Conventionally, k_e is determined as the constant of proportionality between electrical potential gradient and flow rate. There is good qualitative agreement in the results of different studies.

In Khan's (1991) modified theory of electroosmotic flow through soil (see equation 2-2), the true electroosmotic flow is directly proportional to the current carried by the surface of the charged solid constituents of soil, which means that the electroosmotic velocity is directly related to the surface conductance of the soil particles. Hence, the E-O flow is independent of electrolyte concentration in the pore fluid.

Yin and co-workers (1995) backed up Khan's theory. They found that there is no apparent relationship between electroosmotic mobility and the applied electric field. The term, electroosmotic mobility, refers to the average velocity achieved by the pore water, relative to the solid skeleton, due to an externally applied electrical field of unit strength. The mobility appears to be proportional to the specific conductance of the soil specimen. Table 4.4 gives their results.

The mobile ions in the pore solution mainly come from the surface of the clay particles, so a higher ionic concentration and hence a higher conductance for a clay with

Table 4.4 Mobility Testing Data and Results

Specimen	Porosity	Sample Length cm	V[a] volts	I[b] mA	κ[c] m mho/cm	E[d] v/cm	Slope cm/s	Mobility ($x10^{-4}$) $cm^2/s \cdot v$
S1	0.59	1.34	3.5	46.4	0.41	2.54	0.0492	0.55
	0.59	1.34	2.35	30.4	0.40	1.75	0.0375	0.65
S2	0.44	3.01	1.06	21.8	1.40	0.35	0.0140	1.65
	0.44	3.01	1.08	21.8	1.38	0.36	0.0160	1.77
	0.37	2.69	1.58	21.8	0.84	0.58	0.0150	1.27
	0.37	2.69	1.54	21.8	0.86	0.57	0.0150	1.25
S3	0.61	2.04	2.65	17.3	0.30	1.30	0.0390	0.89
	0.61	2.04	2.81	17.3	0.28	1.38	0.0400	0.86
C1	0.58	1.85	5.65	33.6	0.25	3.05	0.0330	0.33
	0.58	1.85	1.86	10.4	0.24	1.01	0.0167	0.51
	0.58	1.85	5.91	43.8	0.32	3.19	0.0565	0.55
C2	0.58	2.33	2.95	21.7	0.39	1.27	0.0233	0.57
	0.58	2.33	2.82	21.5	0.40	1.21	0.0239	0.62
C3	0.58	2.05	2.60	23.6	0.42	1.27	0.0217	0.53
	0.58	2.05	2.55	23.8	0.43	1.24	0.0175	0.44
	0.58	2.05	2.80	24.1	0.40	1.37	0.0278	0.63

Note: [a]Voltage across specimen; [b]Current through the system;
[c]Specific conductance of the soil; [d]Electric field.

Source: Yin et al, 1995

a lower initial water content is expected. As shown in this table, specimen S2 has the lowest initial water contents and has the highest specific conductance and electroosmotic mobility.

Except S2, we can see that all other tests have a mobility value in the scope of 0.3-0.9x10^{-4} $cm^2/s \cdot volt$. Eight of them have a mobility around 0.6x10^{-4} $cm^2/s \cdot volt$. This shows that the mobility could be regarded as a relatively constant value in a low level electric field. For kaolinite, Yin et al concluded that mobility value of 0.6x10^{-4} $cm^2/s \cdot volt$ and κ=0.4m mho/cm are representative values. It should be noted that both the electroosmotic permeability (k_e) and the mobility could not be considered phenomonological constants.

4.4.2.3 Hydraulic Transport Velocity

Flux due to hydraulic gradient is given by Darcy's law

$$v_h = k_h \frac{\partial h}{\partial x} \qquad [4\text{-}20]$$

where

k_h = hydraulic conductivity of the soil [LT^{-1}]

h = hydraulic head [L]

Numerous methods exist for evaluating the hydraulic conductivity of fine-grained soils. Extensive research indicates that the microstructure and soil fabric influence the fluid transport in fine-grained soils. Dispersed micro-structure results in lower hydraulic conductivity than flocculated micro-structure (Mitchell et al. 1965).

In equation 4-9, the hydraulic convection is included as a contributory factor to

the advection velocity. This reflects the net flow theoretically. But the extend of contribution from the hydraulic flow should be examined thoroughly.

For kaolinite, a typical fine-grained soil used in electrokinetic remediation tests, the hydraulic conductivity is fairly low, and thus the flow rate resulting from the hydraulic flow is only a tiny portion of that generated by electroosmosis. In bench-scale experiments, hydraulic head is usually less than 2, while the electric gradient is about 100 volts/m. Comparing the coefficient of permeability (5.0×10^{-7} cm/s for hydraulic in clay, 5×10^{-5} $cm^2/s \cdot v$ for electroosmotic), we clearly see that the hydraulic flow in the electrokinetic processing may be negligible. Further more, the electrokinetic soil remediation continuously changes soil fabric, pore fluid chemistry, and diffuse double layer and thus changes the hydraulic conductivity.

Neglecting Darcy's advection in our numerical modeling will simplify the equations and avoid the complex solution process without losing accuracy. Yet this is not saying that the hydraulic flow is of no influence to the processing. Because of the low hydraulic permeability, the electroosmotic flow results in insufficient water flow. A negative pore water pressure (suction) is developed to compensate the flux. This suction value depends on the ratio of permeabilities (k_e/k_h). The higher this ratio, the higher the suction. This will balance the electroosmotic flow and decrease the net water flow. This effect may actually be included in experimental k_e values for fine grained soils.

4.4.3 Fluid Flux

Fluid flux is an important phenomenon during electrokinetic processing. It is caused by hydraulic gradient and electric gradient. As we have discussed above, the hydraulic gradient is very small and is neglected. So the total fluid flux is only composed of flow caused by electroosmosis. The total fluid flux, J_w, is thus

$$J_w = -k_e \frac{\partial \phi}{\partial x} \qquad [4\text{-}21]$$

This expression will be useful later when we study the flux boundary conditions.

4.4.4 Charge Flux

Charged ion migration between the electrodes under an electric field forms the observable electric current, which is the direct measurement of the ion movement. A basic assumption is that there are interconnected flow channels through the soil medium to make it possible for the charge flow between the electrodes. As we discussed in section 4.3.2, the charge flux has two parts: flux that is introduced by diffusional flow and flux that is caused by migration flow. The path for charge flux might be soil solids, diffuse double layer, pore fluid, and their interface. Contribution of these paths vary for different soil media and electrolytes. To simplify the analysis, we will not consider the path of soil solids for charge transport.

4.4.4.1 Diffusional Charge Flux

The diffusional charge flux or current, according to Faraday's law for equivalence of mass flux and charge flux, can be obtained from the diffusional mass flux. From equation 4-1

$$i_{diff} = -\sum_{j=1}^{N_{species}} z_j F D_j \frac{\partial c_j(x)}{\partial x} \qquad [4\text{-}22]$$

where $N_{species}$ is the total number of ion species present in the solution.

4.4.4.2 Migrational Charge Flux

The mass transport due to migration includes both the direct migration and also the ion migration carried by fluid flux.

The advection on flux, from equation 4-21, leads to

$$i_{adv} = \sum_{j=1}^{N_{species}} z_j F c_j J_w \qquad [4\text{-}23]$$

where i_{adv} is the charge flux due to advection.

Since J_w is a constant for any species in a given time and given location, and, required by electrical neutrality, we have,

$$\sum_{j=1}^{N_{species}} z_j c_j = 0 \qquad [4\text{-}24]$$

so, there is no net charge flow due to the advection of fluid ($i_{adv} = 0$).

From equations 4-11, applying Faraday's law, we get

$$i_e = \sum_{j=1}^{N_{species}} z_j F u_j^* c_j \qquad [4\text{-}25]$$

where i_e is charge flux due to direct ionic migration, u_j^* is the effective ionic migration velocity of species j which is given in equation 4-10.

If we define σ^* as effective electric conductivity of the porous medium, which equals

$$\sigma^* = \sum_{j=1}^{N_{species}} z_j F v_m{}^j c_j \qquad [4\text{-}26]$$

where $v_m{}^j$ is the effective ionic mobility of species j. Referring to equations 4-11 and 4-16, then 4-25 can be written as

$$i_e = -\sigma^* \frac{\partial \phi}{\partial x} \qquad [4\text{-}27]$$

where ϕ is electric potential.

4.4.4.3 Local Electric Current

Resulting from the above charge flux, the electric current at a given point can be obtained through

$$\begin{aligned} i &= i_e + i_{diff} \\ &= -F \sum_{j=1}^{N_{species}} z_j D_j \frac{\partial c_j}{\partial x} + \sigma^* E \end{aligned} \qquad [4\text{-}28]$$

where $E = -\partial\phi/\partial x$, noted as local electric field strength.

Since we have assumed zero electrical capacitance for the soil, the electric current should be a constant along the specimen.

4.5 Chemical Reactions

When the mass transferred through the soil is reactive chemical species, usually several chemical reactions will happen: the sorption and desorption reactions, aqueous phase reactions and precipitation/dissolution reactions. These reactions will change the concentration distribution, and thus will display in the governing equations. Simply, we can use a single term r(c) to represent the influence of reactions to the transport process. The reaction term, r, is expected to reflect a mixed effect of all those possible reactions. Contributions of different chemical reactions to the transport of one species vary depending on a lot of factors. Usually these factors include, but not limited to, the physico-chemical properties of the soil, the specific ion, chemical equilibrium in the pore fluid, and ionic concentration. Since we have assumed that chemical reactions reach equilibrium very quickly, no chemical kinetics which will change the concentrations before they reach equilibrium will be considered. So we are able to analyze the influence of chemical reactions independently, taking them out of the transport process, which will simplify the numerical implementation. For example, we are able to deal with the reaction term, r, after each time step, after reaching instantaneous equilibrium, analyze and redistribute the concentration altered by reactions, and start the next time step of the transport.

4.5.1 Adsorption/Desorption

Adsorption attachment may be the result of one or a combination of electrostatic forces. These forces, according to Hamaker and Thompson (1972), could include van der Waals/London forces, hydrogen bonding, charge transfer, ligand exchange, ion exchange, direct and induced ion-dipole and dipole-dipole interactions, and chemi-sorption.

For clays, cation and other positively charged species are adsorbed on the negatively charged clay surfaces. This adsorption may be reversible through the process of desorption. Also, for those ions contained in the double-layer, electroosmotic flow can break their binding. In electrokinetic decontamination processing, acidification of the soil due to H+ ion generated by the anode electrolysis reaction is the fundamental mechanism that facilitates desorption of those adsorbed ions and species. Increase in H+ ion concentration (decrease in pH value) will result in desorption of cations. The adsorption/desorption capability somehow depends on the surface charge density of clay mineral, characteristics and concentration of cation species, and existence of organic matter and carbonates in the soil (Harter 1983, and Yong et al. 1990).

A one-dimensional mass transfer equation with sorption is shown in equation 4-29 (Freeze and Cherry, 1979)

$$\frac{\partial c}{\partial t} = -v_x \frac{\partial c}{\partial x} + D\frac{\partial^2 c}{\partial x^2} - \frac{\rho_b}{n}\frac{\partial q}{\partial t} \qquad [4\text{-}29]$$

where

ρ_b = solid phase(soil) density [M/L^3]

n = pore water fraction (porosity)

q = mass of chemical adsorbed normalized by mass of soil [M/M]

v_x = a combined velocity term [L/T]

D = diffusion coefficient [L^2/T]

There are several models to describe sorption of metal ions on soils. A linear relationship between the sorped concentration and the concentration in the aqueous phase

is adapted in this study. For linear equilibrium adsorption

$$\frac{\partial q}{\partial t} = \frac{\partial q}{\partial c}\frac{\partial c}{\partial t} = k_d \frac{\partial c}{\partial t} \qquad [4\text{-}30]$$

Substituting 4-30 into 4-29

$$\left[1 + \frac{\rho_b}{n} k_d\right]\frac{\partial c}{\partial t} = -v_x \frac{\partial c}{\partial x} + D\frac{\partial^2 c}{\partial x^2} \qquad [4\text{-}31]$$

$$r_f = 1 + \frac{\rho_b}{n} k_d \qquad [4\text{-}32]$$

where

k_d = partitioning coefficient [L^3/M]

r_f = retardation factor (dimensionless)

The retardation factor defines relative rate of transport of a nonsorped species to that of a sorped species, r_f = 1 for nonsorped species. It reflects the influence of adsorption toward the chemical front relative to the bulk flow. Of course, as we have discussed before, the retardation is closely related with pH of pore fluid. The effect is low in low pH soils which is often our situation when we are conducting electrokinetic soil restoration. Progress has been made recently in modeling the sorption process (Yeh and Tripathi 1989, Selim 1992). pH effect, redox reactions, ionic strength, etc. are being considered to give a more clear figure of sorption reaction.

4.5.2 Water Auto-Ionization and Species Production

Two types of reactions are observed: homogeneous chemical reactions which occur throughout the bulk of the fluid and heterogeneous electrochemical reactions occurring at electrodes.

The latter reactions have been discussed in Chapter 3. And because this kind of reactions will control the boundary conditions for hydrogen and hydroxyl ion transport, we will further study their effects and numerical expressions later.

The homogeneous reactions in the pore fluid itself are assumed to be fast dissociation-association reactions. A representative aqueous phase reaction is the water auto-ionization. Metal ions presented in the aqueous phase may tend to combine with others to produce precipitation. These processes are reversible, depending upon the pH, ionic concentration, ionic presence, etc.

These reactions involving water are:

$$H_2O \rightleftharpoons H^+ + OH^- \qquad [4\text{-}33a]$$

weak acids

$$HA_c \rightleftharpoons H^+ + A_c^- \qquad [4\text{-}33b]$$

and weak bases

$$BOH \rightleftharpoons B^+ + OH^- \qquad [4\text{-}33c]$$

where A_c^- and B^+ represent monovalent acid and base species respectively.

Shapiro et al.(1989) stated that the typical reaction time is usually less than 10^{-5} seconds, far quicker than the time scales associated with convection, diffusion, and electromigration. Saville and Palusinski (1986) assumed that the forward and reverse

reaction rates balance and thus the production rates maintain the solution at chemical equilibrium.

Production rates are determined by following chemical equilibrium constants for water, weak acids, and weak bases respectively. Where [ ] denotes concentration in mol/m^3.

$$K_{H_2O} = [H^+][OH^-] \qquad [4\text{-}34a]$$

$$K_a = \frac{[H^+][A_c^-]}{[HA_c]} \qquad [4\text{-}34b]$$

$$K_b = \frac{[B^+][OH^-]}{[BOH]} \qquad [4\text{-}34c]$$

4.6 The Modified Governing Equation - General Model

From the theoretical development discussed in this chapter, a modified governing equation which handles the transient multispecies transport under changing electric field is obtained. This governing equation, coupled with a set of supportive equations which describe the electric field, the current, the chemical reactions, and also the electrode reactions, forms the general mathematical system for the modeling of the multicomponent electrokinetic process. Only the one-dimensional partial differential equation for mass

transport of the general case is presented here. All other equations and analysis are studied later corresponding with specific ionic transport.

The differential equation is obtained from equation 4-6, 4-15, 4-19, and 4-32

$$\frac{\partial n c}{\partial t} = D^* \frac{\partial^2 c}{\partial x^2} - E[k_e + v_m]\frac{\partial c}{\partial x} - c[k_e + v_m]\frac{\partial E}{\partial x} + n r(c) \qquad [4\text{-}35]$$

where D^* = effective diffusion coefficient; $[L^2T^{-1}]$

k_e = effective electroosmosis mobility; $[L^2V^{-1}T^{-1}]$

v_m = effective electromigration mobility; $[L^2V^{-1}T^{-1}]$

E = electric field strength $-\partial\phi/\partial x$; $[VL^{-1}]$

r = the term of chemical reactions; $[MT^{-1}]$

With v_m as defined in Equation 4-15, equation 4-35 can be re-written as :

$$\frac{\partial n c}{\partial t} = D^*_{eff}\frac{\partial^2 c}{\partial x^2} - E\left\{k_e + [v_{m,o} - (\alpha v_{m,o} + \beta)c^{1/2}]\right\}\frac{\partial c}{\partial x} - c\left\{k_e + [v_{m,o} - (\alpha v_{m,o} + \beta)c^{1/2}]\right\}\frac{\partial E}{\partial x} + n r(c) \qquad [4\text{-}36]$$

The electric field in the above equation is calculated using current and the local electric conductivity. We will further study this in the next section.

Note that the above equation is directly constructed on a familiar mass transport equation. For a non-reactive particle passing through a porous medium without electrical field, the above equation is simplified to a diffusive solute transport equation. Since we have removed the hydraulic advection term due to the low hydraulic conductivity of clayey soil, there is no advection presence in the basic diffusive equation.

Equation 4-36 or 4-35 will be employed as the master one-dimensional transport equation in this study. For each participating species, one differential equation is applied. Therefore for N species in the system, we will generate N differential equations, plus boundary conditions, electric neutrality condition, and chemical reaction equations. These complicated equation systems will be developed on the selected multiple species concerned in this study.

Also note that the resulting equation 4-35 is an initial value question. We need both initial condition and two boundary conditions for solving this equation for each species. Initial conditions can be evaluated from initial concentration distribution and initial electrical potential distribution. Boundary conditions are more difficult to be generalized. They will be studied case by case.

4.7 Electric Field Distribution

Previous teams of modelers often assumed a constant electric field across the soil sample all through the processing to simplify their models. This assumption may be viable for the early stage of the process, but an oversimplification for later stages could lead to a erroneous understanding toward the nature of the E-K test.

Data from Lehigh researchers show that the electric field does change with time across the sample, as shown in Figure 4.2. A lower and flatter electrical field is observed near the anode side as experiment continues. Others recorded a steep increase of electrical field near the cathode side (Acar and Hamed 1992). Theoretically, when charged ions and particles move through the soil cylinder, the distribution of the charge concentration undergoes a continuous change, which results in the variance of local electric conductance. This will definitely result in electric field change.

Electric current i at any point due to charge flux was given in equation 4-28. Assuming we know the electric conductivity at any position along the specimen and at any time point, we should be able to find out the electrical field distribution.

From equation 4-28, relationship between E and i at time t can be written as

$$E(x) = \frac{i + F \sum_{j=1}^{N_{species}} z_j D_j^* \frac{\partial c_j}{\partial x}}{\sigma^*} \qquad [4\text{-}37]$$

where σ^* is defined in equation 4-26 as the effective electric conductivity. If current density i(t) is known from other calculation, 4-37 will give the electric field strength distribution at any time point t. Note, i(t) here is a space independent value since we have assumed that electrical capacitance is zero for the soil, which means:

$$\frac{\partial i(t)}{\partial x} = 0 \qquad [4\text{-}38]$$

In this case, a constant electrical voltage difference across the electrodes is maintained, so the following equation can be solved

$$\int_0^L E(x)\,dx = -\Delta\phi \qquad [4\text{-}39]$$

where $-\Delta\phi$ is the constant voltage difference with unit [Volt].

Insert 4-37 into 4-39, rearranging the integral, i(t) is obtained as

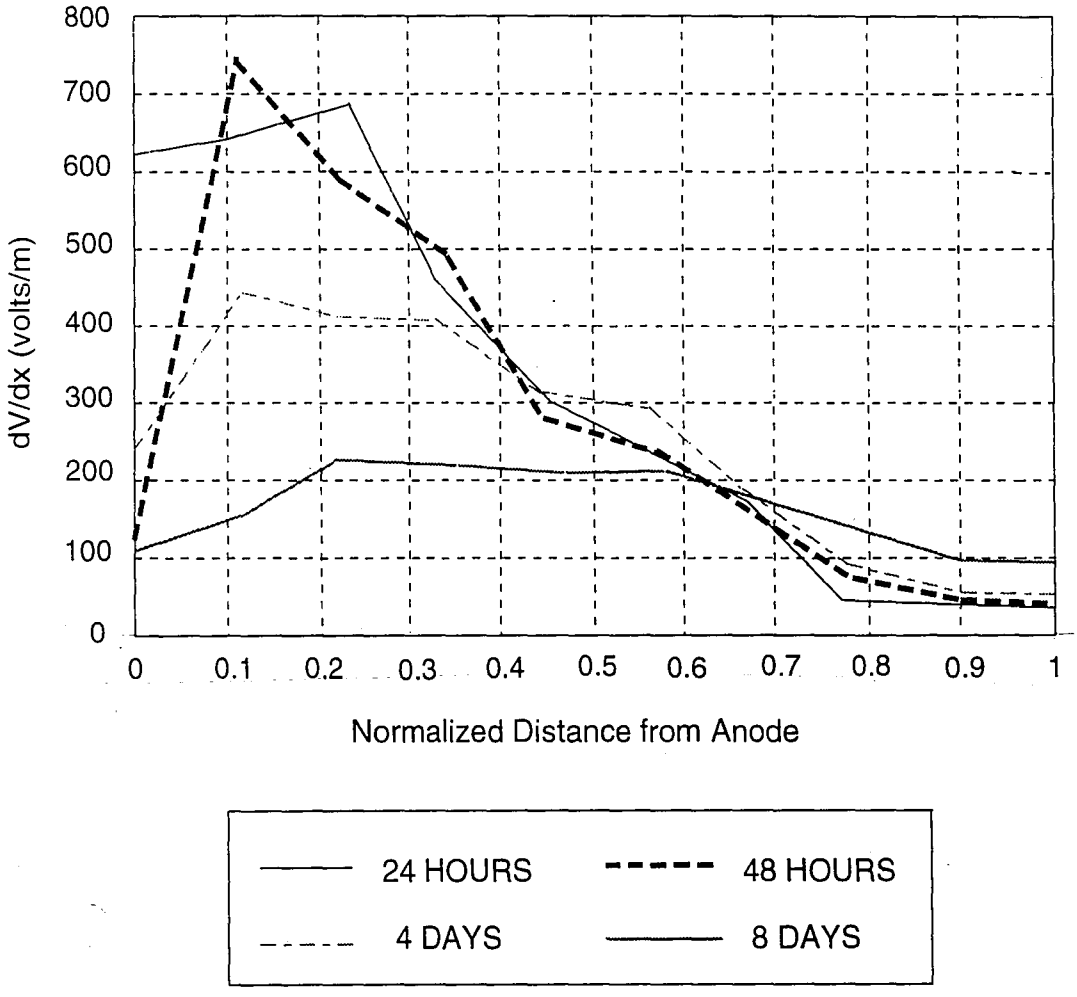

Source: Wittle and Pamukcu 1993

Figure 4.2 Voltage Gradients at Different Time Period for Strontium

$$i = -\frac{\Delta\phi + F\int_0^L \frac{\sum_1^N z_j D^*_j \frac{\partial c_j}{\partial x}}{\sigma^*} dx}{\int_0^L \frac{dx}{\sigma^*}} \qquad [4\text{-}40]$$

After *i* is calculated from above equation, then from 4-37 the field is ready to be evaluated. Note that equation 4-40 is actually seeking an average value of the current to avoid the error carried by a calculation at a single point as described in equation 4-28. If we look at the integral, assuming a relative stable average value for conductivity σ^*, we could have already found that the denominator is

$$\int_0^L \frac{1}{\sigma^*} dx = L\int_0^1 \frac{dz}{\sigma^*} = \frac{L}{\int_0^1 \sigma^* dz} = \frac{L}{\sigma^*_{avg}} \qquad [4\text{-}41]$$

where z is the normalized distance, $z \in [0, 1]$. σ^*_{avg} is the average value of conductivity through the specimen. In the numerator part, the big integral can also be simplified to

$$F\int_0^L \frac{\sum_1^N z_j D^*_j \frac{\partial c_j}{\partial x}}{\sigma^*} dx = \frac{FL}{\sigma^*_{avg}} \int_0^1 \sum_1^N z_j D^*_j \frac{\partial c_j}{\partial z} dz \qquad [4\text{-}42]$$

Insertion of 4-41 and 4-42 into 4-40 will give us a similar expression as equation 4-28.

$$i(t) = -F\int_0^1 \sum_1^N z_j D^*_j \frac{\partial c_j}{\partial z} dz + \sigma^*_{avg} E_0 \qquad [4\text{-}43]$$

where E_0 is the initial field strength.

The above equations 4-41, 4-42 and 4-43 are not valid if the soil conductivity value vary greatly. They are presented here just for comparison to help the understanding.

Note, from above theory development, we can see that, instead of using a constant voltage difference, we may use a constant current density as well. In that case, we do not need to solve 4-40. A direct use of 4-37 will give us the needed field value. Accordingly, no other term in this model need to be changed. Therefore this model is basically applicable to the case of constant current also.

4.8 Initial and Boundary Conditions

As we have mentioned in section 4.6, the general equation describing mass transport must have initial and boundary conditions to generate solution for this differential equation. Initial condition and two boundary conditions are necessary for each species present in the system. Initial conditions can be evaluated by the initial concentration distribution, potential distribution and other values so that an equilibrium state can be maintained at the starting point. Boundary conditions can be obtained through employing different equations which describe different flow status at the boundaries. Generally used boundary conditions are Neumann boundary conditions, Dirichlet boundary conditions, and mixed boundary conditions. When describing flow problems, a Neumann boundary is an insulated boundary (or impermeable boundary) which means there is no flux at the boundary, while a Dirichlet boundary indicates that the value of head (potential, concentration, etc.) is constant at the boundary.

Previous researches often used constant boundary conditions to simplify the

solution procedure. Such boundaries are not be able to describe the nature of the electrokinetic flow realistically. Due to the existence of flux at boundaries, i.e., caused by the electrode reactions and advection of fluid, flux boundary condition is more capable of describing electrokinetic flow status. Figure 4.3 gives an example that reflects the change of concentration at both boundaries due to the electrode reactions and flow condition. This is from data for Pb decontamination by electrokinetics (cited from Wittle and Pamukcu 1993).

A so-called third-type boundary condition is actually a mixed boundary condition. It was first studied by Brenner (1962) Kreft and Zuber (1978), and developed by Parker and Van Genuchten (1984). The boundary conditions applied at the inlet and outlet of the soil column must express the equality between the flux of solute applied at the inside of the column and the flux of solute at the immediate outside of the porous medium. In a one-dimensional solute transport model in porous media, the following boundary condition was used at the inlet (Lafolie and Hayot, 1993):

$$-D^{*}\frac{\partial c}{\partial x}+vc\,|_{x=0}=vc_{0}(t) \qquad [4\text{-}44]$$

where $c_0(t)$ is the concentration of the incoming solution. $c_0(t)$ is often a Dirac or step function.

The boundary condition at the outlet of the column is very similar to the inlet boundary. Assuming that diffusion and dispersion inside the exit reservoir are negligible and the concentration across the boundary is continuous, the outlet boundary becomes Neumann boundary:

$$\frac{\partial c}{\partial x}\,|_{x=L}=0 \qquad [4\text{-}45]$$

Notice that the velocity inside soil is different with that outside of the soil. Flux velocity outside of the soil caused by fluid flux J_w as defined in equation 4-21, and by

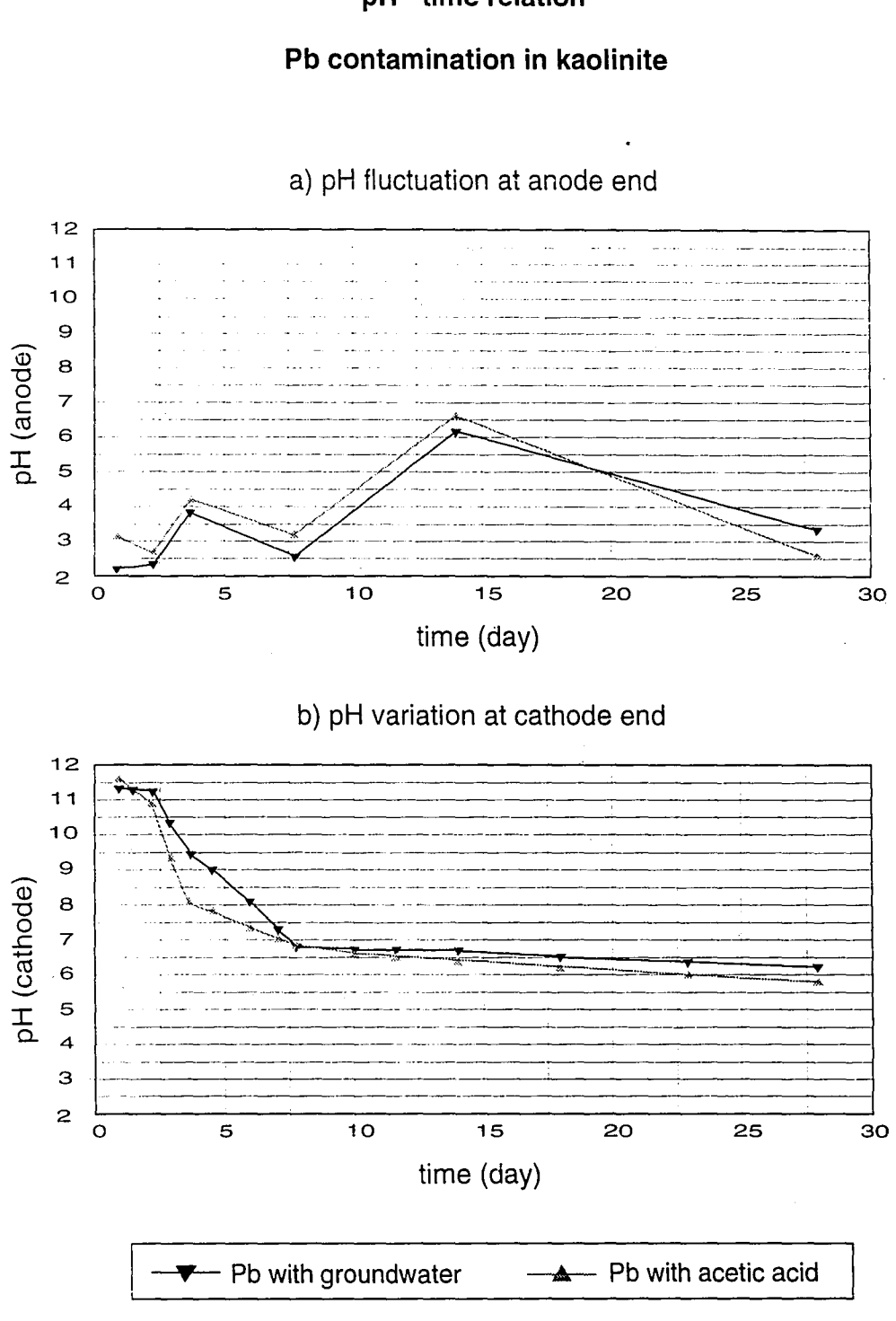

Figure 4.3 pH Changes at Boundaries Due to Flux and Electrolysis

electric current i

$$J\big|_{x=0^-} = J_w c_0\big|_{x=0^-} + \frac{i_j}{zF} \qquad [4\text{-}46a]$$

$$J\big|_{x=L^+} = J_w c\big|_{x=L^+} + \frac{i_j}{zF} \qquad [4\text{-}46b]$$

where i_j is the component of current density generated by the charge flux of species j. While inside the soil, this velocity is the migration velocity

$$v\big|_{x=0^+,x=L^-} = (k_e + v_m) E\big|_{x=0^+,x=L^-} \qquad [4\text{-}47]$$

So the boundary conditions are modified as

$$-D^* \frac{\partial c}{\partial x} + (k_e + v_m) Ec\big|_{x=0} = J\big|_{x=0} \qquad [4\text{-}48]$$

$$-D^* \frac{\partial c}{\partial x} + (k_e + v_m) Ec\big|_{x=L} = J\big|_{x=L} \qquad [4\text{-}49]$$

where J is defined in equation 4-46.

The above boundary condition can also be obtained by analyzing the equivalence of charge flux. Left side of equations 4-48 and 4-49 is actually the charge flux of species j at any position inside the soil column. It should be equal to the charge flux at the immediate outside of the soil column. This leads to the same expression of the boundary conditions as 4-48 and 4-49. The charge flux has been discussed in section 4.4.4.

The validity of boundary condition at outlet side (x=L) is questionable due to the assumption of continuity of the concentration across the boundary. However, according to Van Genuchten and Parker (1984), this assumption does not significantly affect the breakthrough curve when the column Peclet number P_e is high

$$P_e = \frac{vL}{D^*} > 20 \qquad [4\text{-}50]$$

where v = a combined velocity term

L = length of the specimen

which is always able to be maintained in the electrokinetic processing due to relatively high migration velocity.

CHAPTER 5
MODELING LEAD TRANSPORT

5.1 A Multi-Species Transport Process

We have developed a modified differential equation system in the previous chapter and claimed it capable of modeling complex electrokinetic-enhanced multi-species transport.

While we have discussed that heavy metal contamination is a widespread problem, lead plays a very important role among those metal contaminants, and it is the most frequently identified species in hazardous waste sites. Lead is chosen in this study to evaluate the developed theoretical model also because that a series of lead removal tests have been done by both Lehigh researchers (Pamukcu and Wittle 1992) and others (Hamed et al. 1991; Acar and Alshawabkeh 1996; Hsu et al. 1996). The validity of the model may then be established by comparing the model predictions and experimental data.

Various cations and anions may be present in soil pore fluid. The transport of hydrogen and hydroxyl ions is one of the dominant processes in electrokinetic remediation and must be included to describe the pH environment change. Pb(II) is the cation of our concern. NO_3^- is introduced due to the use of lead nitrate salt for preparing the solution. Only these four species are studied here.

Four one-dimesional partial differential equations are developed accordingly. Chemical reactions, including production of lead hydroxide, water auto-ionization and lead sorption, are described in a set of algebraic equations. Electrical potential, conductivity and field strength are evaluated using previously presented equations, depending upon

concentration distributions. Boundary conditions for those partial differential equations are developed from flow status at both ends of the specimen.

This formed an electrokinetic mass transport model for lead removal. The development of this multispecies transport model is described below step by step.

5.2 Acid/Base Distribution

As discussed before, the hydrogen/hydroxyl transport and the resulting acid/base environment change are the important features in electrokinetic process that need to be considered first. pH change influences the chemical reactions especially for heavy metal transport. Cation exchange capacity of the soil particle, sorption and desorption reactions, and chemical productions are all directly influenced by the pH environment in the soil.

Application of direct current to a saturated soil column always involves the electrode reactions which produces H^+ at anode due to oxidation and OH^- at cathode due to reduction of water. The generated concentration of H^+ and OH^- will move toward oppositely charged electrodes under the driving force of the applied electric field. This movement results in redistribution of pH along the specimen. More detailed description is presented in section 3.2.

The mass transport equation is implemented to describe the movement of H^+ and OH^-. Aqueous phase reactions involving these two ions such as water auto-ionization are expressed using algebraic equations presented in section 4.5.2. Boundary conditions for solving the partial differential equations are obtained from implementation of Equations 4-48 and 4-49.

5.2.1 H^+ Transport

The one-dimensional mass transport equation of hydrogen ion is

$$\frac{\partial n\, c_{H+}}{\partial t} = D^{*}_{H+}\frac{\partial^2 c_{H+}}{\partial x^2} - E[k_e + v_m^{H+}]\frac{\partial c_{H+}}{\partial x} - c_{H+}[k_e + v_m^{H+}]\frac{\partial E}{\partial x} - R_{H+} \qquad [5\text{-}1]$$

where R_{H+} is the reduction of H^+ through water auto-ionization reaction. This reaction is the only one concerned within this study involving hydrogen.

Boundary conditions for this equation are (for charge z=1):

1) At the anode

$$-D^{*}_{H+}\frac{\partial c_{H+}}{\partial x} + (k_e + v_m^{H+})Ec_{H+}\Big|_{x=0} = c_0^{H+}J_w + \frac{I}{F} \qquad [5\text{-}2]$$

where c_0^{H+} is the concentration of H^+ flow in from the anode, or say, the concentration in anode compartment.

Note in equation 5-2 the total current I replaces i_j in equation 4-46. Electrolysis reactions (electrode reactions) are assumed to only include the oxidation and reduction of water. Under this assumption, all current is expended in generation of hydroxyl at cathode. Therefore,

$$i_{H+}\Big|_{x=0} = I \qquad [5\text{-}3]$$

$$i_{OH-}\Big|_{x=L} = I \qquad [5\text{-}4]$$

2) At the cathode

$$-D^{*}_{H+}\frac{\partial c_{H+}}{\partial x}+(k_e+v_m^{H+})Ec_{H+}\Big|_{x=L}=c_{H+}J_w \qquad [5\text{-}5]$$

Note that, since continuous flux is assumed at cathode side (see discussion in section 4.8), the advective flux of H^+ into cathode compartment is the fluid flux multiplied by the concentration of H^+ in soil mass at x=L. This is different from that at the anode side which uses the concentration in anode compartment. The H^+ produced at the anode compartment is carried by the electroosmotic flow into soil. The advective flux carry the concentration into the soil and out into the cathode compartment. Therefore the use of different concentration at two boundaries is considered reasonable.

J_w is defined in equation 4-21.

5.2.2 OH^- Transport

The one-dimensional mass transport equation for OH^- is

$$\frac{\partial n\, c_{OH-}}{\partial t}=D^{*}_{OH-}\frac{\partial^2 c_{OH-}}{\partial x^2}-E\left[k_e+v_m^{OH-}\right]\frac{\partial c_{OH-}}{\partial x} \qquad [5\text{-}6]$$

$$-c_{OH-}\left[k_e+v_m^{OH-}\right]\frac{\partial E}{\partial x}-R^{a}_{OH-}-R^{p}_{OH-}$$

where R_{OH-}^{a} denotes the concentration of OH^- participating in water auto-ionization reaction , R_{OH-}^{p} represents the part that is consumed in reaction with lead.

Boundary conditions for OH^- transport are (for z=-1)

1) At the anode

$$-D^{*}_{OH-}\frac{\partial c_{OH-}}{\partial x}+(k_e+v^{OH-}_m)Ec_{OH-}\Big|_{x=0}=c^{OH-}_0 J_w \qquad [5\text{-}7]$$

where c_0^{OH-} is the concentration of OH^- in anode compartment.

2) At the cathode

$$-D^{*}_{OH-}\frac{\partial c_{OH-}}{\partial x}+(k_e+v^{OH-}_m)Ec_{OH-}\Big|_{x=L}=c_{OH-}J_w-\frac{I}{F} \qquad [5\text{-}8]$$

The term - I/F explains that all current is consumed in generation of negatively charged hydroxyl ions in cathode compartment.

5.2.3 Water Auto-Ionization

As given in equations 4-33a and 4-34a, the existence of hydrogen and hydroxyl ions in the solution must satisfy the equilibrium state. In the model, H^+ and OH^- transport independently which raises the importance of the incorporation of water auto-ionization reactions into the model to guarantee the equilibrium state of the two ions in the aqueous phase.

This reaction will generate or consume equal amount of hydrogen and hydroxyl ions which means:

$$R_{H+}=R^{a}_{OH-}=\Delta c \qquad [5\text{-}9]$$

where Δc is the part of hydrogen or hydroxyl ions which participate the reaction.

The equilibrium requires

$$c_{H+} c_{OH-} = K_w = 10^{-14} \qquad [5\text{-}10]$$

If we know the concentrations c_{H+} and c_{OH-}, it becomes easy to calculate Δc.

5.2.4 H^+ Retardation

Previous findings (Mitchell 1993; Yong et al. 1990; Alshawabkeh and Acar 1996) show that kaolinite has a low cation exchange capacity (about 0.01 mg/g) and low buffering capacity. It seems that retardation for H^+ transport may not be a significant phenomenon. However, according to Alshawabkeh (1994), due to the change of pH environment and thus the change of tortuosity factor and the presence of other species, there is significant influence of retardation to the transport of H^+. It is necessary to estimate a retardation factor for specific transport process to reflect this influence so that the model prediction is more reliable. A retardation factor can be obtained through experimental data (Alshawabkeh and Acar, 1996).

The one-dimensional differential equation for H^+ transport with retardation factor is given as

$$R_d \frac{\partial n c_{H+}}{\partial t} = D^*_{H+} \frac{\partial^2 c_{H+}}{\partial x^2} - E[k_e + v_m^{H+}] \frac{\partial c_{H+}}{\partial x} - c_{H+}[k_e + v_m^{H+}] \frac{\partial E}{\partial x} - R_{H+} \qquad [5\text{-}11]$$

where R_d is the retardation factor.

5.3 Pb(II) Transport

The one-dimensional mass transport equation for lead is

$$\frac{\partial n\, c_{Pb}}{\partial t} = D_{Pb}^{*} \frac{\partial^2 c_{Pb}}{\partial x^2} - E\left[k_e + v_m^{Pb}\right] \frac{\partial c_{Pb}}{\partial x} - c_{Pb}\left[k_e + v_m^{Pb}\right] \frac{\partial E}{\partial x} - R_{Pb}^{p} - R_{Pb}^{s} \qquad [5\text{-}12]$$

where R_{Pb}^{p} reflects the number of moles of lead precipitated, while R_{Pb}^{s} is due to the sorption/desorption of lead onto/from soil particles.

No electrode reaction was considered for Pb(II). Therefore boundary conditions for lead transport are set as:

1) At the anode

$$-D_{Pb}^{*} \frac{\partial c_{Pb}}{\partial x} + (k_e + v_m^{Pb}) E c_{Pb}\Big|_{x=0} = c_0^{Pb} J_w \qquad [5\text{-}13]$$

2) At the cathode

$$-D_{Pb}^{*} \frac{\partial c_{Pb}}{\partial x} + (k_e + v_m^{Pb}) E c_{Pb}\Big|_{x=L} = c^{Pb} J_w \qquad [5\text{-}14]$$

Note at all times that concentration of Pb(II) in anode compartment c_0^{Pb} remains zero.

5.4 NO_3^- Transport

The mass transport equation for NO_3^- can be given similarly as that of the other three species. The boundary conditions are same as those of lead.

NO_3^- is the least reactive species compared with other three, and it does not have a significant importance in the electrokinetic removal process of lead. Inclusion of NO_3^- in the model is mainly to maintain the charge neutrality of the system. Therefore the presence of this species itself in the model does not have a definite meaning. Therefore, we are not concerned about the fate of NO_3^-, but predict the charge concentration that it represents which is used to achieve the electrical neutrality in the system and to analyze the distribution of the electrical field.

By preserving electrical neutrality as described in equation 4-24, the concentration of NO_3^- can be obtained simply from

$$c_{NO_3^-} = \sum_{j=1}^{3} z_j c_j \qquad [5\text{-}15]$$

where j = 1..3 refers to H^+, OH^-, and Pb^{2+}. Note, we are assuming c_j an average value at an element so that a numerical solution can be carried out easily. Figure 5.1 describes the implementation of this assumption.

5.5 Chemical Reactions With Pb(II)

In section 4.5, a number of chemical reactions involved during electrokinetic processing were discussed. Besides water auto-ionization reaction, reactions associated

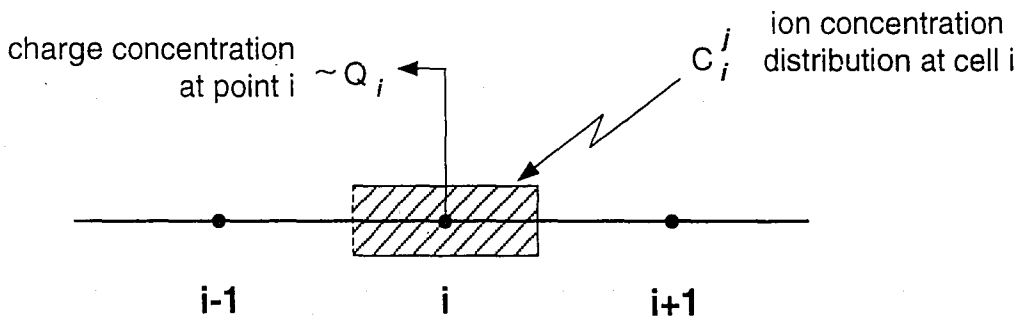

Figure 5.1 Equivalence of Continuous Concentration Distribution and Point Charge

with lead, including sorption/desorption and precipitation/dissolution, are examined below. They are presented in the mass transport equation 5-12 as R_{Pb}^{s} and R_{Pb}^{P} respectively. Algebraic equations describing these processes are developed to evaluate their influences assuming the maintenance of local equilibrium.

5.5.1 Precipitation/Dissolution

Equation 4-33c presents a general form of weak base reaction in aqueous phase. pH change is the major factor that influences the reaction direction and production rate. A reasonable conclusion can be drawn that precipitation reactions will most likely take place near the cathode side where there is a higher pH environment.

Lead hydroxide precipitation/dissolution reaction is

$$Pb(OH)_2 \rightleftharpoons Pb^{2+} + 2OH^- \qquad [5\text{-}16]$$

and the equilibrium of this state requires

$$c_{OH-}^2 \, c_{Pb} \leq K_{Pb(OH)_2} = 2.8 * 10^{-16} \qquad [5\text{-}17]$$

From equation 5-16, 2 moles of OH^- is required per 1 mole of Pb(II) to generate 1 mole of $Pb(OH)_2$. This means that the change in hydroxyl molar concentration due to the precipitation reaction is twice as the change in Pb(II) molar concentration. Therefore,

$$R_{Pb}^{P} = 2 R_{OH-}^{P} \qquad [5\text{-}18]$$

Hydroxyl ions also participate in water auto-ionization as described in Equation 5-9. The total change in OH^- concentration is the sum of the changes in H^+ and Pb(II)

concentrations due to precipitation/dissolution reaction. The decrease of concentration due to consumption is always defined as a positive value in mass transport equations (refer to the expressions of Rs).

5.5.2 Lead Adsorption

Lead ion, Pb(II) present in pore fluids, is highly adsorbed by clay minerals. Selectivity of kaolinite for Pb is higher than Ca, Cu, Zn, and Cd (Alloway 1990). According to Yong et al. (1990), for a given type of clay lead adsorption is mainly controlled by its concentration and the pH value of the solution. Figure 5.2 presents the experimental data reproduced from Yong et al. (1990). Their results showed that the ratio between adsorbed lead to total lead in kaolinite increases linearly with pH increasing up to 5.

The following empirical relation developed by Alshawabkeh and Acar (1996) is used in this study to represent the lead adsorption of kaolinite at different pH values.

$$\begin{aligned} R_{Pb}^{s} &= 0.27 c_{Pb}(pH - 1) && 1.0 < pH < 4.7 \\ R_{Pb}^{s} &= 0 && pH < 1.0 \\ R_{Pb}^{s} &= 0.011 && pH > 4.7 \end{aligned} \qquad [5\text{-}19]$$

where c_{Pb} is the total lead concentration including both adsorbed and solute concentration in M (mol/L). When pH is larger than 4.7, the adsorbed lead no longer fits the experimental data which was obtained in a dilute concentration (Yong et al. 1990). The largest possible adsorbed lead is limited by the cation exchange capacity, CEC of the clay, and thus the maximum value can be estimated through CEC = 1.06 meq/kg. Usually adsorbed lead is expressed in the concentration unit of mg/kg. Accordingly,

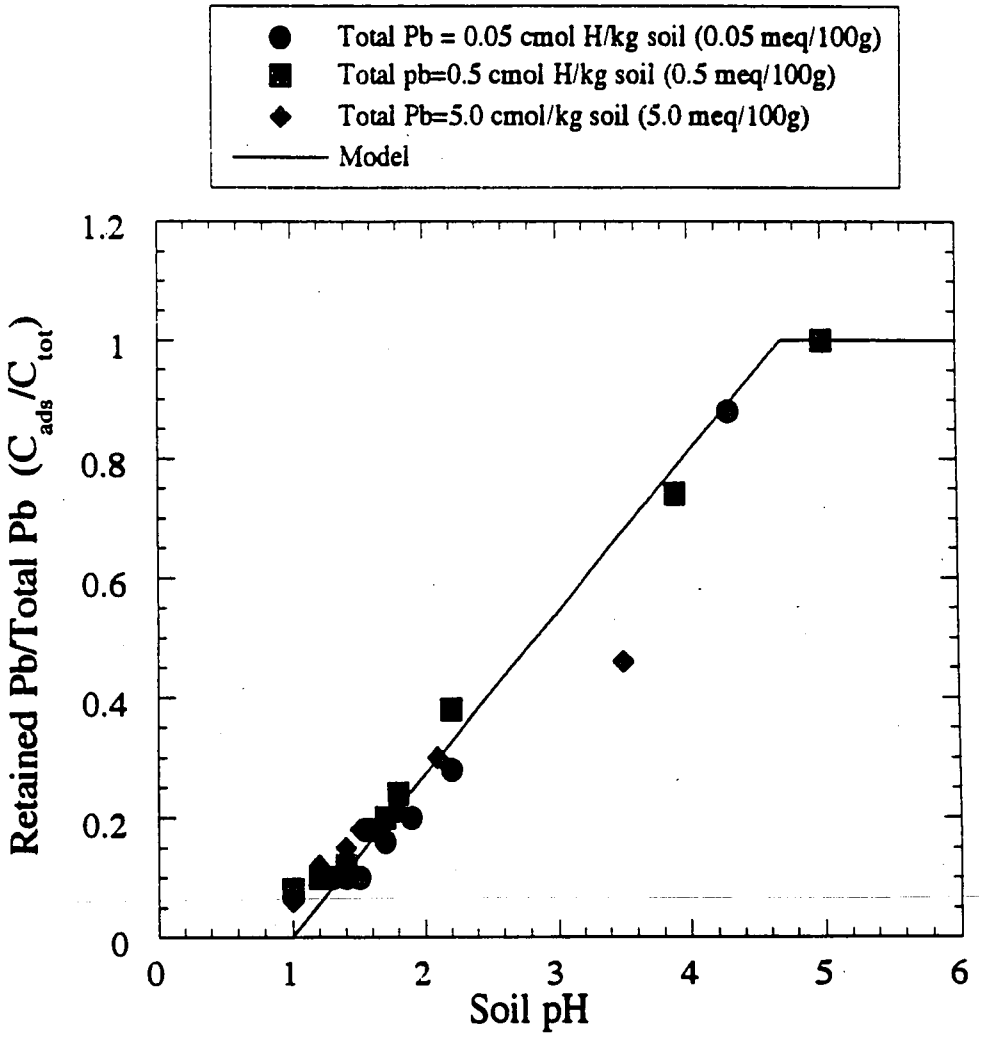

Figure 5.2 Lead Sorption ~ pH Value Relation

(Data From Yong et al. 1990)

equation 5-19 can be transferred to

$$
\begin{aligned}
s_{Pb} &= R^{s}_{Pb}\left(\frac{n}{\rho_d}\right)(207.2*1000) \qquad 1.0 < pH < 4.7 \\
s_{Pb} &= 0 \qquad\qquad\qquad\qquad\qquad pH < 1.0 \\
s_{Pb} &= 0.5\,CEC * 207.2 * 10^{6} \qquad pH > 4.7
\end{aligned}
\qquad [5\text{-}20]
$$

where n is soil porosity, ρ_d is its dry density, 207.2 is atomic weight of lead. s_{Pb} in Equation 5-20 gives the adsorbed lead in mg/kg.

This empirical relation is also plotted in Figure 5.2 to compare with the experimental data.

Although several chemical reactions have been considered in this study, they only reflect a part of the complex reactions and the effort to quantitatively account for part of these reactions. We know that the same ion can form multiple species in the solution, especially metal ions in weak acids. The redox potential, pH environment, electric field strength, and ion concentration in the solution will all affect the existing form of the metal ion. Further work is needed to understand and qualitatively evaluate the complexity of ion reactions during electrokinetic processing.

5.6 System Set-up

Untill now, we have analyzed the transport equations for lead transport in the presence of multispecies in pore fluid. In this system, 11 unkown variables are needed to be solved. They are: four concentrations, i, E, R_{H+}, $R_{OH-}{}^{a}$, $R_{OH-}{}^{p}$, $R_{Pb}{}^{s}$, and $R_{Pb}{}^{p}$. Three

mass transport equations 5-6, 5-11, 5-12, and equation 5-15 are used to handle the mass transport processes. They are supported by boundary conditions as described in equations 5-2, 5-5, 5-7, 5-8, 5-13 and 5-14. Equations 4-37 and 4-40 are solved for E and i, and equations 5-9, 5-10, 5-17, 5-18 and 5-19 are solved for all the chemical reaction terms, Rs. These equations form the complete model system for lead transport by electrokinetics.

The method of numerical simulation of this model system is developed next. Solution procedure is given in the detail of the general form of the partial differential mass transport equations presented in this chapter.

CHAPTER 6
NUMERICAL IMPLEMENTATION

6.1 Finite Difference Method

For the one-dimensional mass transfer equation 4-36, finite difference method (FDM) is an efficient computation process in seeking the numerical solution. A possible numerical dispersion can be avoided by proper spatial and temporal discretization. Since the FDM is based on the principle of mass conservation, the mass balance discrepancy at each step should be very small.

6.1.1 Discretization Method

The partial derivative $\partial c(x,t)/\partial x$ may be approximated through forward, backward, or central difference. These three interpolation methods are all developed from the definition of partial derivative and the Taylor's expansion.

Figure 6.1 gives a detailed illustration for forward difference, while a scheme for all three methods is shown in Figure 6.2 .

From Figure 6.1, forward difference in space for $\partial c/\partial x$ is

$$\left(\frac{\partial c}{\partial x}\right)_i = \frac{c_{i+1} - c_i}{\Delta x_i} \qquad [6\text{-}1]$$

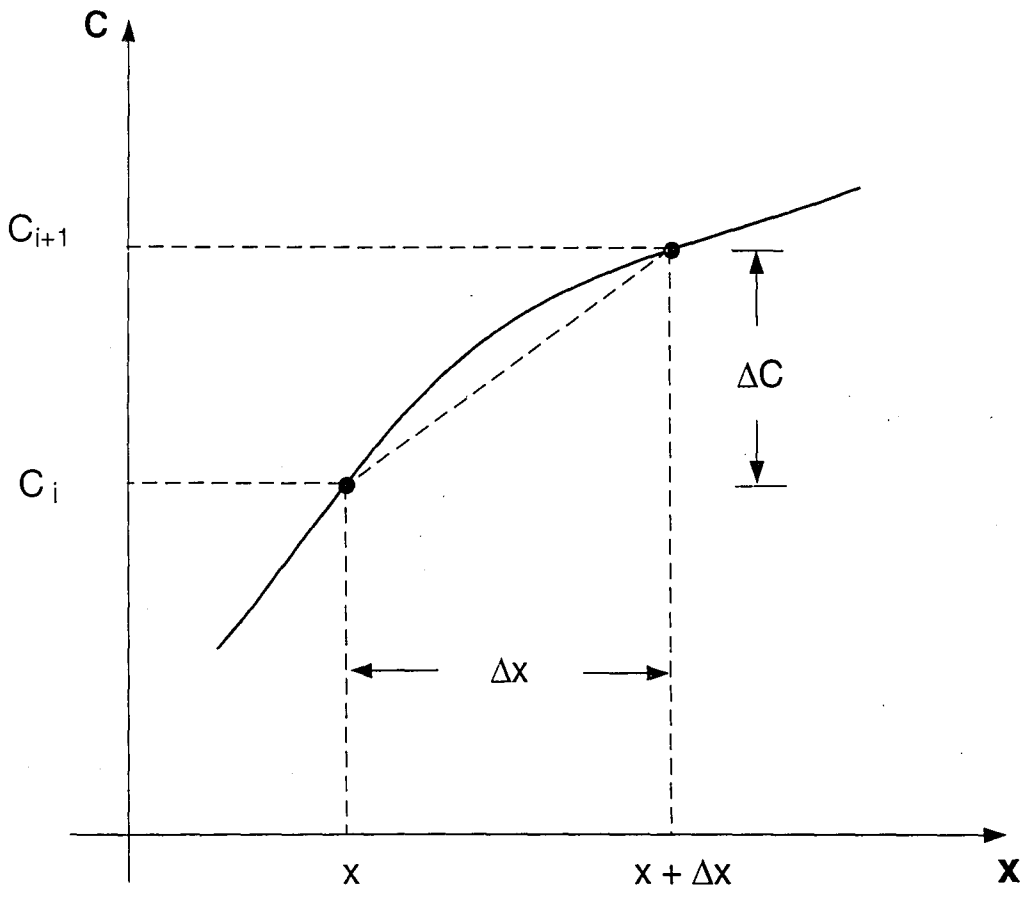

Figure 6.1 Scheme of Forward Difference

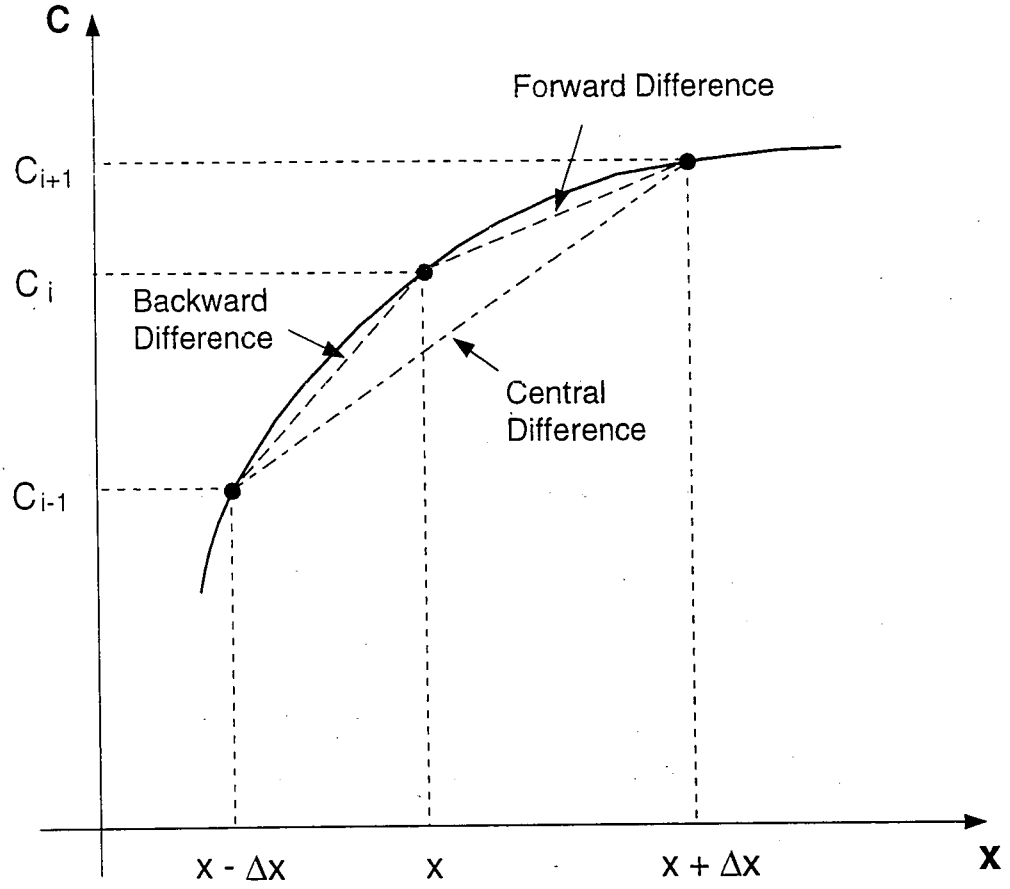

Figure 6.2 Comparison of Forward Difference, Backward Difference, and Central Difference

where Δx_i is the space increment from nodal point $i \rightarrow i+1$; c_{i+1} and c_i are concentration values at points $i+1$ and i, respectively.

Backward difference

$$\left(\frac{\partial c}{\partial x}\right)_i = \frac{c_i - c_{i-1}}{\Delta x_i} \qquad [6\text{-}2]$$

And central difference

$$\left(\frac{\partial c}{\partial x}\right)_i = \frac{1}{2}\left[\frac{c_{i+1} - c_i}{\Delta x_i} + \frac{c_i - c_{i-1}}{\Delta x_i}\right] = \frac{c_{i+1} - c_{i-1}}{2\Delta x_i} \qquad [6\text{-}3]$$

Among these three methods, the central difference is the average of forward and backward interpolation. It can provide the best approximation to slope at point i. We will choose the central difference as approximation to the first derivative.

For the second derivative $\partial^2 c/\partial x^2$, a mixed interpolation will be helpful. Taking forward difference on outside derivative and backward difference on inside one:

$$\left(\frac{\partial^2 c}{\partial x^2}\right)_i = \frac{\partial}{\partial x}\left(\frac{\partial c}{\partial x}\right)_i \approx \frac{\left(\frac{\partial c}{\partial x}\right)_{i+1} - \left(\frac{\partial c}{\partial x}\right)_i}{\Delta x_i} \qquad [6\text{-}4a]$$

$$\approx \frac{\frac{c_{i+1} - c_i}{\Delta x_i} - \frac{c_i - c_{i-1}}{\Delta x_i}}{\Delta x_i}$$

$$\left(\frac{\partial^2 c}{\partial x^2}\right)_i = \frac{c_{i+1} - 2c_i + c_{i-1}}{(\Delta x)_i^2} \qquad [6\text{-}4b]$$

are obtained.

6.1.2 Spatial and Temporal Discretion

In our one-dimensional transport model, spatial discretization is not as important as it is in a three-dimensional modeling, although we do need to think about the velocity distribution along the sample. A modified grid system might be an advantage to simulate the velocity field difference, to prevent numerical dispersion, and to save the machine processing time and storage space. This may be particularly important when dealing with a large model with large amount of nodal points, or if the medium has spatially changing material properties.

Simulating a clay sample of homogeneous properties on bench-scale, space grids need not be many and thus a fixed grid system should suffice.

A major concern after choosing the fixed grid is: how to avoid the possible numerical dispersion and secure the accuracy of the output? A fine enough grid should be the answer when applying the FDM. Due to the low electrokinetic flow rate in clay and sludge, sparse grids will possibly generate significant errors at each time step. Keller (1960) proposed a sufficient condition for nonoscillatory solution of the diffusion-advection equation, which reads as:

$$\Delta x \leq \frac{D_{eff}^*}{v} \qquad [6\text{-}5a]$$

$$\Delta t \leq \frac{\Delta x^2}{D_{eff}^*} \qquad [6\text{-}5b]$$

where v is a combined convection velocity term.

Figure 6.3 shows the schematic of the discretization used in the computation.

6.1.3 Numerical Modeling

For convenience, define a coefficient A^* as :

$$A^* = -\left\{k_e + \left[v_{m,o} - \left(\alpha v_{m,o} + \beta\right)c^{1/2}\right]\right\}E \qquad [6\text{-}6]$$

define another coefficient B^* as:

$$B^* = -\left\{k_e + \left[v_{m,o} - \left(\alpha v_{m,o} + \beta\right)c^{1/2}\right]\right\}\frac{\partial E}{\partial x} \qquad [6\text{-}7]$$

where E is the electrical field which is given in equation 4-37.

Equation 4-36 is thus simplified to

$$D_{eff}^* \frac{\partial^2 c(x,t)}{\partial x^2} + A^* \frac{\partial c(x,t)}{\partial x} + B^* c(x,t) = \frac{\partial c(x,t)}{\partial t} \qquad [6\text{-}8]$$

The effect of chemical reaction production r(c) to the mass flow can be incorporated during computing process through a scheme that will be discussed later, and

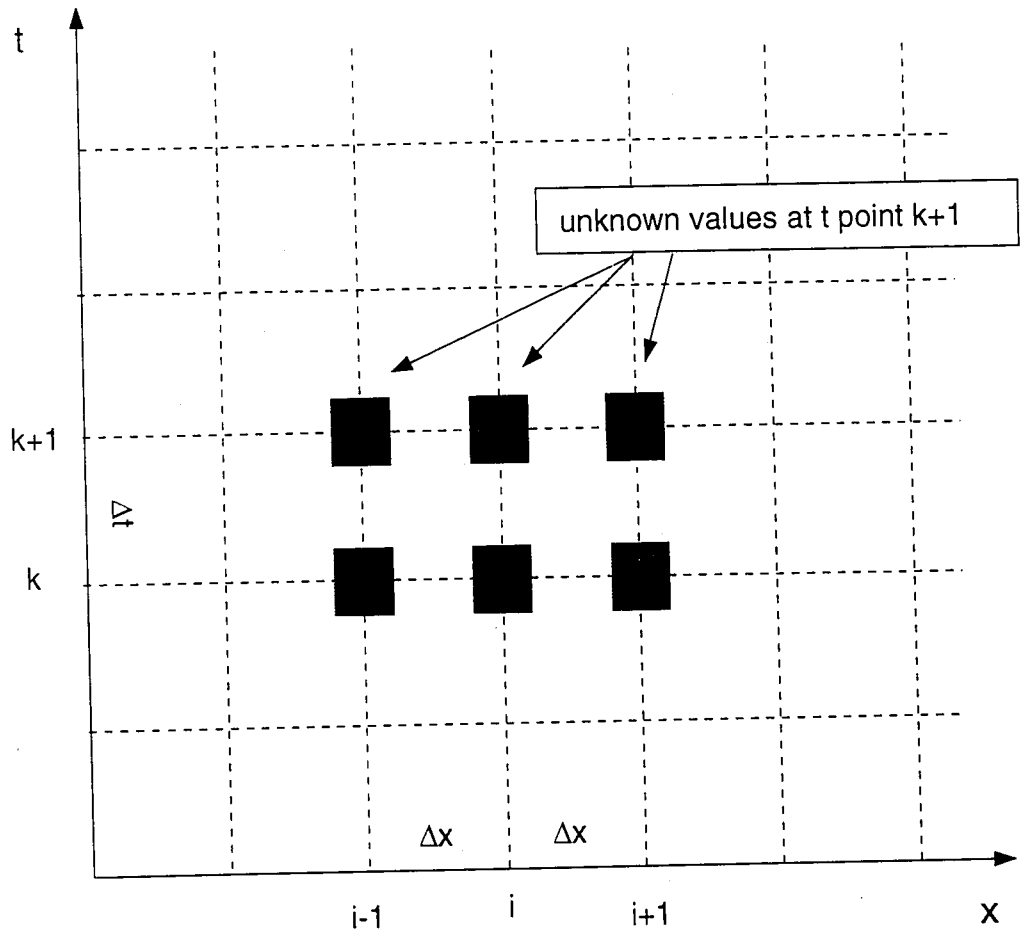

Figure 6.3 Scheme of Spatial and Temporal Discretization

thus is omitted in equation 6-8.

x is replaced by the normalized length, x (z is not used to represent normalized length to avoid confusion that may arises with the expression of electron charge)

$$x = \frac{x}{L} \qquad [6\text{-}9]$$

where x = normalized distance coordinate

x = real distance coordinate

L = real length of soil sample

Equation 6-8 is modified to

$$D_{eff}^{*} \frac{\partial^2 c(x,t)}{\partial x^2} \frac{1}{L^2} + A^{*} \frac{\partial c(x,t)}{\partial x} \frac{1}{L} + B^{*} c(x,t) = \frac{\partial c(x,t)}{\partial t} \qquad [6\text{-}10]$$

To keep the expression of spatial dimension consistent, redefine x as the normalized coordinate x ,

$$\frac{D_{eff}^{*}}{L^2} \frac{\partial^2 c(x,t)}{\partial x^2} + \frac{A^{*}}{L} \frac{\partial c(x,t)}{\partial x} + B^{*} c(x,t) = \frac{\partial c(x,t)}{\partial t} \qquad [6\text{-}11]$$

Substitute,

$$D' = \frac{D_{eff}^{*}}{L^2}$$

$$A' = \frac{A^{*}}{L} \qquad [6\text{-}12]$$

Note, this will eliminate the longitudinal dimension of D^{*}_{eff} and A^{*}. Simply replacing c(x,t) with c will generate a neat expression as follows:

$$D' \frac{\partial^2 c}{\partial x^2} + A' \frac{\partial c}{\partial x} + B^* c = \frac{\partial c}{\partial t} \qquad [6\text{-}13]$$

In this equation, for a given experiment, D′ is a constant property of the species *j*, A′ and B* can be obtained from their original definition. Applying the Finite Difference discretization equations (Equation 6-3, 6-4b) to Equation 6-13, the numerical form is obtained as follows:

$$\left[\frac{1}{2}D'\right]_i \frac{c_{i-1}^{k} - 2c_i^{k} + c_{i+1}^{k}}{(\Delta x)_i^2} + \left[\frac{1}{2}D'\right]_i \frac{c_{i-1}^{k+1} - 2c_i^{k+1} + c_{i+1}^{k+1}}{(\Delta x)_i^2}$$

$$+ \left[\frac{1}{4}A'\right]_i \frac{c_{i+1}^{k} - c_{i-1}^{k}}{(\Delta x)_i} + \left[\frac{1}{4}A'\right]_i \frac{c_{i+1}^{k+1} - c_{i-1}^{k+1}}{(\Delta x)_i} \qquad [6\text{-}14]$$

$$+ \frac{1}{2}B^* c_i^{k} + \frac{1}{2}B^* c_i^{k+1} = \frac{c_i^{k+1} - c_i^{k}}{\Delta t}$$

where k, k+1 denotes consecutive time steps.

Equation 6-14 is supposed to be naturally stable and with no numerical dispersion. Convergence check may not be needed if not for consideration of the coefficients A′ and B*. Since both A′ and B* involve the concentration function c, while c varies each time step altering the values of E and migration velocity v_m , a sub-iteration between the time steps is necessary. In other words, additional iteration levels need to be introduced at each time step to check with the convergence of coefficients A′ and B*.

Including the sub-iteration levels, Equation 6-14 is modified as:

$$\left[\frac{D'}{2}\right]_i \frac{c_{i-1}^{k} - 2c_i^{k} + c_{i+1}^{k}}{(\Delta x)_i^2} + \left[\frac{D'}{2}\right]_i \frac{c_{i-1}^{k+1^{(n+1)}} - 2c_i^{k+1^{(n+1)}} + c_{i+1}^{k+1^{(n+1)}}}{(\Delta x)_i^2}$$

$$+ \left[\frac{\left(A'\right)^{k+1^{(n)}}}{4}\right]_i \frac{c_{i+1}^{k} - c_{i-1}^{k}}{(\Delta x)_i} + \left[\frac{\left(A'\right)^{k+1^{(n)}}}{4}\right]_i \frac{c_{i+1}^{(k+1)^{(n+1)}} - c_{i-1}^{k+1^{(n+1)}}}{(\Delta x)_i} \qquad [6\text{-}15]$$

$$+ \left[\frac{\left(B^*\right)^{k+1^{(n)}}}{2}\right]_i c_i^{k} + \left[\frac{\left(B^*\right)^{k+1^{(n)}}}{2}\right]_i c_i^{k+1^{(n+1)}} = \frac{c_i^{k+1^{(n+1)}} - c_i^{k}}{\Delta t}$$

where n represents the iteration level. The above equation shows that values of A' and B^* at time step k+1 under iteration level n will be used to calculate the concentration distribution c at the same time step k+1 but under a higher iteration level n+1. At the first iteration level n=0 at the beginning of time step k, A' and B^* are obtained from the concentration distribution of time step k-1. This approach will be discussed further later.

Rearranging Equation 6-15 :

$$\left\{\left[\frac{D'}{2(\Delta x)^2}\right]_i - \left[\frac{\left(A'\right)^{k+1^{(n)}}}{4(\Delta x)}\right]_i\right\} c_{i-1}^{k+1^{(n+1)}} - \left\{\left[\frac{D'}{(\Delta x)^2}\right]_i - \left[\frac{\left(B^*\right)^{k+1^{(n)}}}{2}\right]_i + \frac{1}{\Delta t}\right\} c_i^{k+1^{(n+1)}}$$

$$+ \left\{\left[\frac{D'}{2(\Delta x)^2}\right]_i + \left[\frac{\left(A'\right)^{k+1^{(n)}}}{4(\Delta x)}\right]_i\right\} c_{i+1}^{k+1^{(n+1)}} \qquad [6\text{-}16]$$

$$= -\left[\frac{D'}{2}\right]_i \frac{c_{i-1}^{k} - 2c_i^{k} + c_{i+1}^{k}}{(\Delta x)_i^2} - \left[\frac{\left(A'\right)^{k+1^{(n)}}}{4}\right]_i \frac{c_{i+1}^{k} - c_{i-1}^{k}}{(\Delta x)_i} - \left\{\left[\frac{\left(B^*\right)^{k+1^{(n)}}}{2}\right]_i + \frac{1}{\Delta t}\right\} c_i^{k}$$

Equation 6-16 is the prevailing equation for numerical simulation of the governing

partial differential equation 4-36.

6.2 Global Matrix

From finite difference equation 6-16, a tri-diagonal coefficient matrix (global matrix) can be formulated. The n finite difference equations are:

$$
\begin{cases}
a_1 c_1 + b_1 c_2 + 0 + \ldots\ldots\ldots\ldots + 0 = d_1 \\
e_2 c_1 + a_2 c_2 + b_2 c_3 + \ldots\ldots\ldots\ldots + 0 = d_2 \\
\vdots \\
0 + 0 + \ldots + e_i c_{i-1} + a_i c_i + b_i c_{i+1} + 0 + \ldots + 0 = d_i \\
\vdots \\
0 + 0 + \ldots\ldots\ldots\ldots + 0 + e_n c_{n-1} + a_n c_n = d_n
\end{cases}
\qquad [6\text{-}17]
$$

This will result in the following matrix form:

$$
\begin{bmatrix}
a_1 & b_1 & 0 & \ldots & \ldots & 0 \\
e_2 & a_2 & b_2 & 0 & \ldots & 0 \\
0 & e_3 & a_3 & b_3 & 0 \ldots & 0 \\
\ldots & \ldots & \ldots & \ldots & \ldots & 0 \\
\ldots & \ldots & \ldots & \ldots & \ldots & 0 \\
\ldots & \ldots & \ldots & 0\ e_{n-1} & a_{n-1} & b_{n-1} \\
\ldots & \ldots & \ldots & \ldots & e_n & a_n
\end{bmatrix}
\begin{bmatrix} c_1 \\ c_2 \\ \cdot \\ \cdot \\ \cdot \\ c_{n-1} \\ c_n \end{bmatrix}
=
\begin{bmatrix} d_1 \\ d_2 \\ \cdot \\ \cdot \\ \cdot \\ d_{n-1} \\ d_n \end{bmatrix}
\qquad [6\text{-}18]
$$

where vector $\{c_i\}$ is the unknown concentration distribution. In general form

$$A \cdot c = d \qquad [6\text{-}19]$$

The coefficients a, b, e, and d are:

$$a_i = -\left[\frac{D'}{(\Delta x)^2}\right]_i + \left[\frac{\left(B^*\right)^{k+1^{(n)}}}{2}\right]_i - \frac{1}{\Delta t} \qquad [6\text{-}20]$$

$$b_i = \left[\frac{D'}{2(\Delta x)^2}\right]_i + \left[\frac{\left(A'\right)^{k+1^{(n)}}}{4(\Delta x)}\right]_i \qquad [6\text{-}21]$$

$$e_i = \left[\frac{D'}{2(\Delta x)^2}\right]_i - \left[\frac{\left(A'\right)^{k+1^{(n)}}}{4(\Delta x)}\right]_i \qquad [6\text{-}22]$$

$$d_i = -\left[\frac{D'}{2}\right]_i \left[\frac{c_{i-1}^{\,k} - 2c_i^{\,k} + c_{i+1}^{\,k}}{(\Delta x)_i^2}\right] - \left[\frac{\left(A'\right)^{k+1^{(n)}}}{4}\right]_i \frac{c_{i+1}^{\,k} - c_{i-1}^{\,k}}{(\Delta x)_i} - \left\{\left[\frac{\left(B^*\right)^{k+1^{(n)}}}{2}\right]_i + \frac{1}{\Delta t}\right\} c_i^{\,k} \qquad [6\text{-}23]$$

Boundary elements will be influenced by the flux boundary conditions which are described in equations 4-48, 4-49, or the specific ions describedby equations 5-2, 5-5, 5-7,

5-8, 5-13, 5-14. Incorporation of the boundary conditions will modify the coefficients at i=1 and i=n.

6.3 Decomposition Method

Thomas algorithm is employed to solve equation 6-19 with the tri-diagonal matrix A. A general discussion of this algorithm is given below.

Assume A has factorization

$$L \cdot U = A \qquad [6\text{-}24]$$

where L is the lower triangular matrix and U is upper triangular matrix.

Since all elements in matrix A are zero except those on the tri-diagonal lines, it is easy to prove that all elements in L and U are zero except those on their tri-diagonal lines. As a result, 3n-2 non-zero elements in A are the only resource to build the 3n-2 conditions in L and U. As a specific case of Doolittle decomposition, we can expect L and U have the form

$$L = \begin{bmatrix} 1 & 0 & & & 0 \\ l_2 & 1 & & & \\ & l_3 & 1 & & \\ & & & \ddots & \\ 0 & & & l_n & 1 \end{bmatrix} \qquad U = \begin{bmatrix} u_1 & v_1 & & & 0 \\ & u_2 & v_2 & & \\ & & u_3 & & \\ & & & \ddots & v_{n-1} \\ 0 & & & & u_n \end{bmatrix} \qquad [6\text{-}25]$$

After the decomposition, we can solve linear equations

$$Ly = d$$
$$Uc = y \qquad [6\text{-}26]$$

Thomas algorithm is composed of a forward iteration process to seek for matrix decomposition and a backward iteration process to obtain the solution.

Forward solution:

for i=1 $w_1 = b_1/a_1$; $g_1 = d_1/a_1$

i=2, 3, . . . , n-1 $w_i = b_i / (a_i - e_i w_{i-1})$

i=2, 3, . . . , n $g_i = (d_i - e_i g_{i-1})/(a_i - e_i w_{i-1})$

Backward solution:

$c_n = g_n$

for i=n-1, n-2, ... , 2, 1 $c_i = g_i - w_i c_{i+1}$

The convergence is checked to satisfy the following condition

$$\left| \frac{c_i^{k+1^{(n+1)}} - c_i^{k+1^{(n)}}}{c_i^{k+1^{(n)}}} \right| \le e_{rror} \qquad [6\text{-}27]$$

where e_{rror} is the preset data dispersion tolerance.

6.4 Incorporation of Initial and Boundary Conditions

In solving the numerical model, we need to furnish initial and boundary conditions for each species. Due to the existence of source for hydrogen and hydroxyl ions, they do have flux through boundaries. For lead, zero-flux boundary conditions are assumed.

6.4.1 Initial Conditions

Soil specimen is assumed to be mixed homogeneously with solutions, and thus the initial concentration distribution for each species is averaged along the soil sample cylinder.

For each species, there is

$$c^j(x,0) = c_0^j \qquad 0 \le x \le 1 \qquad [6\text{-}28]$$

where j refers to the different ions or species, and c_0^j is the initial concentration of species j. x is the normalized distance following its use in equation 5-10.

Since both ends of a soil specimen in the experiments are in contact with distilled water initially, the actual value of c at the ends (x=0, x=1) may be slightly different than that of the internal sections of the soil. Nevertheless, this is assumed not to likely influence the simulation.

Under ambient pH, clayey soils possess negative surface charge. The soil's initial pH value is used to determine the initial concentration values of H^+ and OH^- ion. Lead concentration in solute is adjusted by considering any possible sorption reaction under the initial pH value, using equation 5-19.

6.4.2 Boundary Conditions

For the general form of boundary conditions as described in 4-48 and 4-49, finite difference method is used to discretize those differential equations.

Forward difference is used for boundary x=0, and backward difference is used for x=L. To avoid numerical dispersion, the boundary node in our case should be at the end of specimen, or very close to the edge to reflect the status of boundary flux. Therefore a finer element or special handling during the computation is required, especially when a zero-flux boundary condition is assumed - such as the boundary conditions for lead in this study.

When using 4-48 and 4-49 to describe flux at the boundary elements, equations for i=1 and i=n in matrix A and vector d are altered. A modified matrix equation 6-18 is the basis for mass transport simulation by the numerical method. The way that boundary conditions influence equation 6-18 is different with different species, due to their different flux situation, and is not necessary to be repeated here.

Appendix A presents the details of the integration of boundary conditions.

6.5 Evaluation of Chemical Reactions

The evaluation of chemical reactions is a complex process. Several reaction phenomena are considered in this study, including water auto-ionization, lead sorption, lead precipitation/dissolution. They are described using the algebraic equations 5-10, 5-17, and 5-19.

These reactions are associated with each other. For example, OH^- joins with H^+

to produce water, at the same time it also takes part in the lead precipitation/dissolution reactions; and Pb^{2+} itself also undergoes sorption/desorption reactions.

A full equilibrium at the limit state in the solute is assumed, which means the equilibrium conditions described by equations 5-10, 5-17, and 5-19 are all maintained at their limit states. So the chemical reactions may be evaluated sequentially and as a full system.

As shown in Figure 6.4, the scheme follows that first equation 5-10 is checked with the calculated concentration of H^+ and OH^-, and then sorption reaction takes place under the new H^+ concentration. After sorption, Pb(II) together with OH^- goes through precipitation/dissolution reaction and the new Pb(II) concentration is compared with initial Pb(II) concentration. If the difference is not within the tolerance, the above process is repeated.

While the sorption equation 5-19 and equation 6-29 for water auto-ionization are easy to solve,

$$(c_{H+} - \Delta c)(c_{OH-} - \Delta c) = K_w \qquad [6\text{-}29]$$

a special effort is put on solving lead precipitation equation 6-30.

$$(c_{OH-} - 2\Delta c)^2 (c_{Pb} - \Delta c) \le K_{Pb(OH)_2} \qquad [6\text{-}30]$$

Exact solution is sought for this equation. The solution scheme is as follows:

Define

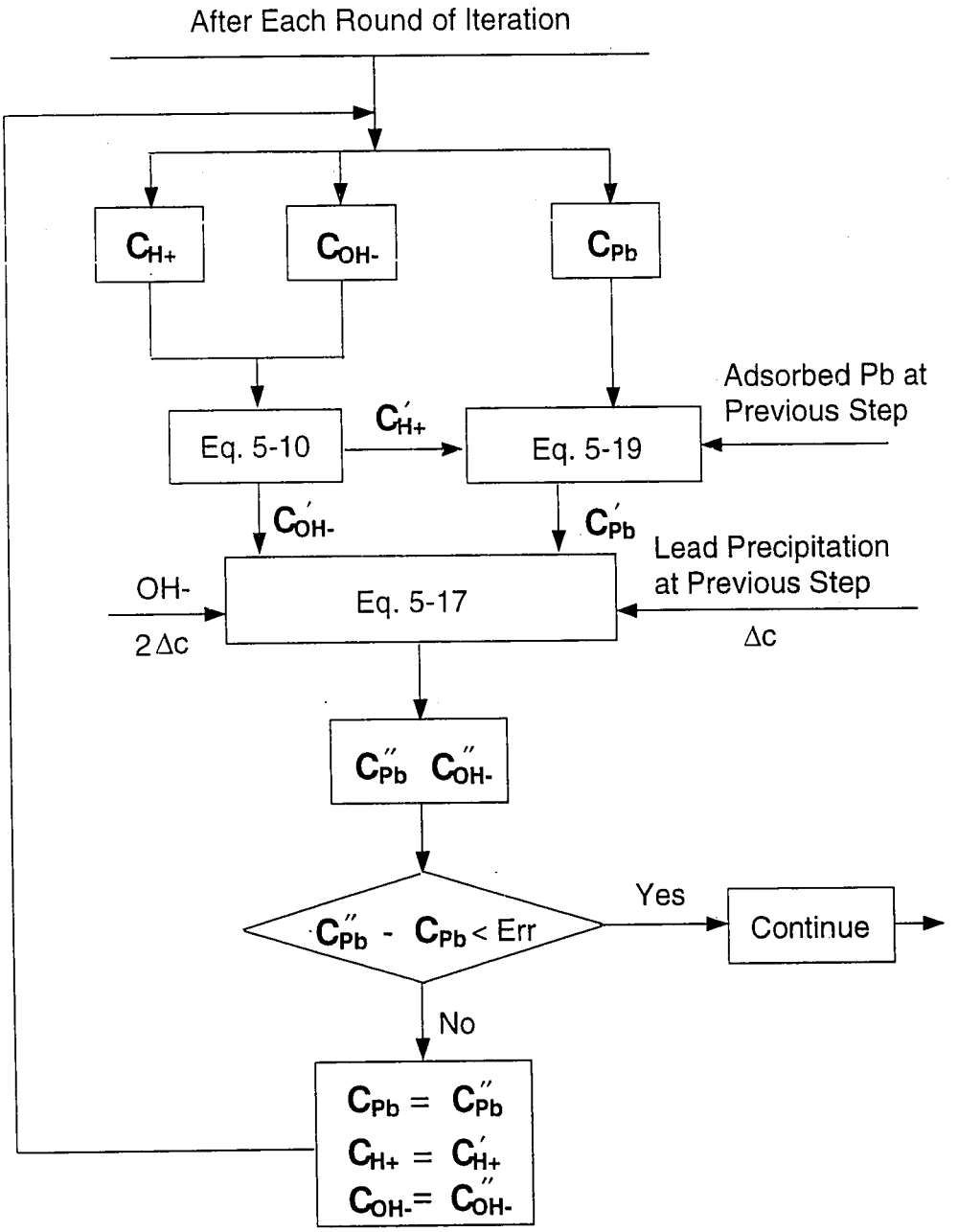

Figure 6.4 Flow Chart for Evaluating Chemical Reactions

$$a = -c_{Pb} - c_{OH-}$$

$$b = \frac{c_{OH-}^2 + 4c_{OH-}c_{Pb}}{4} \qquad [6\text{-}31]$$

$$c = -\frac{c_{OH-}^2 c_{Pb} - K_{Pb(OH)_2}}{4}$$

and

$$Q = \frac{a^2 - 3b}{9}$$

$$R = \frac{2a^3 - 9ab + 27c}{54} \qquad [6\text{-}32]$$

then a real root of equation 6-30 is obtained from

$$\Delta c = -2\sqrt{Q}\cos(\frac{\theta}{3}) - \frac{a}{3} \qquad [6\text{-}33]$$

where,

$$\theta = \arccos(\frac{R}{\sqrt{Q^3}}) \qquad [6\text{-}34]$$

There are two other real roots of the equation 6-30. Those roots are excluded because they do not satisfy the concentration situation, ie., they will cause a negative value of OH^- concentration.

However, one problem remains. We know that the same ion can form multiple species in the solution, especially metal ions in weak acids. The redox potential, pH

environment, electric field strength, and ion concentration in the solution will all affect the form of the metal ion. Because of this complexity, simply applying equilibrium constraints to metal ions may not be realistic.

6.6 Solution Procedure

At the beginning of the numerical simulation of lead removal, initial concentration and uniform electric field are specified at time step k=0. Forward time difference method is used in time discretization, $t_{k+1} = t_k + \Delta t$.

Mass transport equations are solved to obtain the new concentrations of all but NO_3^- ion species, at all space elements. These new concentrations are then input into chemical reaction equations to get a new set of concentration distributions under chemical equilibrium state. These results are then used to calculate the concentration of NO_3^-, new electric field distribution and electrical conductivity. If error between the calculated concentration and the concentration at iteration level n=0 is within the preset tolerance, then the simulation marches forward to next time step k+1, otherwise it goes back to a higher iteration level and repeats the above process under new electrical field condition. This process goes through all time steps and all space elements along the specimen. A simple description of the employed solution procedure is presented in Figure 6.5 .

The benefit of simulating lead removal by electrokinetic process in this scheme is clear. It separates the evaluation of chemical reactions from the mass transport equations which saves great CPU time and simplify the problem. The validity of this so-called sequential iteration method applied was verified by several other researchers also (Yeh and Tripathi 1991, Alshawabkeh and Acar 1996). The chemical reactions do not depend on spatial derivatives and thus it's reasonable to evaluate them separately and sequentially. But the greatest advantage of this scheme may be that it allows more freedom to modify

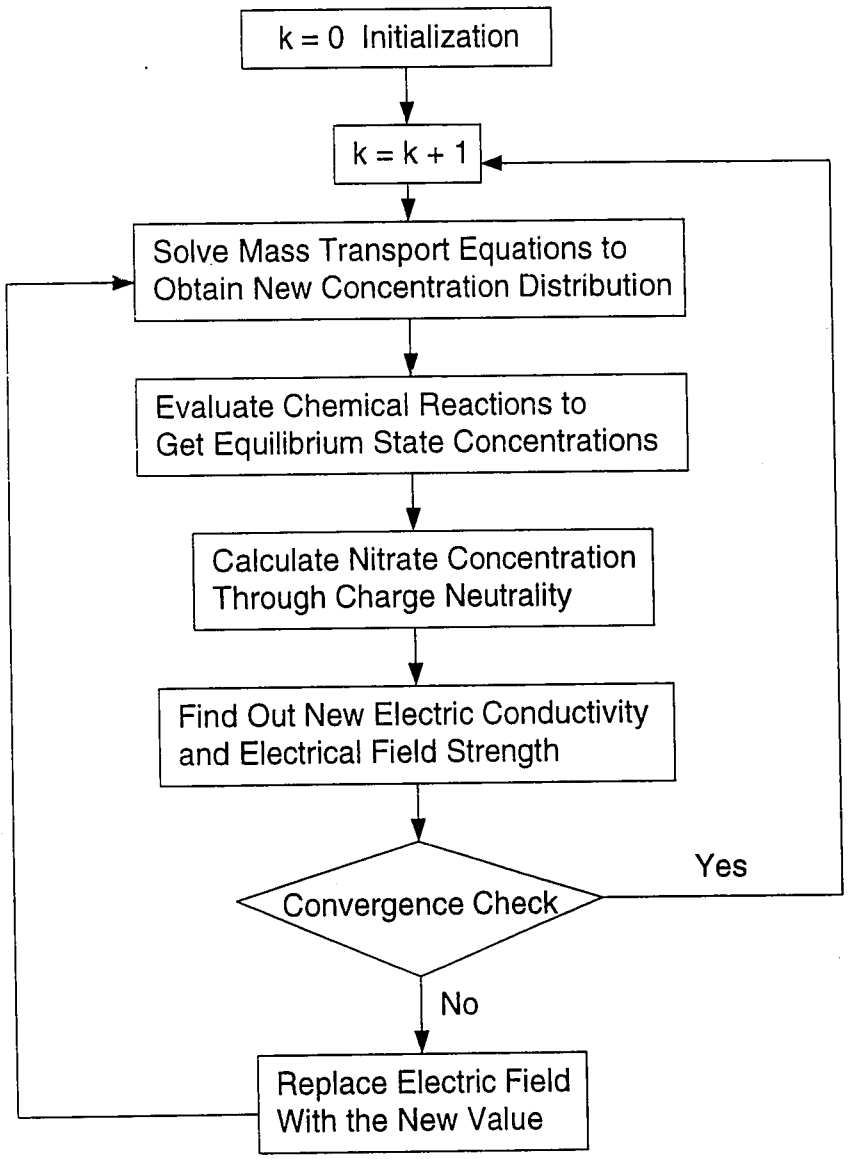

Figure 6.5 A Simple Description of Solution Procedure Used in Numerical Simulation

the simulation process, for example, it's possible in this procedure to account for the influence of soil consolidation (suction) more easily. The pore water pressure could be obtained directly from the electric field strength through their relationship (See Alshawabkeh and Acar 1996).

The standard convergence check could be made easier by comparing the new calculated electric field or voltage with their original counterparts. This is the same as checking concentrations theoretically with reduced CPU time.

Further details of the solution scheme used in this study will be presented in next chapter while describing the computing programs. The numerical solution is achieved using object-oriented programming compiled and tested on IBM Risc/6000 workstation.

CHAPTER 7
PROGRAMS AND RESULTS

7.1 Introduction

The purpose of developing computerized numerical simulation is to provide solutions to a complicated modeling system, where the analytical solutions are not possible. A verified program running on a powerful computer could be used as a further analysis tool for both research and practical application. It is easier to evaluate the importance of a specific factor on the physical system simply by adjusting its value or existence in the program structure, instead of long waiting and complex handling of an experiment. This computing program could also function as a core simulation processor for a more advanced software package, such as a knowledge-based artificial intelligence system. For the latter purpose, the program is expected to be easy to maintain and be accessible by other programs.

Chapter 4 and 5 presented the new multispecies mass transport model under transient electric field accompanied by coupled chemical reactions. Numerical solution scheme for these partial differential equations is developed in Chapter 6. Sequential iteration method between mass transport equations and chemical reaction equations is employed in the programming. Computer programs are written in C++ on IBM RISC/6000 workstation running with AIX UNIX operating system, but are also tested on Sun SPARC workstations.

Program list and input and output samples are provided in the Appendices of this thesis. Description of the program structure and the results of the analysis are presented

in this chapter.

7.2 Summary of Program

C++ and Object-oriented Programming (OOP) technology are used in writing these programs. Though C++ does not provide advancement over Fortran or other scientific programming languages in terms of mathematical computation, it offers much more flexibility and capacity for integration and further expansion. Its readability is also better than other procedural languages.

7.2.1 About OOP

The procedural paradigm (i.e. Fortran, Pascal) has been predominant over the past years. A system is modeled as a flow of control from one procedure to another. The high level view of a system is a procedure that is successively decomposed into sub-procedures. Each sub-procedure plays a role to fulfill the overall task of a program. One criticism of a system designed around procedures is that data tends to be ignored in favor of procedures and yet procedures are most likely to change during the software life cycle. Another disadvantage is that many tasks are not easily modeled by the decomposition of procedures.

Object-oriented concepts structure the solution of a given task in a different way than using procedures. They offer much more flexibility for representing a model at the conceptual and implementation level. The central entities within an object-oriented model are objects. Procedures are not ignored but are packaged within the objects along with

data. Control is determined by messages that pass between objects.

The core concept in OOP technology is the so called "object". Objects are physical instantiation of a class. Each object belongs to a class. A class provides a description for objects of a particular type. The class description is made up of attributes and operations which together comprise a set of class members. Attributes define the state of an object and operations govern the behavior of an object. All these concepts form the basis of object-oriented paradigm.

An OOP language like C++ allows a high degree of reuse which certainly leads to the increased productivity and an easier-to-maintain system. Programs using object-oriented language are relatively easy to modify. Yet the most advanced aspects of OOP lie on its powerful libraries for graphical user interface design. Using C++ in the electrokinetic modeling programs leaves room for future expansion of the programs into a more integrated software.

7.2.2 Class Hierarchy

Figure 7.1 presents the conceptual structure of the programs. The classes are developed based on this structure.

Each specie is defined as an aggregate object which is composed of several objects that are defined by various classes. In Figure 7.1, each specie is defined by its physico-chemical properties, its initial concentration distribution and its concentration history (the concentration distribution for a species along the time step). Both distribution and history classes are directed to the solver and are assigned value through the class of value distribution.

There are 6 classes and 2 library functions defined in the simulation programs

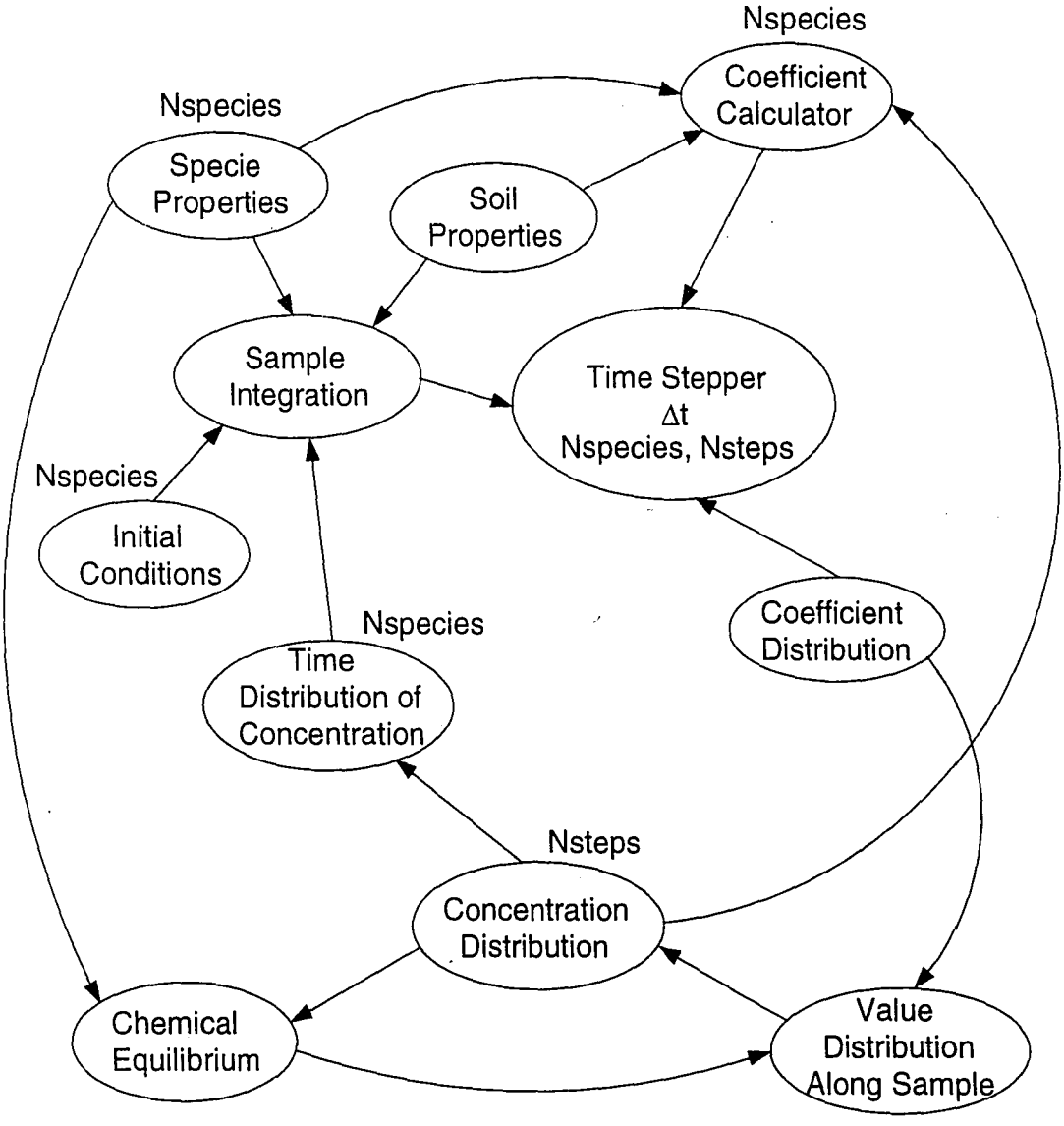

Figure 7.1 Structure Diagram for Electrokinetic Mass Transport Computing Programs

which are utilized by the main program to conduct the simulation process. These classes and functions are described below.

ekconcen.c A species object class that represents the concentration of a species across soil column. It has two attributes: number of space element and values of concentration. It also has several methods that enable it to manipulate the concentration distributions. It inherits from class ekvalued.c.

ekconchi.c This class represents concentrations across time and space. It records the concentration history. It has attributes of time points and space points. It is constructed on class ekconcen.c.

ekinit.c A class that reads and operates initial conditions. It works by a method that assigns initial values and conditions to different objects.

eksolver.c An object class that solves mass transport equations for each species. It has methods that distribute calculated coefficients to all points.

ekvalued.c An object class that represents the distribution of a value across the soil column. It also has two attributes: number of points and the value. It has methods that operate on any value generated through the simulation process.

tokenzr.c This class offers the methods that define ways to identify the input characters. These methods are used in ekinit.c for reading the input file.

eksoilpr.h Describes general properties such as initial electric field and length of soil sample.

ekspecco.h A structure that represents the properties of chemical species.

The main program controls time step. It calculates the coefficients and evaluates the chemical equilibrium at each time step and at every iteration level. It assures the convergence of the simulation, analyzes the generated data, and creates the output files. More efforts can be made here to separate some processes from the main program to keep the main program simple.

7.2.3 Flow Chart for Modeling Lead Transport

A traditional flow chart of the program modeling lead transport is given in Figure 7.2.

Program starts by initializing the objects for each species. *Ekinit* first reads in data from input data file, then these data are categorized into several different groups according to the properties they describe. A structure derived from *ekspecco* is used to store the properties of each species. Species objects are initialized with the concentration data. Initial electrical field and the length of soil sample are put in structure derived from *eksoilpr* which is designed to hold the general properties that are same to all species. *Ekvalued* is used to distribute the concentration profile into a desired density of space points. This is important to easily change the element size or assign data to any point.

Coefficients for solving the PDEs are then computed in the main program with the furnished concentration profiles through those species objects. The results are passed into *eksolver* to formalize and solve the numerical equations, one species each time, using the scheme that is discussed before.

After the concentration profiles for the first three species are obtained (H^+, OH^-, Pb(II)), the chemical reactions are evaluated. Assuming that every equilibrium is maintained (referring to section 5.5), a convergence standard is set so that the difference

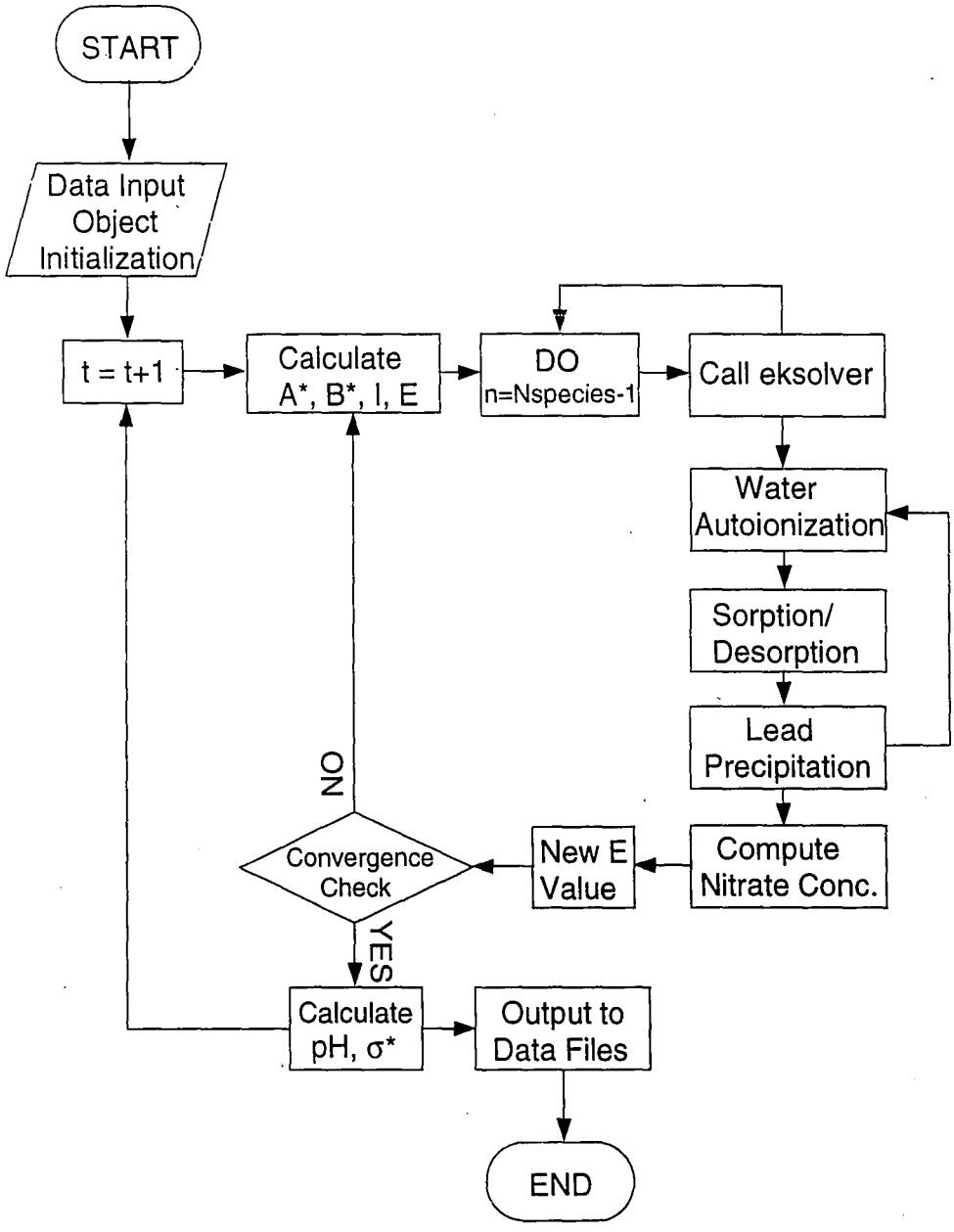

Figure 7.2 Flow Chart for Programs Modeling Lead Transport

between the lead concentration in solution before and after chemical reactions is within a preset tolerance.

NO_3^- is then calculated through charge neutrality. Note here that only the concentration of dissolved lead participates in the calculation of the charge neutrality, electrical field and mass transport.

New electrical field strength E is computed and compared with the initial value. If the error falls within the tolerance limits, then the processing continues; otherwise the PDEs are solved with new set of electrical field values and the process is repeated until the convergence standard is satisfied.

Electric conductivity (σ^*) and pH value at each point are calculated then*. All the concentration profiles are recorded by *ekconchi* objects.

Next step is taken forward in time.

* Note, in the case hydraulic advection is considered, the hydraulic pressure profile (pore pressure) can be calculated here using final electrical field data at each time step.

7.3 Modeling Lead Transport

Some initial data input is necessary to perform the computation, . Parameters required for modeling lead transport and removal include: properties of soil and ion species, initial and boundary conditions. Among these parameters, coefficients related to chemical reactions and lead sorption/desorption have been discussed before. Accurate estimates of these parameters are critical for a good prediction using the model. For a qualitative model whose main purpose at current stage is to asses whether or not it could provide a reasonable prediction, accurate values of parameters and constants are not

sought through strict experiments. All data used in the program and presented below are evaluated either through previous laboratory tests conducted at Lehigh University or approximated from data reported in the literature. To compare with the results of other models especially with those of Alshawabkeh and Acar model (1996), the measurement units used in this model are similar with theirs. The units chosen for input and output data are listed in Table 7.1.

7.3.1 Tortuosity Factor of Soil

Kaolinite is chosen as the porous medium used in this model. Table 4.1 indicates that the tortuosity factor, τ, varies from 0.1 to 0.5. A value of 0.25 is used in this model following Alshawabkeh and Acar (1996) model.

7.3.2 Diffusion Coefficients

Diffusion coefficients are previously presented in Tables 4.2 and 4.3. Diffusion values are directly taken from these tables. Equation 4-8 is used to apply the diffusion of ions in porous media by multiplying with the tortuosity factor τ. Electro-migration mobilities in dilute solution are also obtained from these tables.

7.3.3 Electroosmotic Permeability

Table 7.1 Units of Parameters Used in Program

Parameter	Unit
Length (L)	*cm*
Time (t)	*day*
Faraday's Constant (F)	*Coulomb/mol*
Concentration (c)	*mol/l*
Adsorbed mass or in precipitation	*mg/kg*
Diffusion Coefficient (D)	cm^2/day
Electroosmotic Permeability (k_e)	$cm^2/V \cdot day$
Electro-migration Mobility (v_m)	$cm^2/V \cdot day$
Electric Potential (ϕ)	*Volt*
Electric Field (E)	*V/cm*
Current (I)	*A*

As discussed in section 4.4.2.2, the coefficient of electroosmotic permeability is around 10^{-4} to 10^{-5} cm^2/Vs for kaolinite. For lower activity clays and at higher water contents, this value is higher. Most researchers have used a k_e value on the order of 10^{-5} cm^2/Vs. Mitchell and Yeung (1991) used a value of 2×10^{-5} cm^2/Vs for illitic Altamont clay. Alshawabkeh and Acar (1992) used 1×10^{-5} cm^2/Vs for kaolinite. Hamed (Hamed et al. 1991) reported a maximum k_e value of 10^{-5} cm^2/Vs in lead-spiked kaolinite samples.

A constant value of 10^{-5} cm^2/Vs is used in current analysis for electroosmotic permeability.

Table 7.2 gives the values of constants that used in the current model. The compositional and engineering properties of Georgia kaolinite which works as the porous media in the model are summarized in Table 7.3.

7.3.4 Initial and Boundary Conditions

The boundary conditions that are applied to solve the mass transport equations have been discussed in Chapters 4 and 5. In the modeling system, there are 3 partial differential equations describing the transport of H^+, OH^-, and Pb(II) which require 6 boundary conditions. NO_3^- is solved through the preservation of electrical neutrality.

Initial concentrations for H^+ and OH^- are taken as 10^{-5} M and 10^{-9} M respectively assuming the soil pH is 5 at the beginning. Initial lead concentration is taken as 0.05 M or 3223 mg/kg. Note, all these initial values are taken only to supply rational information to model a case of lead transport and to verify the model's predictions. They are subject to change when modeling a specific experiment.

Table 7.2 Values of Parameters Used in Modeling Multi-species Transport

Parameter	Value
F	96,485.31 C/mol
τ	0.25
D_{H+}	8.05 cm^2/day
D_{OH-}	4.57 cm^2/day
D_{Pb}^{2+}	0.82 cm^2/day
D_{NO3-}	1.64 cm^2/day
k_e	0.864 cm^2/V·day
T	298 K
L	20 cm
n	0.56

Table 7.3 Characteristics of Georgia Kaolinite (From Hamed 1990)

Mineralogical Composition (% by Weight)	
Kaolinite	98
Illite	2
Index Properties (ASTM D 4318)	
Liquid Limit (%)	64
Plastic Limit (%)	34
Specific Gravity (ASTM D 845)	2.65
% Finer than 2 μm Size	90
Activity	0.32
Porosity	0.56
Cation Exchange Capacity (meq/100gm of dry soil)	1.06
Maximum Dry Density (tons/m^3)	1.37
Optimum Water Content (%)	31.0
Initial pH of Soil [a]	4.7 ~ 5.0
Compression Index (C_c)	0.25
Permeability of Specimens Compacted at the Wet of Standard Proctor Optimum ($\times 10^{-8}$ cm/sec)[b]	6 ~ 8

[a] pH measured at 50% water content

[b] Flexible Wall Permeability at Full Saturation

After the initial sorption reaction, the lead concentration in solution together with hydrogen and hydroxyl concentrations are used to obtain the initial value of nitrate concentration. Since the nitrate ions presented in the model are less reactive and is chosen to balance the electrical charge, they are of less importance in the analysis of the system. Table 7.4 lists the initial and boundary conditions used in the program.

Since the species concentrations change greatly with time, the range of time increments for obtaining a stable solution also changes in time, so does the element size. There is no available formulation specified to choose the time step and element size for a stable solution of modeling a system with such dramatic change in its parameters. Various combinations of time steps and element sizes were tried in the model. For a specific element size, different time steps were used until a relatively stable solution was obtained. It should be noted that "a relatively stable" means that in most trials, the program becomes unstable when a steep concentration gradient forms close to cathode side and thus a sharp front of electric conductivity develops in this area. This leads to the first and second derivatives of voltage in the transport equations to become too large. This often happens in the late stages of the modeling, for example, after four or five weeks in time of transport. More analysis and suggestions on this observation are given later.

A time step of 0.1 day and a finite element size of 2 mm are used in computing. Choosing such a fine element size was mainly due to avoiding the possible problems caused by boundary flux. When time step is changed, the numerical solution also change. But the solutions fall into a narrow range and a convergent solution is achieved always.

7.4 Results and Analysis

Program was run on RS/6000 IBM workstation to give predictions on lead

Table 7.4 Initial and Boundary Conditions

	Initial Values	Boundary Conditions
C_{H+}	10^{-5} M	equations 5-2, 5-5
C_{OH-}	10^{-9} M	equations 5-7, 5-8
C_{Pb}^{2+}	0.05 M	equations 5-13, 5-14
E	0.1 V/cm	algebraic equation 4-37 (no BCs)

$\Delta\phi$ = 2 volt

transport and removal using the preset conditions and initial data given above. Due to time constraints, no matching experiments were conducted in lab. Therefore the analysis of the results are made mainly based on previous research data and the emphasis is put on qualitative discussion of theoretical rationale of the predictions.

7.4.1 H^+ Transport and pH Distribution

H^+ is the prevailing species in a multi-component electrokinetic process, as was been discussed in Chapter 3. H^+ generated from the anode reaction is driven through the soil column by electric field and convection flow, meets with OH^- that is generated at cathode side and reacts complying to the water phase chemical equilibrium. This flux changes the pH environment of soils and fluids, and greatly influences the physico-chemical properties of soils and chemical equilibrium of ionic species and thus influences the transport process of other species.

Figures 7.3, 7.4 and 7.5 describes the transport of H^+ and OH^-, and soil pH changes in time across the soil predicted by the model, respectively. The mass flux of H^+ at anode decreases pH of soil at anode side to around 2, while flux of OH^- at cathode increases soil pH near cathode to about 7 (Figure 7.5).

Previous research showed an increase of pH to above 10 in cathode compartment (Pamukcu and Wittle 1992, Acar and Hamed 1991). In Figure 7.5, the pH only increases to about 7 at the cathode end of soil specimen. Report from Wittle and Pamukcu (1992) shows that there are buffer effects between electrode compartments and soil column. While the pH in the catholyte rises to 10-11, the value in soil that is close to the cathode may not be that high.

Besides the buffering effects, one more reason why pH in the soil at cathode end is lower compared with its value in the cathode compartment is the continuous consump-

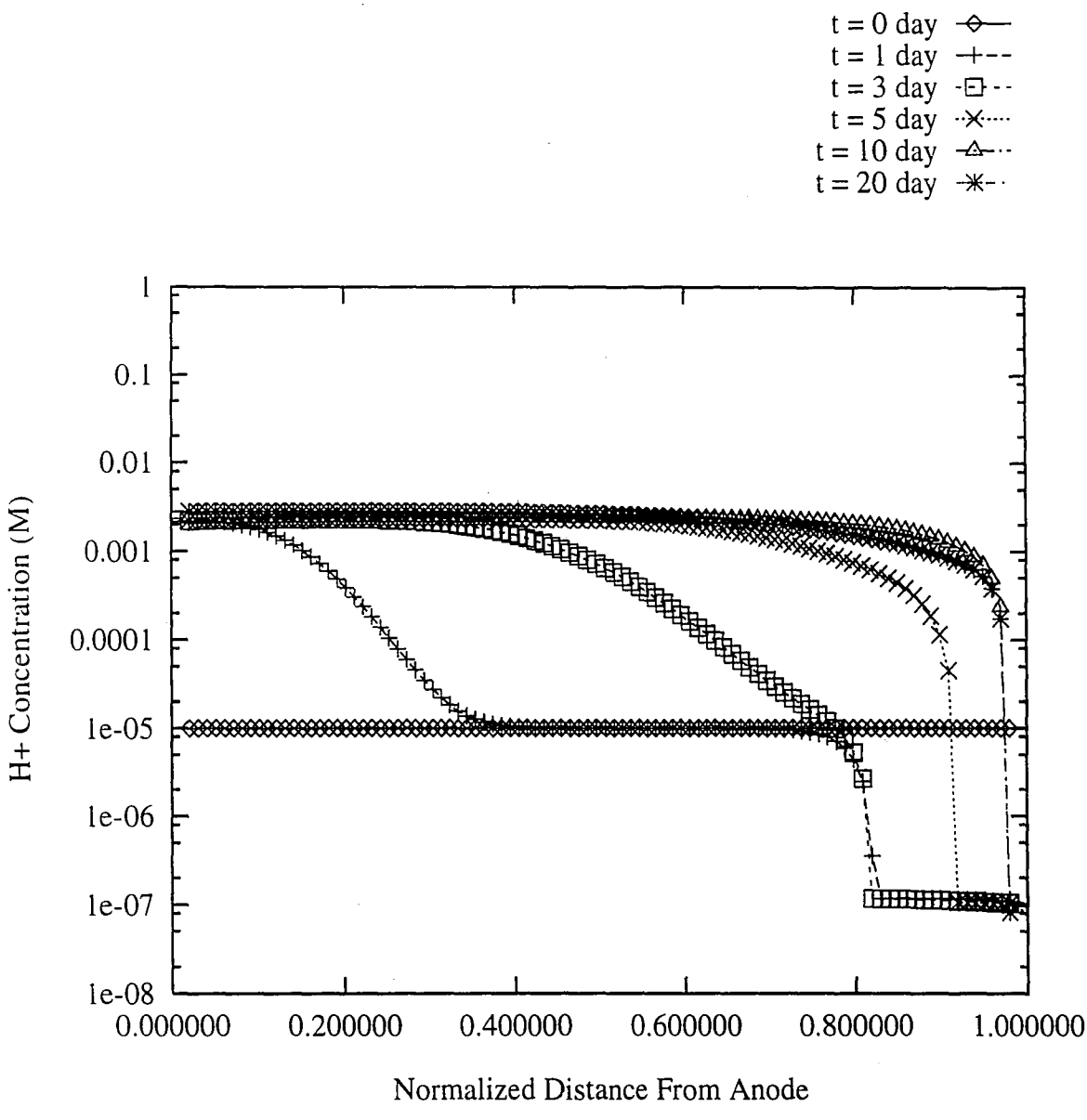

Figure 7.3 Hydrogen Transport Across the Soil Column

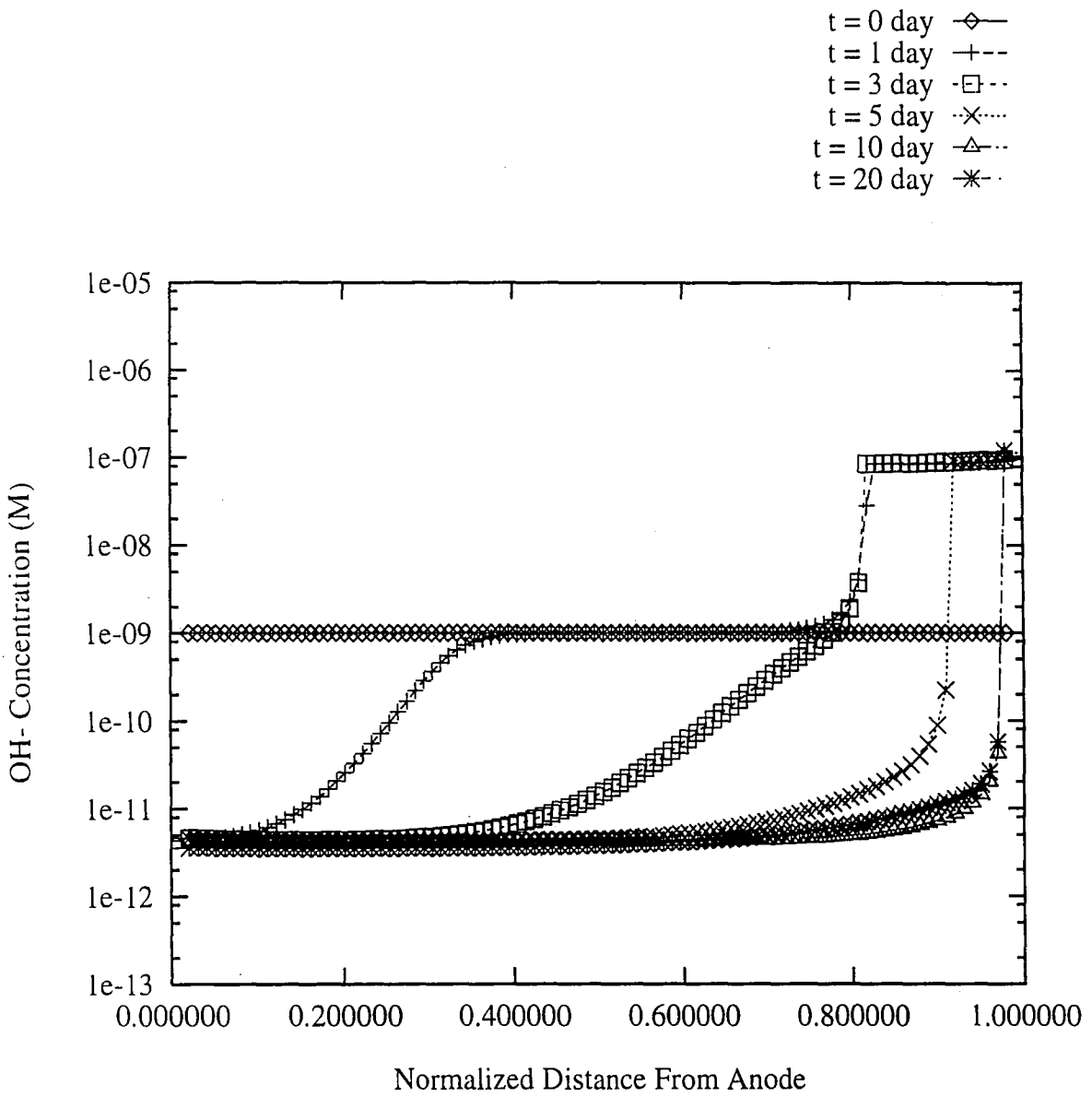

Figure 7.4 Hydroxyl Transport Across the Soil Column

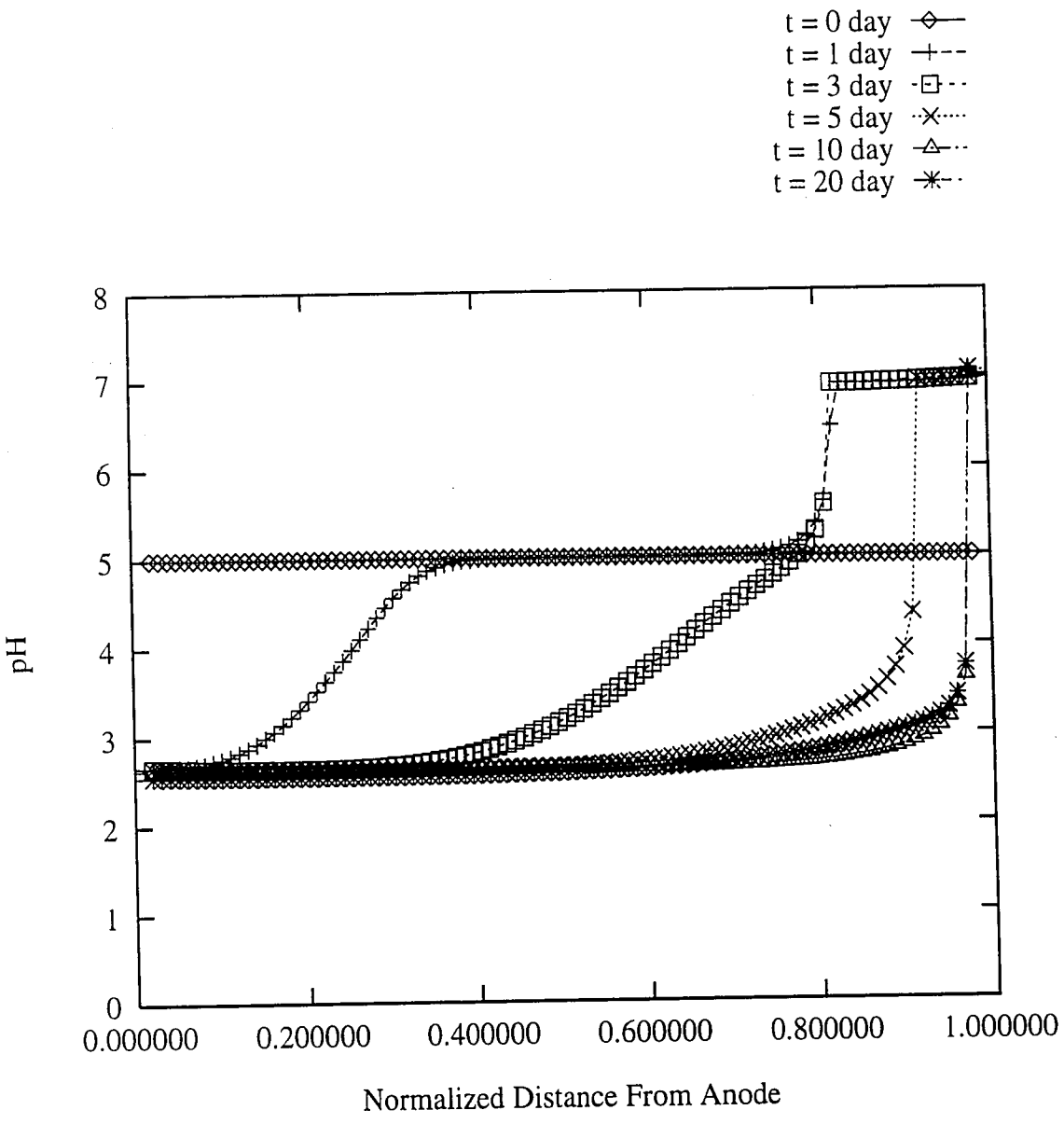

Figure 7.5 Predicted pH Profiles Along the Soil Column in Time

tion of OH^- due to chemical reactions in the soil at that location.

There are two types of reactions that OH^- participates. One is the water-auto-ionization; the other is lead precipitation reaction. The latter makes a decisive influence on the decrease of OH^- concentration near cathode end. Restrained by chemical equilibrium state, Pb(II) that moves toward the cathode side tends to combine with OH^- in a high pH environment to produce precipitation. Equations 5-17 and 5-18 govern the reaction process. The initial lead concentration is very high (0.05M) compared with the concentration of OH^-. Indeed most of the generated OH^- that flow into the soil from cathode compartment will be consumed by the Pb(II) in generation of $Pb(OH)_2$. As a result, the pH in soil near cathode zone will not go as high as it is in the catholyte. The predicted value of about 7 is reasonable.

Figure 7.5 also shows a trend that H^+ moves much faster toward cathode than OH^- toward anode. This complies well with experimental data and research reports that have been discussed in chapter 3. The model predicts that the acid front meets base at a place very close to cathode, at a point between 0.7-0.8 by normalized distance from anode. As the process continues, the acid front moves forward, drives the base front back to a thin soil film near the end of the soil column. In the simulation presented, this occurrence takes place after 10 days into the process. This state is relatively steady thereafter, meaning that new arriving ions of both H^+ and OH^- meet at this point to produce water.

7.4.2 Electric Conductivity and Electrical Field Strength

The electrical field is one of the key parameters in electrokinetic soil processing technology. An electrical voltage difference is applied to the ends of the soil specimen and thus an electrical field is generated through the soil medium. When charged ions transport under the influence of this externally applied electrical field, their concentration

distributions change with time and thus lead to the change of local electrical conductivity (Equation 4-26). The change of local electric conductivity directly alters the value of voltage gradient at that specific point. In other words, the distribution of electrical field strength is changed. The changing electrical field and electric conductivity are the results of mass transport through the soil column, and they thus describe the transport process of the species indirectly.

Figure 7.6 is the model predicted electric conductivity across the soil column. Equation 4-26 is used to evaluate the conductivity using charged concentrations that are present in the pore fluid. From that equation, it is apparent that the higher the total species concentration at a point, the higher the conductivity. The high initial concentrations result a high initial conductivity, as high as over 240 *C/V/day/cm* (or about 3 mS/cm). The decrease of dissolved lead concentration is prevailing over the increase of H^+ concentration due to a far higher initial concentration of Pb(II) than H^+ (0.05M to 10^{-5}M), and thus leads to the decrease of the conductivity across the soil. Basically, the change of the conductivity is decided by the initial conditions, the ionic mobility of each species and the production rate of H^+ at anode.

The conductivity becomes very low in the area close to the cathode. This reflects the great decrease of ionic species concentrations in this area. This low conductive area will require more voltage difference over it to keep a consistent current with other parts of the soil column. Finally a nonlinear electric potential profile will develop across the specimen.

This tendency is observed in Figure 7.7 where the electric potential distribution with time is presented. A uniform conductivity distribution at the beginning results a linear distribution of voltage across the soil. As the electrokinetic processing continues, we can expect a flatter potential curve except in the region close to cathode, where the electrical potential is likely to have the biggest gradient ($\partial V/\partial x$). This tendency agrees well with the experiment data that is reported by Wittle and Pamukcu, 1993 and Acar and Alshawabkeh (1996).

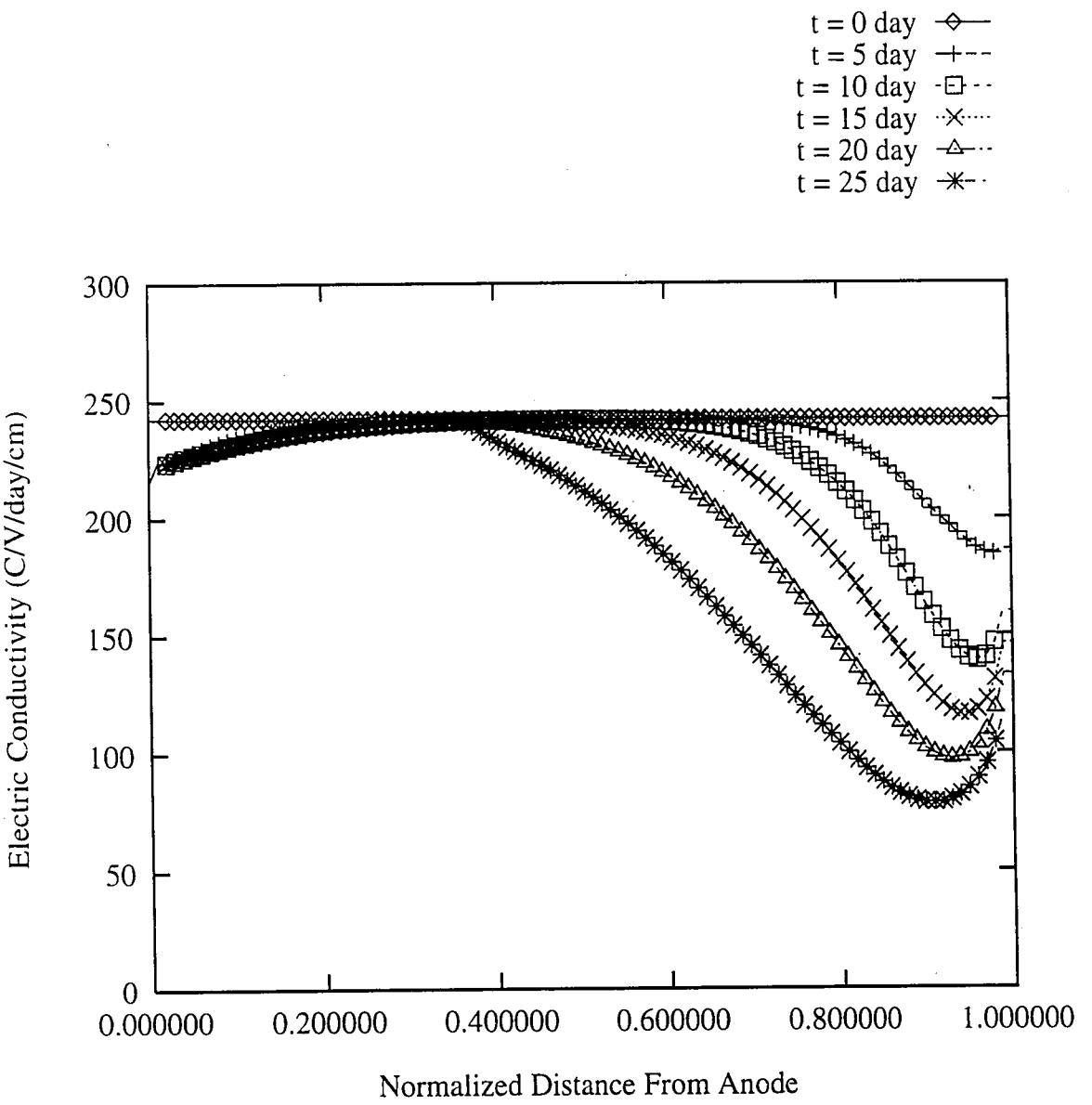

Figure 7.6 Electric Conductivity Profile Across Soil Specimen

A large electrical potential gradient (electrical field strength) means a lot to the electrokinetic enhanced mass transport process. From the mass transport equations, the potential gradient plays an important role in deciding the rate of species transport. Figure 7.8 displays the change of electrical field strength with time. The initially uniform distribution of potential gradient becomes non-linear in later stages due to the changes in electrical conductivity. A zone with high potential gradient develops close to the cathode side while near anode side the field strength keeps dropping. The rise of potential gradient near cathode is because of the drop of conductivity within that area, while the decrease of field strength in other side of soil is due to the decrease of electrical current. A reasonable expectation can be drawn from this figure that as processing continues, the potential gradient near cathode will continue to increase to a large value, while in other parts of the soil column, the field strength will become smaller and smaller to a value near zero.

Comparing Figures 7.6, 7.7, and 7.8, it can be observed that they describe the electrical field and the mass transport phenomena from different ways, yet they support each other for better understanding of their meaning. It should be noted that in figure 7.6, the conductivity value at the cathode interface rises up from the low depression behind it, which reflects that a higher concentration is present there than in the region before it. This, as will be shown later for lead transport, is due to the presence of higher lead concentration. This occurrance can also be observed in figures 7.8, where the gradient drops toward the cathode interface.

While theoretically, Pb(II) should keep moving toward the cathode under the electrical field, the dissolved lead should have its lowest concentration in soil at the cathode end. Such a model prediction is mainly caused by two factors. First, by comparing Figures 7.3 and 7.6, we can see that the increase in conductivity value at cathode end happens after about 10 days of processing. After 10 days, the H^+ front meetswith OH^- and reaches a stable state in a region very close to the cathode. To the left of this region (toward the anode), the pH environment becomes very low and it is unlikely that lead precipitation will take place there. Therefore the dissolved lead con-

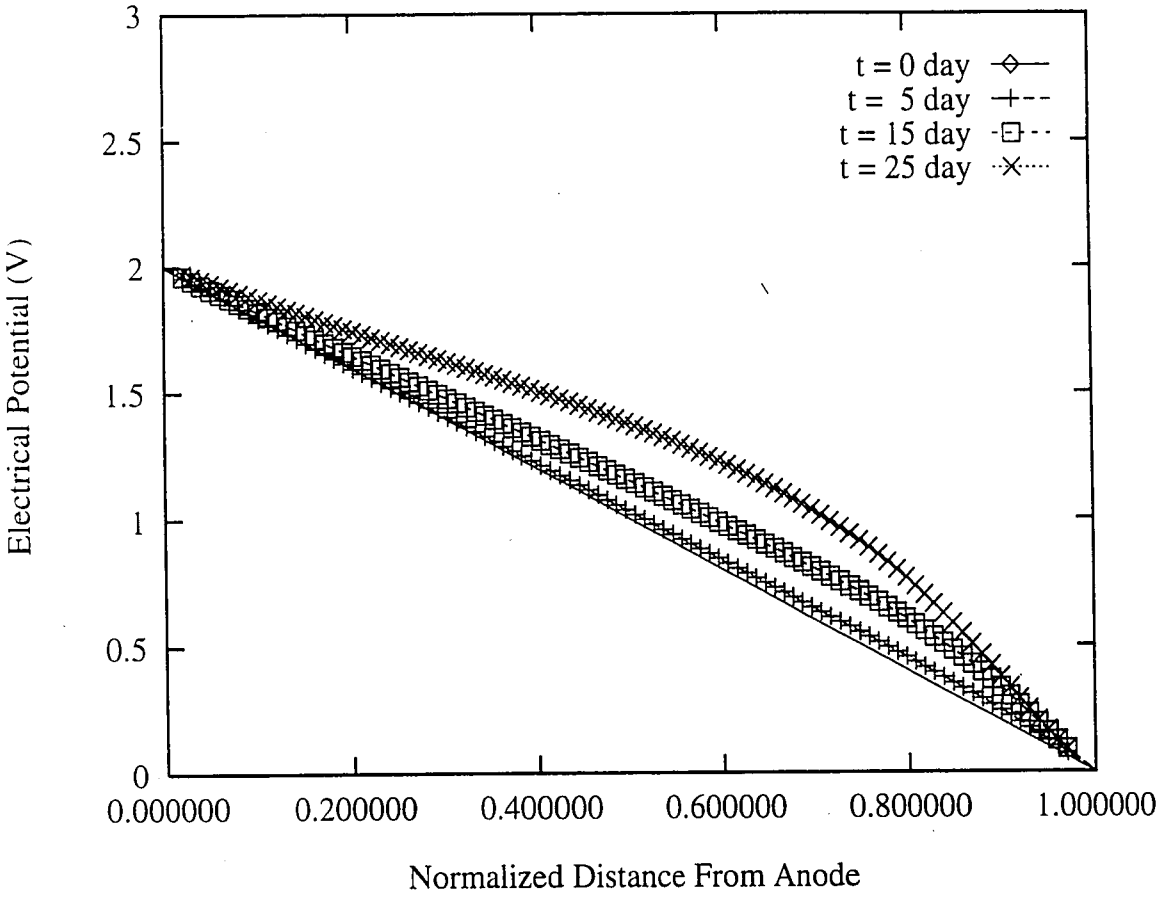

Figure 7.7 Predicted Electrical Potential Difference Profiles

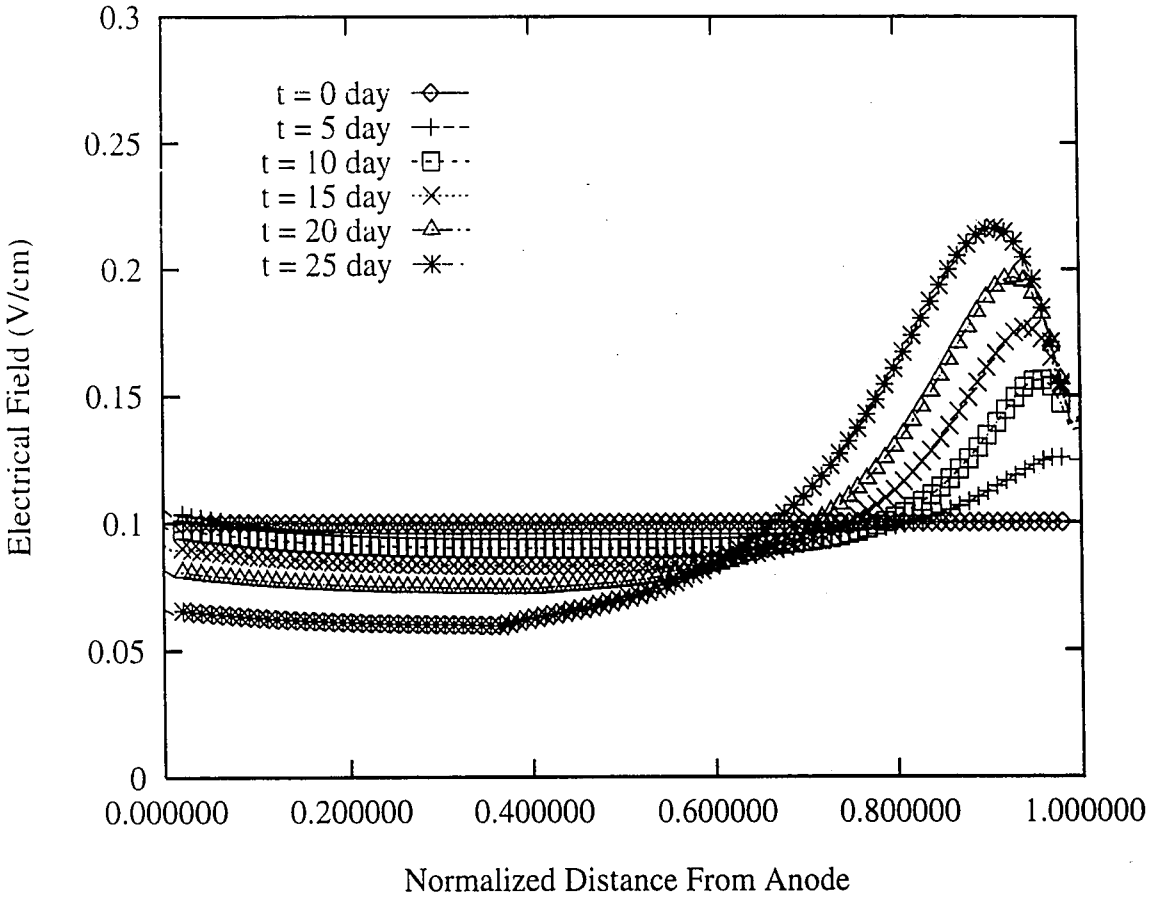

Figure 7.8 Electrical Field Distribution Across Soil Column

centration tend to rise before the acid/base interface.

The other reason is due to the influence of the boundary conditions. While a finite difference method is able to offer a stable solution for a system of partial differential equations, it is not very good in handling complex flux boundary condition. Although effort has been made to assure the least influence of boundary flux, a possible accumulation of numerical dispersion in describing the boundary conditions using the finite difference method over many iterations of time could affect the solution, especially at points near the boundaries.

7.4.3 Pb(II) Transport

The model generates four predictions for lead transport. They are presented in Figures 7.9 through 7.14. Figure 7.9 shows the dissolved lead concentration distribution profile in units of M (mol/l) while Figure 7.10 gives the same curves in units of weight concentration (mg/kg) for the convenience of comparison. Figure 7.11 displays the adsorbed lead profile at 0 and 35 days in units of mg/kg; Figure 7.12 gives the precipitated lead profile in mg/kg; and Figure 7.13 describes the total lead transport in mg/kg. Synthesis of these four profiles will generate a complete image for lead transport in a multicomponent system under electrical field. Figure 7.14 shows the components of final lead profile at the 35th day of processing.

It is noted that only the dissolved lead participates in the transport, the adsorbed lead and precipitated lead do not move. Only when lead dissolves into aqueous state from adsorbed or precipitated state it then can be transported. Therefore the profiles of adsorbed lead and precipitated lead are not the result of mass transport but the result of chemical reactions.

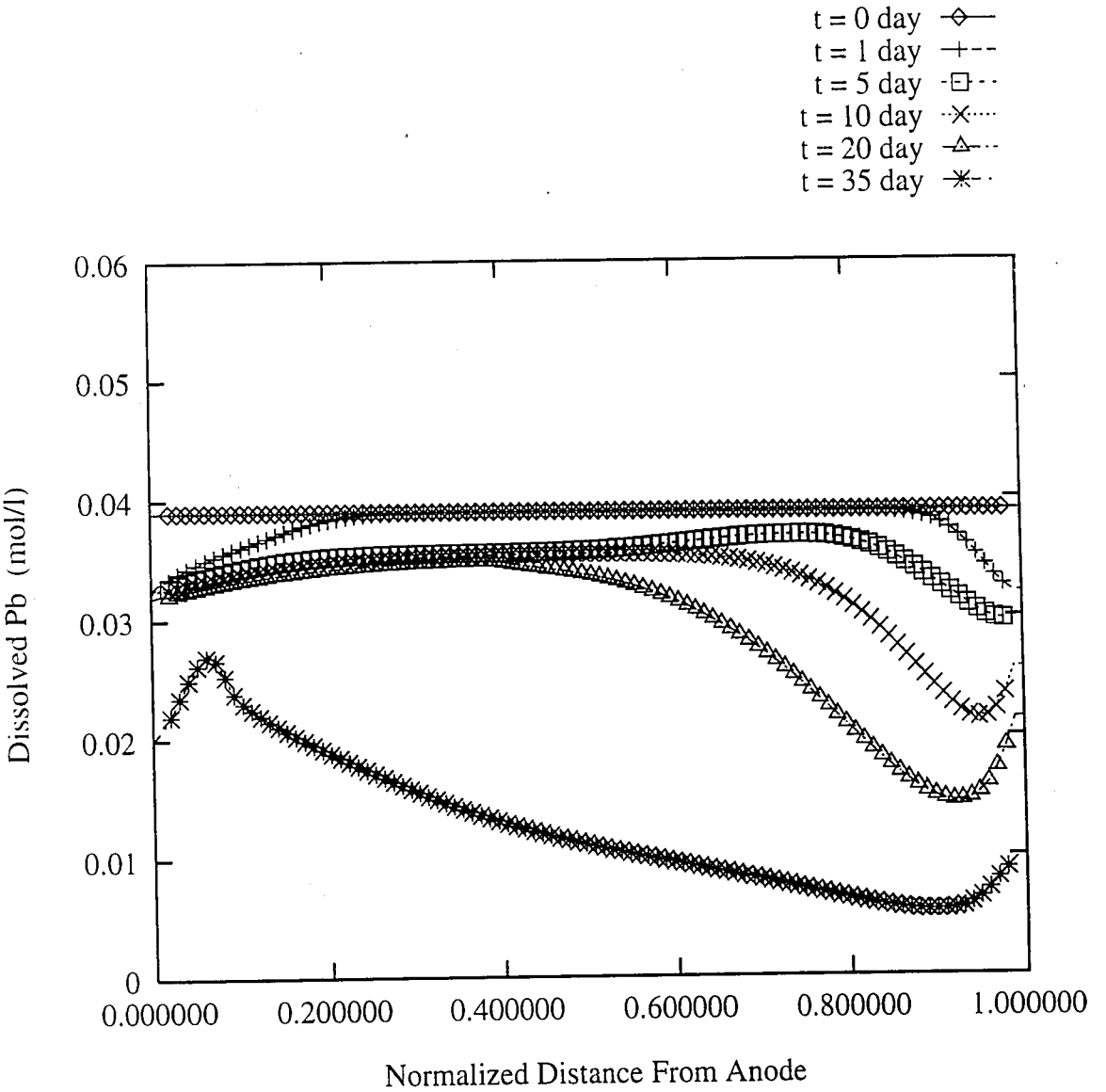

Figure 7.9 Dissolved Lead Concentration Distribution

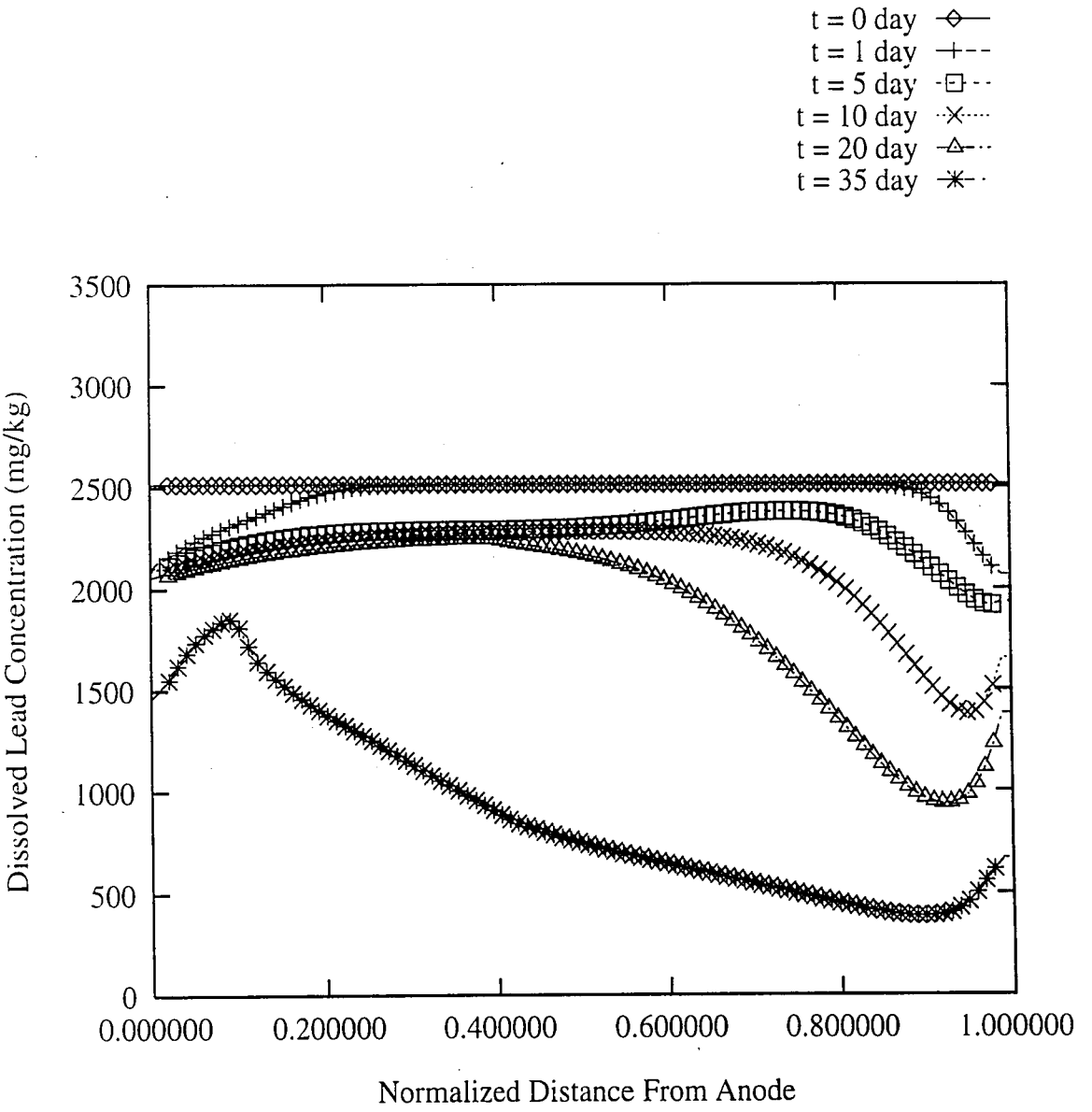

Figure 7.10 Dissolved Lead in Weight Concentration

Dissolved lead continuously transports towards the cathode under the electric field. The precipitation reaction taking place in a region near the cathode consumes the dissolved lead. This is the main reason of the presence of low Pb(II) concentration in that region (Figure 7.9). This leads to a low conductivity in the region and a high potential gradient over it. The high E value drives ionic lead faster towards the cathode and further decreases Pb(II) concentration in the region. Because the electric potential difference used in this simulation is relatively weak (2v/20cm), the high lead concentration front did not move as quickly as the field strength decreased. Transport rate of lead is slow at the normalized distance between 0 - 0.1 and the balance of the electromigration and diffusion results in the formation of high lead concentration front in this zone.

Adsorbed lead profile is presented only at the 35th day of processing besides its initial uniform distribution. A significant change of adsorbed lead concentration was not observed from model prediction until after about 30 days. As a result of decreased Pb(II) concentration and/or the decreased pH in soil pore fluid, the desorption starts at that time and a decrease of adsorbed lead concentration is observed. The desorption first occurs at a location in soil where the decrease of both pH and Pb(II) are the most significant. Very close to the cathode side, desorption is not observed due to a high pH environment (Figure 7.10).

The lead precipitation profile (Figure 7.11) displays the weighted concentration distribution of $Pb(OH)_2$ instead of Pb(II) only. Precipitation, like adsorption, retards lead transport, but at the same time decreases the Pb(II) concentration in pore fluid. As lead transport continues, the lead precipitation within a narrow zone very close to the cathode can go significantly high. This high lead precipitation near the cathode could also decrease the soil porosity in that region, block the flow path, and thus decrease the E-O flow. The net effect will be a decrease in the efficiency of electrokinetic processing. Enhancement techniques to prevent such a precipitation, such as the use of pH controlling agents at the cathode can be employed.

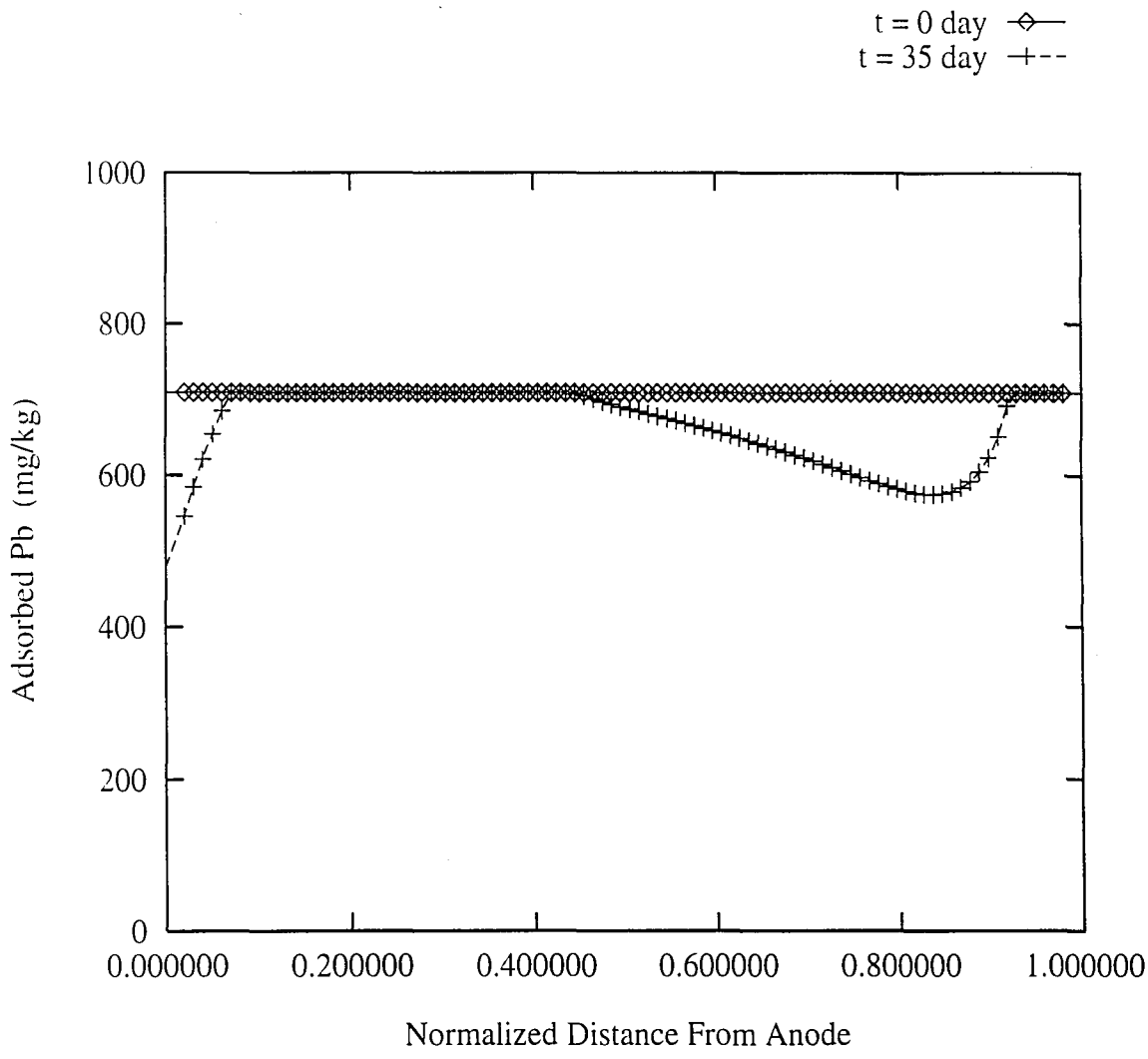

Figure 7.11 Adsorbed Lead Profile

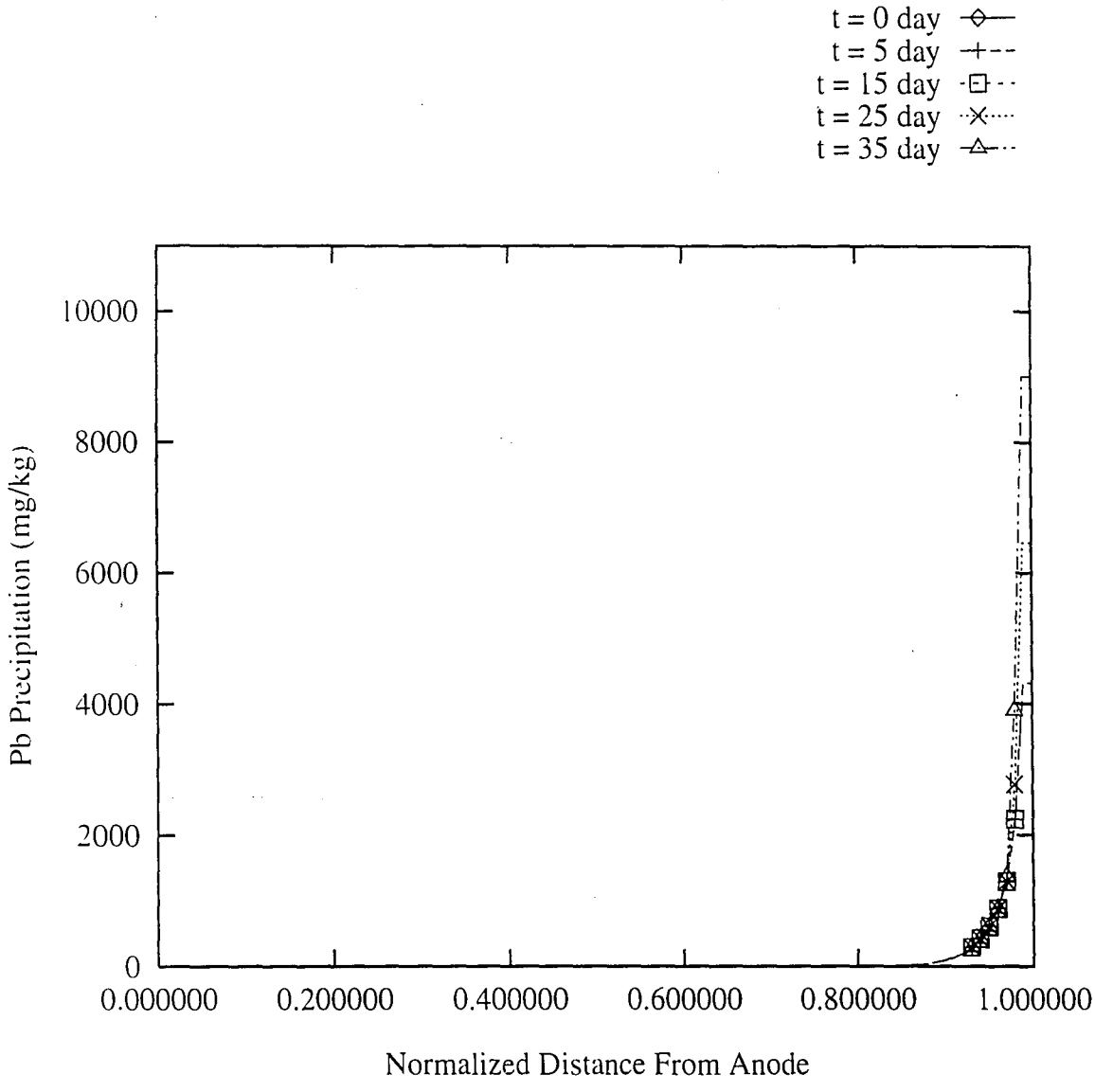

Figure 7.12 Lead Precipitation Profile

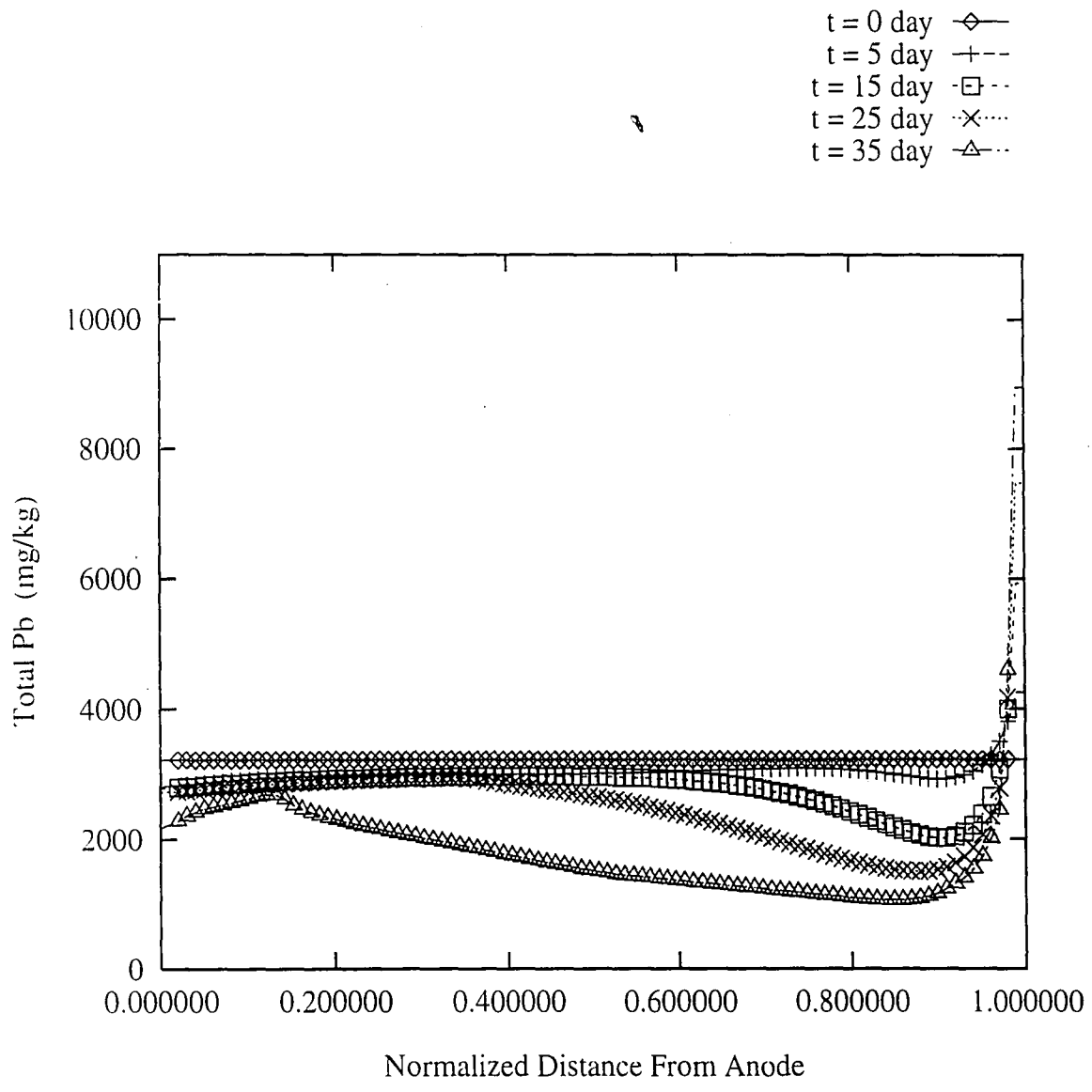

Figure 7.13 Total Lead Concentration Distribution Across Soil Column

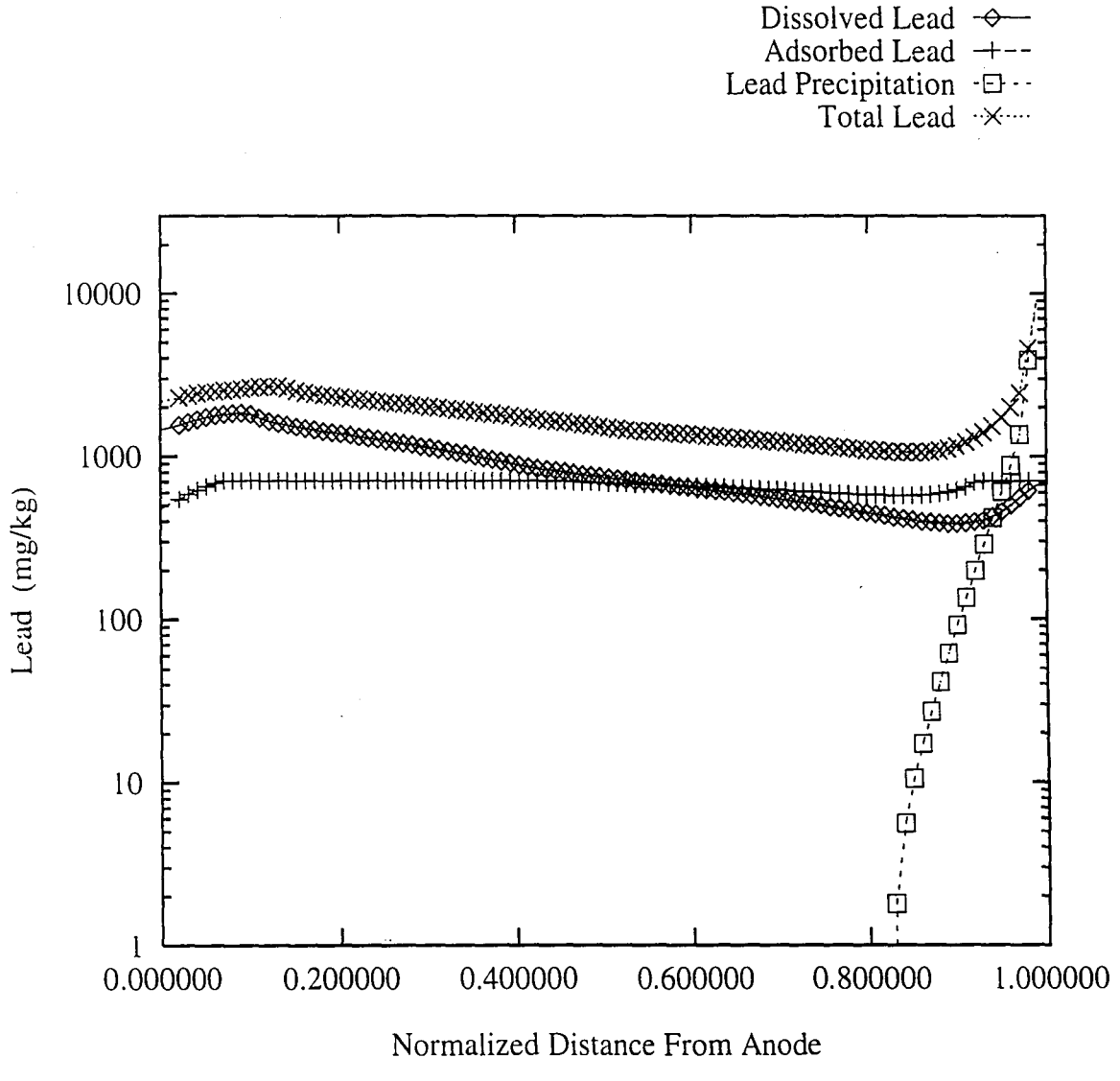

Figure 7.14 Lead Profile After 35 Days into Processing

The total lead transport and removal is shown in Figure 7.12. The model predicts an overall fall of lead concentration across the soil except in a thin film at the cathode side. In that zone, the total lead increases from initially below 4,000 mg/kg to about 9,000 mg/kg after 35 days. That increase is largely contributed by lead precipitation.

A relatively low rate of mass transport is predicted using the model. This is due to the low potential difference applied across the soil specimen (2 volt/20 cm). The low voltage generates low electrical current and thus leads to a low rate of transport. Again, the reason for using low initial electric field was because of the finite difference method that employed in this model and also because of the constant electrical potential difference condition under which this model is developed.

A high electrical field generates a high current flow which is used in the boundary conditions for H^+ and OH^- (Equations 5-2, 5-8). Finite difference method is not good at handling flux boundary conditions which vary greatly, and a higher current presented in the boundary equations could lead to numerical instability and give unrealistic solutions. Choosing a lower electric field can avoid such computing problems. Reports from both Lehigh's experiments and Alshawabkeh and Acar (1996) record a low initial voltage difference across the specimen. Alshawabkeh and Acar (1996) use an even smaller initial field strength (< 0.1V/cm) in their model.

In this work it was attempted to model the mass transport process under a constant applied potential difference across the soil column. Varied voltage that can be achieved by controlling the electrical current is not available in this program. In future modeling, a step voltage may be used to reach a higher transport rate. Accordingly experiments are required to check with the model prediction.

The predicted concentration distribution of NO_3^- is given in Figure 7.15. Since the nitrate concentration is computed from charge neutrality and Pb(II) has the biggest value of charge valence and initial concentration, the predicted nitrate concentration profile is very similar to dissolved lead concentration profile (referring to Figure 7.9) except its value was influenced by the increasing concentration of hydrogen ions.

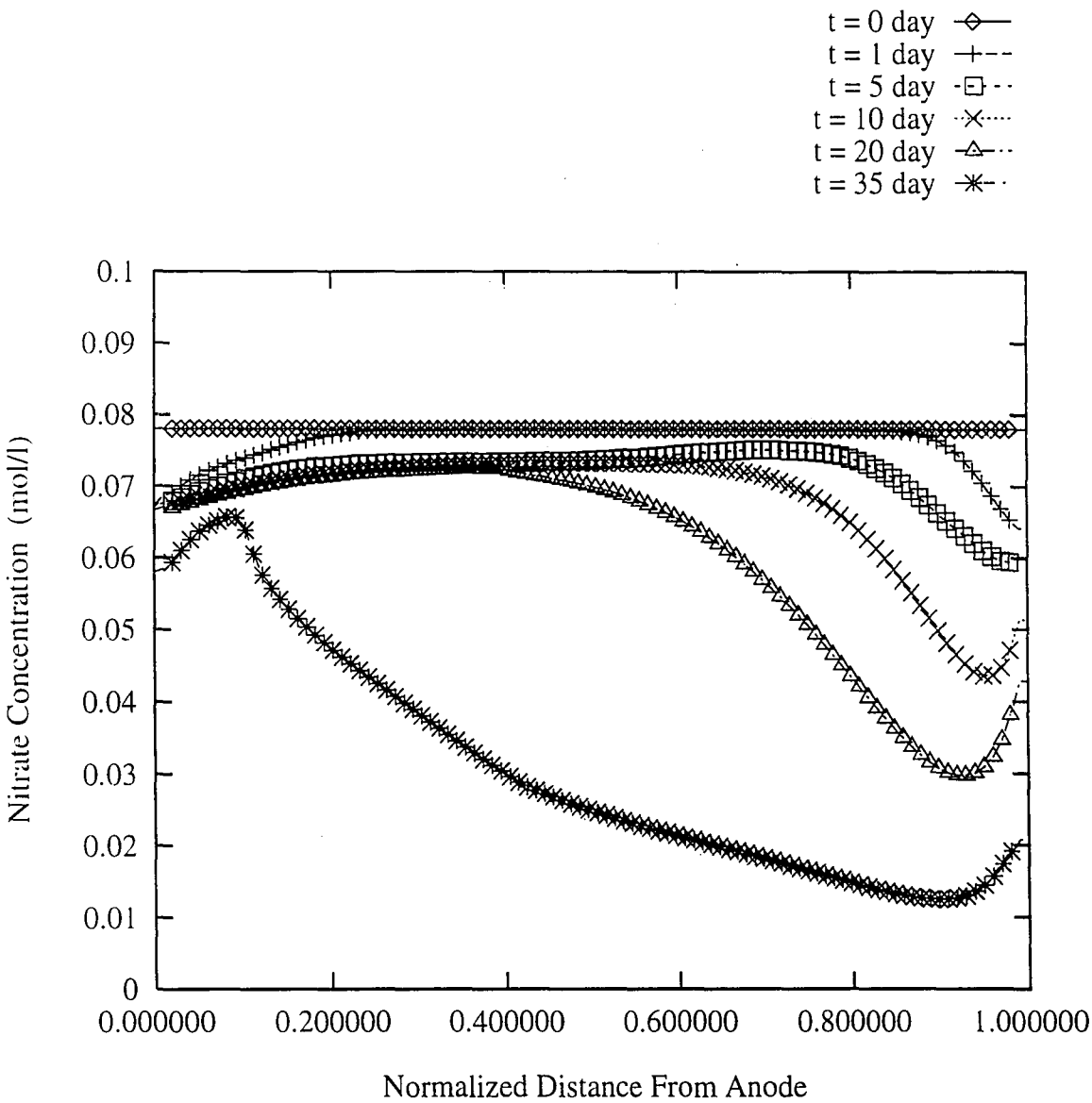

Figure 7.15 Nitrate Concentration Distribution Across the Specimen

CHAPTER 8
CONCLUSIONS AND RECOMMENDATIONS

8.1 Summary and Conclusions

Pollution of natural resources, especially due to heavy metal contaminants, is paid more and more serious attention to preserve the environment of planet earth. There are currently a variety of remediation technologies but most of them can barely handle soils with low hydraulic conductivities and their efficiency in restoring metal contaminated fine-grained deposits is usually undesirable. Innovative in-situ remediation technologies are in demand.

Electrokinetic soil processing is a promising and cost-effective technology that has emerged in recent years. Low level direct electric current is applied to contaminated soils which generates electrical field between electrodes through the soil. Electrolysis reactions at the electrodes produce acid or base concentrations. Hydrogen ions transport from anode toward the cathode under the electrical field while the hydroxyl ions transport from cathode to anode. Due to their different transport rates, an acid front develops and moves toward cathode side and leads to an acidified soil environment. Low pH values cause desorption and dissolution process of metal ions that are adsorbed by soil particles or present as precipitation products in the soil pore fluid. Chemical species in pore fluid transport toward different electrodes depending on their electric charge, driven by chemical gradients, electroosmotic flow, hydraulic gradient (if any, in a porous media with moderate hydraulic conductivity), and electrical field. Many experimental studies on electrokinetics have already demonstrated its feasibility of removing heavy metal contaminants and other cationic species from soils.

A modified mathematical model is developed to describe the process of multicomponent species transport under transient electrical field. Principles of mass conservation are applied to formulate one-dimensional flux equations for charge, species and fluid in saturated porous medium. Chemical reactions, such as electrolysis, precipitation/ dissolution, sorption/ desorption and water auto-ionization, are studied and included in the model. A constant electrical voltage difference across the ends of soil column and a changing electrical field are simulated by the model.

Finite Difference Method is used for numerical discretization to obtain solutions of the partial differential equations. An object-oriented program (OOP) is developed to perform the numerical modeling for one-dimensional transport of Pb(II), hydrogen, hydroxyl and nitrate ions under constant voltage difference condition. The program is also capable of modeling the process under constant current condition, as well as including the consideration of pore water pressure after a few simple modifications.

The model predictions describe reasonably well the mass transport process in electrokinetic processing, along with the change of electric field and electric conductivity. Several major conclusions from the model predictions are summarized below.

1. A non-linear yet unperturbed distribution of electrical potential difference across the column is expected. The tendency of the electrical potential change is understood and rationalized.

2. The decrease of electrical current under constant voltage difference is due to the decrease of overall electric conductivity which is the result of ion transport and removal from the soil. The precipitation of lead hydroxides and the movement of acid/base interface are major contributing factors for non-linear electric potential distribution.

3. A lower pH in cathode soil than in cathode compartment is observed due to the buffer effects, the water auto-ionization and lead precipitation reactions.

4. The electrical field developed in soil close to the cathode results in a large electrical gradient which causes numerical difficulties and leads to unstable computation after 35 days of simulation. This high electrical field occurs where sharp fronts of species concentration and pH profiles are observed. Finer discretization of this zone is required for accurate modeling of the process.

5. The continuity of mass transport and the stable state of the modeling is controlled by the transport of hydrogen and hydroxyl ions. Cations are continuously transported towards the cathode and accumulate there as long as there is continuous transfer of hydrogen and hydroxyl ions. Higher or lower initial cation concentration (i.e., Pb(II)) do not influence the stability of the model because at a late stage of the processing, hydrogen concentration distribution becomes dominant over other species (higher mobility and concentration) and so does its gradient close to the cathode.

8.2 Significance of This Study

A brief comparison of this study with previous model results is summarized below.

The model developed in this research brings together a multicomponent system, transient electrical field and complex chemical reactions. Model predictions of this study can better describe the reality of the electrokinetic process than single species transport model or a model with a constant electrical field assumption.

Of all the published models, only the one developed by Alshawabkeh and Acar (1996) is comparable with this model. The other recent model from Denisov et al. (1996) does not take into consideration the chemical reactions and does not have a convincing

numerical solution to compare results with.

The contribution of this study lies in two aspects: a constant electrical potential difference across the soil specimen is simulated; the concept of equivalent ionic mobility in limited concentration is implemented.

Constant electrical potential difference is easy to control in practice but difficult to simulate in a model. Model development and predictions under this condition for the first time reveal the principles of electrokinetic soil processing under constant voltage applied to the soil. It shows that a high initial voltage may not be applicable due to the very high initial conductivity of the pore fluid. Together with Alshawabkeh and Acar's model (1996) which is developed under constant current control, this study provides advancement over the existing E-K mass transport models.

In Alshawabkeh and Acar's model (1996), an experimental retardation factor is used to address the difference of transport rate between tests and model predictions. A detailed analysis was not conducted. In this study, the equivalent ionic mobility is introduced trying to explain the influence of concentrations toward the migration velocity. Instead of simply selecting a retardation factor, the mechanism of why ionic mobility is lower in the pore fluids than it is in dilute solutions is described in equation 4-12 and is implemented in the model.

Some differences between this model prediction and Alshawabkeh's results could be caused by several reasons. Besides the above differences in the two models, other possible influences come from: the low electrical potential difference applied in this study, different coefficients used in each model and different numerical solution scheme. The finite difference method used in this study could not describe well the flux boundary conditions and is very likely the most important factor causing the slight different predictions. The combined influences have made it very difficult to detect specifically deviations between the two predictions. A more detailed comparison of this model prediction with that of Alshawabkeh and Acar's model is of less importance due to lack of experimental data and due to the roughness of the solution process of this model at its

current stage.

8.3 Recommendations for Future Studies

Further development of the model and the program is suggested for better understanding of the transport process and for better performance of the modeling system. The following future studies are recommended:

1. Specifically designed bench-scale experiments and field tests are necessary to compare data with this particular model predictions and to modify the program. Experimental data is expected to include not only the lead transport and removal but also other ionic species. These data are needed to generalize the system for a general multi-species mass transport model. This generalization will render the development of a knowledge-based modeling system more closer to reality.

2. Although Finite Difference Method works well in solving regular differential equations, it does not handle complex boundary conditions well. Finite Element Method should be implemented in space discretization to better handle the boundary conditions. The other advantage of FEM is that it is easier and more stable than FDM to integrate different initial and boundary conditions. Its advantages in 2-D or 3-D simulation for a large scale system are also evident.

3. Special analysis and treatment should be made in handling the large gradient of electrical potential that is developed with time in a region close to the cathode. A finer element size or smaller time step or other numerical technologies to limit the gradient so as to avoid or delay the

numerical dispersion need to be studied and applied.

4. The presence of lead or other metal ions in solutions is not limited to the forms we have discussed. For example, except Pb(II) and $Pb(OH)_2$, lead could also appear in complex ionic forms depending on the redox potential and the pH environment. The effect of this complexation on species transport should be addressed and clarified through both experiment and mathematical analysis. Other chemical reactions and reactions of other species should be studied as well. The model should be modified to include these considerations for better accuracy and generalization.

5. It would be desirable to integrate the development of pore water pressure. This can reveal the contribution of electroosmosis toward the transport process. Information on suction and soil consolidation status is useful to evaluate the efficiency of processing and builds a connection between electrochemistry and soil mechanics.

6. Further study on equivalent ionic mobility is required. In current analysis, equation 4-12 is used to convert the ionic mobilities in dilute solution to their equivalency in fluid with limited concentrations. But equation 4-12 is only accurate for a binary electrolyte system. In the case of the presence of multispecies, complex chemical reactions may exist and a binary situation is not maintained. A better understanding of the influence between species and a suitable mathematical description are expected.

REFERENCES

Acar, Y.B., Gale, R.J., Alshawabkeh, A.N., Marks, R.E., Puppala, S., Bricka, M. and Parker, R., "Electrokinetic remediation: Basics and technology status", J. Hazardous Materials, v.40, pp117-137 (1995)

Acar, Y.B., Puppala, A., Marks, R., Alshawabkeh, A. and Gale, R.J., "An investigation of selected enhancement techniques in electrokinetic remediation", Electrokinetics Inc., Report to U.S. Army Waterways Experiment Station, 212p. (1994)

Acar, Y.B., Hamed, J., Alshawabkeh, A., Gale, R., "Cd(II) removal from saturated kaolinite by application of electrical current", Geotechnique, v.44, No.3, pp.239-254 (1994)

Acar, Y.B., A.N. Alshawabkeh, and R.J. Gale, "Fundamentals of extracting species from soils by electrokinetics", Waste Management, Vol.13, pp 141-151 (1993)

Acar, Y.B., Alshawabkeh, A.N., "Principles of electrokinetic remediation", Environ. Sci. Technol., Vol.27, No.13, 2638-2647 (1993)

Acar, Y.B., "Electrokinetic soil processing; A review of the state of the art", ASCE Grouting Conference, Special Publication No.30, Vol.2 : 1420 (1992)

Acar, Y.B., Li, H., and Gale, R.J., "Phenol removal from kaolinite by electrokinetics", ASCE, J. of Geotechnical Engineering. Vol. 118, No.11, 1837-1852 (1992)

Acar, Y.B., Gale, R., Putnam, G., Hamed, J., and Wong, R., "Electrochemical processing of soils: Theory of pH gradient development by Diffusion, Migration and linear Convection", J. Electro Analytical Chem., Louisiana State University (1989)

Acar, Y.B. and Hamed, J., "Electrokinetic soil processing in remediation/treatment; Synthesis of available data", Bulletin of the Transportation Research Record, No.1312, Soils Geology and Foundations, Geotechnical Engineering, 152 (1991)

Alloway, B.J., Heavy metals in soils, John Wiley & Sons Inc., New York, p339. (1990)

Alshawabkeh, A.N., and Y.B. Acar, "Electrokinetics remediation. II: Theoretical model", J. Geotechnical Eng. Vol.122, No.3, 186-196 (1996)

Alshawabkeh, A.N., and Y.B. Acar, "Removal of contaminants from soils by electro-kinetics: A theoretical treatise", J. Environmental Sci. and Health, A27(7), 1835-1861 (1992)

Adamson,W.A., Physical Chemistry of Surfaces, Fifth Edition. Wiley, New York, 1990

Banarjee, S., Horng, J., Ferguson, P., and Nelson, O., "Field-scale feasibility study of electrokinetic remediation", U.S. EPA, Risk Reduction Engineering Laboratory, Office of Research and Development (1988)

Brenner, H. "The diffusion model of longitudinal mixing in beds of finite length. Numerical values", Chem. Eng. Soc., 17: 229-243 (1962)

Bruell, C.J., Segall, B.A., and Walsh, M.T., "Electroosmotic removal of gasoline hydrocarbons and TCE from clay", J. Environ. Engin., 118, (1992)

Casagrande, L., "Electro-osmotic stabilization of soils", J. Boston Soc. Civil Engr, 39, 285-317 (1952)

Chan, D.Y.C., Pashley, R.M., and Quirk, J.P., "Surface potential derived from co-ions exclusion measurements on homoionic montmorrilonite and illite", Clays & Clay Minerals: 32, 131-138 (1984)

Cussler, E.L. Diffusion: Mass transfer in fluid systems, Cambridge University Press, (1984)

Debye, P. Polar Molecules, Chemical Catalogue Company, Reinhold, New York. (1936)

Denisov, G., Hicks, R.E., and Probstein, R.F., "On the kinetics of charged contaminant removal from soils using Electric fields", J. Colloid and Interface Sci., Vol. 178, 309-323 (1996)

Dukhin, S.S, and Shilov, V.N., Dielectric Phenomena and Double Layer in Disperse Systems and Polyelectrolytes, John Wiley and Sons, Inc., pp 192 (1974)

Ferris, A.P. and Jepson, W.B., "The exchange capacities of kaolinite and the preparation of homoionic clays", J. Colloid and Interface Sciences, Vol.51, No.2, pp245-259 (1975)

Gray, D.H. and J.K. Mitchell, "Fundamental aspects of electro-osmosis in soils", J. Soil Mech. and Found., 93, 209-236 (1967)

Gray, D.H., Somogyi, F., "Electro-Osmotic dewatering with polarity reversals", J. Geotech Engr. Div., ASCE, Vol. 103, No. GT1, pp51-54 (1977)

Hamaker, J.W., and J.M. Thompson, "Adsorption" in Organic Chemicals in the Soil", New Orleans, LA, USA Environment, Vol.6, C.A. Goring and J.W. Hamaker, Eds., New York: Marcel Dekker, Inc., pp 49-143 (1972)

Hamed, J. "Decontamination of soil using Electro-osmosis", Dissertation, Louisiana State University, LA (1990)

Hamed, J., Acar, Y.B., Gale, R.J., "Pb(II) removal from kaolinite by electrokinetics", ASCE, Journal Geotech. Eng., Vol.117, No.2, 241-271 (1991)

Hamnet, R. "A study of the processes involved in the electro-reclamation of contaminated soils", MS thesis presented to the University of Manchester, at Manchester, England. (1980)

Harter, R.D. "Effect of soil pH on adsorption of Lead, Copper, Zinc, and Nickel", Soil Sci. Soc. Am. J., No. 47, 47-51 (1983)

Hicks, R.E. and Tondorf S., "Electrorestoration of metal contaminated soils", Environ. Sci. & Technol. v.28, No.12 (1994)

Hsu, C., Menon, R.M., Yeung, A.T., "Electrokinetic extraction of lead from kaolinite: II. Experimental studies", Proc. 3rd International Symposium on Environmental Geotechnology, San Diego, June 10-12, Vol.2 (1996)

Keller, H.B., "The numerical solution of hyperbolic partial differential equations by the method of characteristics", Mathematical Methods for Digital Computers, Eds. by Ralston, A., John Wiley and Sons, NY (1960)

Khan, L.I., Pamukcu, S., Kugelman, I., "Electroosmosis in fine-grained soil", Proceeding of the 2nd International Symposium on Environmental Geotechnology, Vol. 1, Lehigh University (1989)

Khan, L.I. "Study of Electroosmosis in soil: A modified theory and its application in soil decontamination", Dissertation, Lehigh University, Bethlehem, PA (1991)

Kortüm, G., and Bockris, J.O'M, TextBook of Electrochemistry, Elsevier Publishing, Volume I, pp180 (1951)

Kreft, A. and Zuber, A., "On the physical meaning of the dispersion equation and its solutions for different initial and boundary conditions", Chem. Eng. Sci., 33:

1471- 1480 (1978)

Lafolie, F. and Ch. Hayot, "One-dimensional solute transport modeling in aggregated porous media. Part 1. Model description and numerical solution", J. Hydrology, 143:63-83 (1993)

Lageman, R., "NATO/CCMS Pilot Study: Demonstration of remedial action technologies for contaminated land and groundwater. Theory and Praxis of Electro-Remediation", Copenhagen, Denmark. (1989)

Leij, F.J., Dane, J.H., and van Genuchten, M.Th., "Mathematical analysis of one-dimensional solut transport in a layered soil profile", Soil Sci. Soc. Am. J., 55:944-953 (1991)

Lockhart, N.C., "Electro-Osmotic dewatering of clays. I. Influence of voltage", Colloids and Surfaces, Vol.6, pp229-238 (1983)

Low, P.F., "Structural component of the swelling pressure of clays", Langmuir 3, 18-25 (1987)

Mitchell, J.K., Fundamentals of soil behavior, Second Edition, John Wiley & Sons, Inc., New York. (1993)

Mitchell, J.K., "Potential uses of electrokinetics for hazardous waste site remediation", Electrokinetically Treatment and its Application in Environmental Geotechnical Engineering for Hazardous Waste Site Remediation, Aug. 4-5 (1986)

Mitchell, J.K. and Yeung, T.C., "Electro-kinetic flow barriers in compacted clay", Transportation Research Record, No. 1288, Soils Geology and Foundations, Geotechnical Engineering, 1-10 (1990)

Miller, S.E., "Characterization of the electrical double layer of montmorillonite", PhD Dissertation, Purdue Univ., West Lafayette, Indiana, 93pp. (1984)

Moldrup, P., Yamaguchi, T., Hansen, J., and Rolston, D.E., "An accurate and numerically stable model for one-dimensional solut transport in soils", Soil Science, Vol. 153, No.4 261-273 (1992)

Parker, J.C. and van Genuchten, M.Th., "Flux-averaged and volume-averaged concentrations in continuum approaches to solute transport", Water Resour. Research, 22:399-407 (1984)

Pamukcu, S., Wittle, J.K., "Electrokinetically Enhanced In-situ Soil Decontamination",

Remediation of Hazardous Waste Contaminated Soils, Marcel Dekker Inc. (1994)

Pamukcu, S. "Electrokinetic removal of coal tar constituents from contaminated soils", Electric Power Research Institute, EPRI TR-103320 (1994)

Pamukcu, S. and Wittle, J.K., "Electrokinetic removal of selected heavy metals from soil", Environ. Prog., 11, 241-250 (1992)

Pamukcu, S. and Wittle, J.K., Experimental Data, (1993)

Probstein, R.F., "Remediation of metal contaminated soil by electric fields", Proc. of the Twentieth Annual USEPA-RREL Research Symposium, EPA/600/R-94/011 210-215 (1994)

Probstein, R.F., Physicochemical Hydrodynamics, An introduction, Butterworth-Heinemann, p191 (1989)

Probstein, R.F., P.C. Renaud, "Quantification of fluid and chemical flow in electro-kinetics", Electro-Kinetic Treatment and its Application in Environmental Geotechnical Engineering for Hazardous Waste Site Remediation, Aug. 4-5 (1986)

Putnam, G., "Development of pH gradients in electrochemical processing of kaolinite", MS thesis, Louisiana State University. (1988)

Raythatha, R., and Sen, P.N., "Dielectric properties of clay suspensions in MHz to GHz range", J. of Colloid and Interface Sci., Vol. 109, No. 2, 301-309 (1986)

Saville, D.A., and Palusinski, O.A., "Theory of electrophoretic separations", AIChE J. 32, 207-214 (1986)

Segal, B.A. and Bruell, C., "Electroosmotic contaminant-removal processes", ASCE, J. of Environmental Engineering, Vol. 118, No.1, 84-100 (1992)

Segal, B.A., O'Bannon, C.E., and Matthias, J.A., "Electroosmosis chemistry and water quality", J. Geotech. Engin. Div., 106, 1143-1147 (1980)

Selim, H.M., "Modeling the transport and retention of inorganics in soils", Advances in Agronomy, V.47, 331-384 (1992)

Shapiro, A.P., Renauld, P., and Probstein, R., "Preliminary studies on the removal of chemical species from saturated porous media by electro-osmosis", Physicochemical Hydrodynamics, 11:785 (1989)

Shapiro, A.P., and Probstein, R.F., "Removal of contaminants from saturated clay by electroosmosis", Env. Sci. Tech., 27, 283-291 (1993)

Stern, O., Z. Electrochemistry, 30, 508 (1981)

Van Genuchten, M.Th. and Parker, J.C., "Boundary conditions for displacement experiments through short laboratory soil columns", Soil Sci. Soc. Am. J., 48:703-708 (1984)

West, L.J. and Stewart, D.I., "Effect of zata potential on soil electrokinetics", Geoenvironment 2000:characterization, containment, remediation, and performance in environmental geotechnics, New York, N.Y. : American Society of Civil Engineers, 1535-1549 (1995)

Wittle, J.K., and Pamukcu, S., "Electrokinetic treatment of contaminated soils, sludges and lagoons", DOE/CH-9206, Final Report, Argonne National Laboratory, Chicago (1993)

Yeh, G.T. and Tripathi, V.S., "A critical evaluation of recent developments in hydrogeochemical transport models of reactive multichemical components", Water Resouces Research, Vol. 25, No.1, 93-108 (1989)

Yeung, A.T., Hsu, C., Menon, R.M., "EDTA-enhanced electrokinetic extraction of lead", J. Geotechnical Eng., ASCE, Vol. 122, No.8, 666-673 (1996)

Yin, J., Finno, R.J., and Feldkamp, J.R., "Electro-osmotic mobility measurement for kaolinite clay", Proceedings of the Specialty Conference on Geotechnical Practice in Waste Disposal. Part 2 (of 2), New Orleans, LA, USA (1995)

Yong, R.N., Warkentin, B.P., Phadungchewit, Y., and Galves, R., "Buffer capacity and lead retention in some clay materials", J. Water, Air, and Soil Pollution. No. 53, 53-67 (1990)

APPENDIX A

NUMERICAL INTEGRATION
OF
BOUNDARY CONDITIONS

Boundary conditions for solving mass transport equations for H^+, OH^-, and Pb(II) are given as

1) For H^+

At the anode:

$$-D^*_{H+}\frac{\partial c_{H+}}{\partial x} + (k_e + v_m^{H+})Ec_{H+}\Big|_{x=0} = c_0^{H+}J_w + \frac{I}{F} \qquad \text{[A-1]}$$

At the cathode:

$$-D^*_{H+}\frac{\partial c_{H+}}{\partial x} + (k_e + v_m^{H+})Ec_{H+}\Big|_{x=L} = c_{H+}J_w \qquad \text{[A-2]}$$

2) For OH^-

At the anode:

$$-D^*_{OH-}\frac{\partial c_{OH-}}{\partial x} + (k_e + v_m^{OH-})Ec_{OH-}\Big|_{x=0} = c_0^{OH-}J_w \qquad \text{[A-3]}$$

At the cathode:

$$-D^*_{OH-}\frac{\partial c_{OH-}}{\partial x} + (k_e + v_m^{OH-})Ec_{OH-}\Big|_{x=L} = c_{OH-}J_w - \frac{I}{F} \qquad \text{[A-4]}$$

3) For Pb(II)

At the anode:

$$-D^*_{Pb}\frac{\partial c_{Pb}}{\partial x} + (k_e + v_m^{Pb})Ec_{Pb}\Big|_{x=0} = 0 \qquad \text{[A-5]}$$

At the cathode:

$$-D_{Pb}^{*}\frac{\partial c_{Pb}}{\partial x}+(k_e+v_m^{Pb})Ec_{Pb}\big|_{x=L}=c^{Pb}J_w \qquad \text{[A-6]}$$

To keep consistent with transport equations, replace x with normal length X, $X\in[0,1]$. J_w is given in equation 4-21 and is

$$J_w=k_eE \qquad \text{[A-7]}$$

therefore the above boundary conditions can be rewritten as:

1) For H^+

At the anode:

$$-\frac{D_{H+}^{*}}{L^2}\frac{\partial c_{H+}}{\partial X}+\frac{(k_e+v_m^{H+})}{L}Ec_{H+}\big|_{X=0}=c_0^{H+}\frac{k_eE}{L}+\frac{I}{FL} \qquad \text{[A-8]}$$

At the cathode:

$$-\frac{D_{H+}^{*}}{L^2}\frac{\partial c_{H+}}{\partial X}+\frac{(k_e+v_m^{H+})}{L}Ec_{H+}\big|_{X=1}=c_{H+}\frac{k_eE}{L} \qquad \text{[A-9]}$$

2) For OH^-

At the anode:

$$-\frac{D_{OH-}^{*}}{L^2}\frac{\partial c_{OH-}}{\partial X}+\frac{(k_e+v_m^{OH-})}{L}Ec_{OH-}\big|_{X=0}=c_0^{OH-}\frac{k_eE}{L} \qquad \text{[A-10]}$$

At the cathode:

$$-\frac{D^{*}_{OH-}}{L^{2}}\frac{\partial c_{OH-}}{\partial X}+\frac{(k_e+v^{OH-}_m)}{L}Ec_{OH-}\Big|_{X=1}=c_{OH-}\frac{k_eE}{L}-\frac{I}{FL} \qquad \text{[A-11]}$$

3) For Pb(II)

At the anode:

$$-\frac{D^{*}_{Pb}}{L^{2}}\frac{\partial c_{Pb}}{\partial X}+\frac{(k_e+v^{Pb}_m)}{L}Ec_{Pb}\Big|_{X=0}=0 \qquad \text{[A-12]}$$

At the cathode:

$$-\frac{D^{*}_{Pb}}{L^{2}}\frac{\partial c_{Pb}}{\partial X}+\frac{(k_e+v^{Pb}_m)}{L}Ec_{Pb}\Big|_{X=1}=c^{Pb}\frac{k_eE}{L} \qquad \text{[A-13]}$$

To simplify the expressions, define

$$D'=\frac{D^{*}}{L^{2}}$$

$$v'=\frac{(k_e+v_m)}{L}E \qquad \text{[A-14]}$$

then equations A-8 ~ A-13 can be generalized into the following two equations:

At the anode:

$$-D'\frac{\partial c}{\partial X}+v'c\Big|_{X=0}=a \qquad \text{[A-15]}$$

At the cathode:

$$-D' \frac{\partial c}{\partial X} + v' c \Big|_{X=1} = b \qquad \text{[A-16]}$$

where c is a generalized concentration, a and b are generalized boundary flux outside soil specimen. The values of a and b are independent with boundary equations and their expressions for each species are given in above equations.

Finite Difference Method is applied to discretize these equations. Using forward difference for equation A-15 and backward difference for equation A-16, the numerical formulations are obtained:

At the anode:

$$\left(\frac{D'}{\Delta X} + v_1'\right) c_1 - \frac{D'}{\Delta X} c_2 = a \qquad \text{[A-17]}$$

At the cathode:

$$\frac{D'}{\Delta X} c_{n-1} + \left(-\frac{D'}{\Delta X} + v_n'\right) c_n = b \qquad \text{[A-18]}$$

where v_1' is the combined velocity of ions in soil at anode with 1 denoting spatial point at anode, v_n' is the combined velocity of ions in soil at cathode with n denoting spatial point at cathode. c_1 and c_n are thus the concentrations at anode and cathode points respectively.

Recall the global matrix described in equation 6-18,

$$\begin{bmatrix} a_1 & b_1 & 0 & \cdots & & & 0 \\ e_2 & a_2 & b_2 & 0 & \cdots & & 0 \\ 0 & e_3 & a_3 & b_3 & 0 & \cdots & 0 \\ \cdots & & & & & & 0 \\ \cdots & & & & & & 0 \\ \cdots & & & & 0 & e_{n-1} & a_{n-1} & b_{n-1} \\ \cdots & & & & & e_n & a_n \end{bmatrix} \begin{bmatrix} c_1 \\ c_2 \\ \cdot \\ \cdot \\ \cdot \\ c_{n-1} \\ c_n \end{bmatrix} = \begin{bmatrix} d_1 \\ d_2 \\ \cdot \\ \cdot \\ \cdot \\ d_{n-1} \\ d_n \end{bmatrix} \qquad \text{[A-19]}$$

To integrate the boundary conditions as described in equations A-17, A-18, coefficients a_1, b_1, e_n, a_n and right hand side values d_1 and d_n are modified to reflect the boundary flux:

$$a_1 = \left[\frac{D'}{\Delta X}\right]_1 + v_1' \qquad \text{[A-20]}$$

$$b_1 = -\left[\frac{D'}{\Delta X}\right]_1 \qquad \text{[A-21]}$$

$$e_n = \left[\frac{D'}{\Delta X}\right]_n \qquad \text{[A-22]}$$

$$a_n = -\left[\frac{D'}{\Delta X}\right]_n + v'_n \qquad \text{[A-23]}$$

and

$$d_1 = a; \qquad d_n = b; \qquad \text{[A-24]}$$

Use the modified matrix to solve the equation 6-19 numerically

$$A' \cdot c = d' \qquad \text{[A-25]}$$

where A′ and d′ are modified matrices that integrate the boundary conditions. The above process gives out the numerical solution of the partial differential equations for mass transport with flux boundary conditions.

APPENDIX B

SAMPLE INPUT AND OUTPUT FILES

Program lists can be obtained through Fritz Engineering Library at Lehigh University.

The followings are the sample input and output files of the program. Due to the length of the files, not all data is listed here.

Filename: input.dat

```
#
#  # signs are comments so one can use these lines
#  to enter reminders about the data used
#  for the simulation
#

#
# any line that starts with a keyword and is followed by an = sign is a
# data line

#
# blank lines are ignored

#
# keyword nSpec is the number of species

nSpec = 4

#
# KeyWord E0 is the Electric field strength

E0 = 0.1          # in volts/cm

#
# keyword path is the actual length of the specimen

path = 20.0      # in cm

##########################################################
##                                                      ##
## Now The Species Follow.  Each Line is of The         ##
## Form:     species# : property_name = value           ##
##                                                      ##
##########################################################

 0 : name       = hydrogen   # name of species;  note H+ is always the first ion in input file
 0 : Vceff      =  .864      # electroosmotic permeability
 0 : Vmo        = 78.96      # electromigration mobility in dilute solution under T = 298K
 0 : alpha      =  .229      # coefficient for calculating equivalent conductance
 0 : beta       = 60.2       # the other coefficient for equivalent conductance
```

```
0 : Deff        =  2.028      # diffusion coefficient with tortuosity 0.25
0 : charge      =  1.00       # charge valence
0 : retard      =  2.6        # H+ retardation factor

#
# next species
#

 1 : name       = hydroxyl
 1 : Vceff      =  .864
 1 : Vmo        = -44.88
 1 : alpha      =  .229
 1 : beta       = 60.2
 1 : Deff       =  1.152
 1 : charge     = -1.00
 1 : retard     =  0.56

#
#next species
#

 2 : name       = lead
 2 : Vceff      =  .864
 2 : Vmo        = 16.094
 2 : alpha      =  .458
 2 : beta       = 120.4
 2 : Deff       =  .20664
 2 : charge     = 2.00
 2 : retard     = 0.56

#
#next specie...
#

 3 : name       =  NO3
 3 : Vceff      =  .864
 3 : Vmo        = -16.094
 3 : alpha      =  .3237
 3 : beta       = 85.15
 3 : Deff       =  .41328
 3 : charge     = -1.00
 3 : retard     =  0.56
```

```
#########################################################
##                                                     ##
## Now The Initial Concentration Vals Follow.          ##
##    For each specie, we need                         ##
##  species# : ValinSoil   = value   # values inside soil column   ##
##  species# : ValatZeroPt = value   # value at anode interface    ##
##  species# : ValatEndPt  = value   # value at cathode interface  ##
##                                                     ##
#########################################################

# first specie      -> H+   # ValinSoil is required to have at least 3 values

 0 : ValinSoil   = .00001, .00001, .00001, .00001, .00001
 0 : ValatZeroPt =  .00001
 0 : ValatEndPt  =  .00001                          # all in units of mole/l

# next specie      -> OH-

 1 : ValinSoil   =  .000000001, .000000001, .000000001, .000000001, .000000001
 1 : ValatZeroPt =  .000000001
 1 : ValatEndPt  =  .000000001

# next specie      -> Pb2+

 2 : ValinSoil   =  .05, .05, .05, .05, .05
 2 : ValatZeroPt =  .05
 2 : ValatEndPt  =  .05

# next specie      -> (NO3)-

 3 : ValinSoil   =  .10, .10, .10, .10, .10, .10, .10, .10, .10, .10, .10
 3 : ValatZeroPt =  .10
 3 : ValatEndPt  =  .10

# End of Input
```

Filename: pH.dat

======== time = 1.00000 day ========

x/L	pH
0.000000	2.671391
0.050505	2.667659
0.101010	2.751850
0.151515	2.990498
0.202020	3.411111
0.252525	3.978393
0.303030	4.561890
0.353535	4.903042
0.404040	4.987257
0.454545	4.998674
0.505051	4.999889
0.555556	5.000048
0.606061	5.000337
0.656566	5.001947
0.707071	5.011338
0.757576	5.069308
0.808081	5.608430
0.858586	6.930855
0.909091	6.936133
0.959596	6.956827
1.000000	6.971460

======== time = 10.00000 day ========

x/L	pH
0.000000	2.636131
0.050505	2.629221
0.101010	2.622680
0.151515	2.618162
0.202020	2.615606
0.252525	2.614668
0.303030	2.614915
0.353535	2.615921
0.404040	2.617336
0.454545	2.618916
0.505051	2.620573
0.555556	2.622495
0.606061	2.625379
0.656566	2.630697
0.707071	2.640939
0.757576	2.660159
0.808081	2.695624
0.858586	2.762471
0.909091	2.897055
0.959596	3.306756
1.000000	7.019555

The files listed here are not complete.

Filename: Pb(II).dat

======== time = 1.00000 day ========

x/L	Pb (M)
0.000000	0.0325678
0.050505	0.0346762
0.101010	0.0360833
0.151515	0.0373752
0.202020	0.0383931
0.252525	0.0388494
0.303030	0.0389732
0.353535	0.0389963
0.404040	0.0389996
0.454545	0.039
0.505051	0.039
0.555556	0.039
0.606061	0.039
0.656566	0.0389998
0.707071	0.0389986
0.757576	0.0389917
0.808081	0.0389637
0.858586	0.0388437
0.909091	0.0378833
0.959596	0.0343538
1.000000	0.0320722

======== time = 35.00000 day ========

x/L	Pb (M)
0.000000	0.0199694
0.050505	0.0261792
0.101010	0.0229349
0.151515	0.0205932
0.202020	0.0187248
0.252525	0.0170195
0.303030	0.0154316
0.353535	0.014027
0.404040	0.0128131
0.454545	0.0118007
0.505051	0.0109403
0.555556	0.010171
0.606061	0.00943571
0.656566	0.00869472
0.707071	0.00792638
0.757576	0.00712336
0.808081	0.00631631
0.858586	0.00564364
0.909091	0.00545236
0.959596	0.007218
1.000000	0.00972191

* Limited by the size of output files, samples of output data for other species, electrical field and conductivity, and other pertinent information are not listed here. They can be found either through Fritz Engineering Library or from thesis advisor.

VITA

The author entered Tsinghua University, Beijing, China, in September, 1987. He received the Bachelor of Engineering degree in Hydraulic Engineering in July of 1992. His interest in undergraduate studies was focused on structural, hydraulic and geotechnical engineering. After graduation, he worked as a research assistant in the same university in areas of geotechnical and environmental water resources engineering.

The author began his graduate school at Lehigh University in August, 1994. He expects to receive his Master of Science degree in Civil & Environmental Engineering in June of 1997. His research interest is in geotechnical engineering and soil remediation.

END OF TITLE